

**POLITECNICO DI TORINO**

Master Degree in Mechanical Engineering

Master's Degree Thesis

**Pressure drop and noise performance  
analysis of an intake silencer in a  
reciprocating piston compressor**



**Academic Supervisor:**

Prof. Carlo ROSSO

**Company Supervisor:**

Eng. Marco ESPOSITO

**Graduate:**

Sabino DI GIOIA

**Academic Year 2018/2019**

# Abstract

Reciprocating piston compressor is one of the most common and oldest type of compressor. They are used worldwide to efficiently operate various tools and machinery. One of the most important drawbacks of many air compressors is the high noise level. There are a lot of sources and causes of noise in this kind of machine, like air intake, air exhaust or vibrational noise. My Thesis project is a result of an internship in technical department of *Abac Aria Compressa S.p.a (Atlas Copco Group)*, which identified the intake part as one of the loudest part of an air compressor. The way to reduce noise level from the intake is to install a silencer, built with a combination of silencing device and air filter. Starting from previous thesis “*Design of suction filter aimed to noise reduction of reciprocating piston compressor*”, it is developed a new silencer design. One of the problems of this project was the high pressure drop down the filter, that can decrease machine’s efficiency. Thus the principle aim will be to look for a new concept, that will be able to not increase too much pressure drop and guarantee a noise performance improvement.

After a first introduction chapter, where a literature review of all topic discussed is presented, *Chapter II* of this dissertation talks about machine that is object of this study, *PAT 49*, commonly called *PAT Due*. Geometric characteristics and actual filter used are reported. It is chosen to point out the most important aspects about this filter, called *Abac Filter*, that are noise performances and pressure drop. Moreover, also the filter proposed in previous thesis, called *Noise 1.0 filter*, is shown.

In *Chapter III and IV* analytical models of pressure drop and noise are reported. The first purpose is to validate pressure drop model by applying it to *Abac* and *Noise 1.0 Filters* and comparing results to experimental values. After this validation it’s possible to applicate this models to new filter configurations.

In *Chapter V* all new designs are shown. Unfortunately for external reasons, it was not possible to test the validity of the models proposed. Hence in the last paragraph next step and further analysis will be presented.

In *Appendix A* all technical drawings are shown.

# Contents

|   |           |
|---|-----------|
| <b>Abstract</b>   | <b>ii</b> |
| <b>1 Introduction</b>                                   | <b>2</b>  |
| 1.1 Reciprocating compressor: basic knowledge . . . . . | 2         |
| 1.2 Introduction to acoustics principles . . . . .      | 4         |
| 1.2.1 Quantification of sound . . . . .                 | 4         |
| 1.2.2 Frequency analysis . . . . .                      | 7         |
| 1.2.3 Psychoacoustics and filter weighting . . . . .    | 8         |
| 1.3 Noise test measurment . . . . .                     | 10        |
| 1.4 Pressure drop in a pipeline . . . . .               | 14        |
| <b>2 PAT Due Project</b>                                | <b>16</b> |
| 2.1 Air filter . . . . .                                | 18        |
| 2.1.1 Acoustic performance . . . . .                    | 20        |
| 2.2 Noise 1.0 Filter . . . . .                          | 21        |
| 2.3 Thesis procedure . . . . .                          | 23        |
| <b>3 Pressure drop: model validation</b>                | <b>25</b> |
| 3.1 PAT 2: Actual filter . . . . .                      | 26        |
| 3.1.1 Foam material . . . . .                           | 27        |
| 3.2 Noise 1.0 Filter . . . . .                          | 28        |
| 3.3 Experimental comparison . . . . .                   | 30        |
| 3.4 Comments . . . . .                                  | 33        |
| <b>4 Noise performance model</b>                        | <b>34</b> |
| 4.1 Silencer general information . . . . .              | 34        |
| 4.2 Transfer Matrix Method . . . . .                    | 35        |

|          |   |           |
|----------|---|-----------|
| 4.2.1    | Transmission loss . . . . .                                 | 37        |
| 4.3      | Helmotz Resonator . . . . .                                 | 38        |
| 4.3.1    | Transmission loss: Helmotz resonator . . . . .              | 40        |
| 4.3.2    | From Helmotz resonator to perforated tube . . . . .         | 43        |
| 4.4      | Expansion chamber . . . . .                                 | 44        |
| 4.4.1    | Extended pipes . . . . .                                    | 48        |
| 4.5      | From Transmission Loss to Sound power level $L_w$ . . . . . | 55        |
| 4.6      | Comments . . . . .  | 56        |
| <b>5</b> | <b>Filter design</b>  | <b>57</b> |
| 5.1      | Design 1 . . . . .  | 59        |
| 5.1.1    | Choice of other designs . . . . .                           | 64        |
| 5.2      | Design 2 . . . . .  | 65        |
| 5.3      | Design 3 . . . . .  | 67        |
| 5.4      | Design 4 . . . . .  | 69        |
| 5.5      | Design 5 . . . . .  | 71        |
| 5.6      | CAD 3D and assembly . . . . .                               | 73        |
| 5.7      | Final comparisons . . . . .                                 | 79        |
| 5.8      | Next steps and further analysis . . . . .                   | 88        |
|          | <b>Bibliography</b>   | <b>90</b> |
|          | References . . . . .  | 90        |
| <b>A</b> | <b>Filter design: 2D representations</b>                    | <b>91</b> |



# List of Figures

|      |   |    |
|------|---|----|
| 1.1  | Thermodynamic cycle of a single stage compressor . . . . .      | 3  |
| 1.2  | Slider crank mechanism . . . . .                                | 3  |
| 1.3  | Free field condition . . . . .                                  | 6  |
| 1.4  | Octave band vs one-third octave band . . . . .                  | 7  |
| 1.5  | Equal loudness contours . . . . .                               | 8  |
| 1.6  | A weighting and C weighting networks . . . . .                  | 9  |
| 1.7  | A-weighting attenuation . . . . .                               | 9  |
| 1.8  | Apollo box . . . . .  | 10 |
| 1.9  | Hemispherical box . . . . .                                     | 11 |
| 1.10 | Position of microphones according Directive 200/14/EC . . . . . | 12 |
| 1.11 | Moody diagram . . . . .   | 14 |
| 2.1  | PAT Due compressor . . . . .                                    | 16 |
| 2.2  | PAT Due compressor: P-v diagram . . . . .                       | 17 |
| 2.3  | Abac Filter: 3D Model . . . . .                                 | 18 |
| 2.4  | No filter vs Abac filter acoustic performance . . . . .         | 20 |
| 2.5  | Noise 1.0 filter: 3D Model . . . . .                            | 21 |
| 2.6  | Acoustic performances comparison . . . . .                      | 22 |
| 2.7  | Size comparison . . . . .                                       | 22 |
| 2.8  | Pressure drop model validation . . . . .                        | 23 |
| 2.9  | Noise 2.0 Model . . . . .                                       | 24 |
| 3.1  | Local resistance coefficient . . . . .                          | 25 |
| 3.2  | Abac filter parts . . . . .                                     | 26 |
| 3.3  | Porosity . . . . .  | 27 |
| 3.4  | Noise 1.0: Filter parts . . . . .                               | 28 |

|      |   |    |
|------|---|----|
| 3.5  | Flow distribution in T-junction . . . . .                       | 28 |
| 3.6  | Honeycomb stage . . . . .                                       | 29 |
| 3.7  | Pressure drop: analytical results . . . . .                     | 30 |
| 3.8  | Noise 1.0 Filter: Pressure drop . . . . .                       | 32 |
| 4.1  | Plane wave propagation in straight pipe . . . . .               | 35 |
| 4.2  | Plane wave propagation in more elements . . . . .               | 36 |
| 4.3  | Helmutz resonator . . . . .                                     | 38 |
| 4.4  | HR and mass-spring oscillation . . . . .                        | 39 |
| 4.5  | Helmutz resonator: sound wave propagation . . . . .             | 40 |
| 4.6  | Transmissison loss of Helmutz resonator . . . . .               | 41 |
| 4.7  | Influence of HR parameters: $l_k=\text{const}$ . . . . .        | 42 |
| 4.8  | Influence of HR parameters: $S_k=\text{const}$ . . . . .        | 42 |
| 4.9  | Influence of HR parameters: $V_c=\text{const}$ . . . . .        | 43 |
| 4.10 | Perforated tube . . . . .                                       | 43 |
| 4.11 | Single expansion chamber . . . . .                              | 44 |
| 4.12 | Transmission loss: single expansion chamber . . . . .           | 45 |
| 4.13 | Influence of $m$ . . . . .                                      | 46 |
| 4.14 | Influence of $L$ . . . . .                                      | 47 |
| 4.15 | Influence of $L$ (0-4500 Hz) . . . . .                          | 47 |
| 4.16 | Single expansion chamber with extended pipes . . . . .          | 48 |
| 4.17 | Decomposition of silencer . . . . .                             | 48 |
| 4.18 | Comparison between single EC model and extended model . . . . . | 49 |
| 4.19 | Case 1 . . . . .  | 50 |
| 4.20 | Case 1: Analytical results . . . . .                            | 50 |
| 4.21 | Case 2 . . . . .  | 51 |
| 4.22 | Case 2: Analytical results . . . . .                            | 51 |
| 4.23 | Case 3 . . . . .  | 52 |
| 4.24 | Case 3: Analytical results . . . . .                            | 52 |
| 4.25 | Case 4 . . . . .  | 53 |
| 4.26 | Case 4: Analytical results . . . . .                            | 53 |
| 4.27 | Case 5 . . . . .  | 54 |
| 4.28 | Case 5: Analytical results . . . . .                            | 54 |

|   |    |
|---|----|
| 4.29 Noise analysis . . . . .                         | 55 |
| 5.1 PAT 2: Sound power level without filter . . . . . | 57 |
| 5.2 Acoustics model . . . . .                         | 58 |
| 5.3 Design 1 . . . . .                                | 59 |
| 5.4 Sound power level- Design 1 . . . . .             | 61 |
| 5.5 Flow distribution- Design 1 . . . . .             | 62 |
| 5.6 Pressure drop-Design 1 . . . . .                  | 63 |
| 5.7 Design 2 . . . . .                                | 65 |
| 5.8 Sound power level- Design 2 . . . . .             | 65 |
| 5.9 Pressure drop-Design 2 . . . . .                  | 66 |
| 5.10 Design 3 . . . . .                               | 67 |
| 5.11 Sound power level- Design 3 . . . . .            | 67 |
| 5.12 Pressure drop-Design 3 . . . . .                 | 68 |
| 5.13 Design 4 . . . . .                               | 69 |
| 5.14 Sound power level- Design 4 . . . . .            | 69 |
| 5.15 Pressure drop-Design 4 . . . . .                 | 70 |
| 5.16 Design 5 . . . . .                               | 71 |
| 5.17 Sound power level- Design 5 . . . . .            | 71 |
| 5.18 Pressure drop-Design 5 . . . . .                 | 72 |
| 5.19 PART A: isometric view . . . . .                 | 73 |
| 5.20 PART B: isometric view . . . . .                 | 74 |
| 5.21 PART B- Axial view . . . . .                     | 74 |
| 5.22 CONNECTION PART- Isometric view . . . . .        | 75 |
| 5.23 FOAM MATERIAL: isometric view . . . . .          | 75 |
| 5.24 FOAM MATERIAL and PART B . . . . .               | 76 |
| 5.25 PART B and CONNECTION PART . . . . .             | 76 |
| 5.26 Filter representation . . . . .                  | 77 |
| 5.27 Head of cylinder . . . . .                       | 77 |
| 5.28 Total assembly . . . . .                         | 77 |
| 5.29 Total number of components . . . . .             | 78 |
| 5.30 Size . . . . .                                   | 79 |
| 5.31 Transmission loss . . . . .                      | 80 |

|  |    |
|--|----|
| 5.32 Sound power level . . . . .                   | 80 |
| 5.33 Sound power level: Low frequencies . . . . .  | 81 |
| 5.34 Sound power level: High frequencies . . . . . | 81 |
| 5.35 Transmission Loss 1,3,4 . . . . .             | 82 |
| 5.36 Sound power level 1,3,4 . . . . .             | 83 |
| 5.37 Transmission Loss 1,2 . . . . .               | 84 |
| 5.38 Sound power level 1,2 . . . . .               | 84 |
| 5.39 Transmission Loss 1,5 . . . . .               | 85 |
| 5.40 Sound power level 1,5 . . . . .               | 86 |
| 5.41 Hybrid solution . . . . .                     | 89 |

# List of Tables

|     |  |    |
|-----|--|----|
| 1.1 | Band comparison . . . . .  | 7  |
| 1.2 | Uncertainty in the determination of sound power levels . . . . .   | 11 |
| 1.3 | Coordinates of microphones . . . . .                               | 12 |
| 1.4 | Coordinates of microphones according Directive 200/14/EC . . . . . | 13 |
| 2.1 | PAT Due parameters . . . . .                                       | 16 |
| 2.2 | Pat Due: Abac Filter . . . . .                                     | 19 |
| 2.3 | Abac Filter: Noise performance . . . . .                           | 20 |
| 2.4 | Noise 1.0 experimental results . . . . .                           | 21 |
| 2.5 | Noise 1.0 filter vs Abac filter . . . . .                          | 22 |
| 3.1 | Description of Abac filter parts . . . . .                         | 26 |
| 3.2 | Local resistance coefficients of Abac Filter . . . . .             | 27 |
| 3.3 | Description of Noise 1.0 filter parts . . . . .                    | 29 |
| 3.4 | Local resistance coefficients of Noise 1.0 Filter . . . . .        | 29 |
| 3.5 | Maximum pressure drop . . . . .                                    | 31 |
| 3.6 | Experimental vs Analytical results . . . . .                       | 31 |
| 3.7 | Noise 1.0: Maximum pressure drop . . . . .                         | 31 |
| 3.8 | Noise 1.0: Experimental vs Analytical results . . . . .            | 32 |
| 4.1 | Helmotz resonator vs Perforated tube . . . . .                     | 44 |
| 4.2 | Example: Expansion chamber parameters . . . . .                    | 46 |
| 5.1 | Design 1: filter parts . . . . .                                   | 59 |
| 5.2 | Design 1: Acoustic element . . . . .                               | 60 |
| 5.3 | Equivalent sound power level- Design 1 . . . . .                   | 61 |
| 5.4 | Design 1: mass flow and velocity . . . . .                         | 62 |

|      |  |    |
|------|--|----|
| 5.5  | Design 1: local resistance . . . . .             | 63 |
| 5.6  | Design 1: maximum pressure drop . . . . .        | 63 |
| 5.7  | Reasons of the choice . . . . .                  | 64 |
| 5.8  | Equivalent sound power level- Design 2 . . . . . | 66 |
| 5.9  | Design 2: maximum pressure drop . . . . .        | 66 |
| 5.10 | Equivalent sound power level- Design 3 . . . . . | 68 |
| 5.11 | Design 3: maximum pressure drop . . . . .        | 68 |
| 5.12 | Equivalent sound power level- Design 4 . . . . . | 70 |
| 5.13 | Design 4: maximum pressure drop . . . . .        | 70 |
| 5.14 | Equivalent sound power level- Design 5 . . . . . | 72 |
| 5.15 | Design 5: maximum pressure drop . . . . .        | 72 |
| 5.16 | PART A: details . . . . .                        | 73 |
| 5.17 | PART B: details . . . . .                        | 74 |
| 5.18 | CONNECTION PART: details . . . . .               | 75 |
| 5.19 | FOAM MATERIAL: details . . . . .                 | 76 |
| 5.20 | Decomposition of each filter . . . . .           | 78 |
| 5.21 | Analytical results . . . . .                     | 79 |
| 5.22 | Design 1,3,4 . . . . .                           | 83 |
| 5.23 | Design 1,2 . . . . .                             | 84 |
| 5.24 | Design 1,5 . . . . .                             | 86 |
| 5.25 | Final comparison . . . . .                       | 87 |
| 5.26 | Explication of the symbols . . . . .             | 87 |

# Ringraziamenti

Alla fine di questo lavoro di tesi, ci terrei a ringraziare in queste poche righe le persone che mi hanno permesso di affrontare questo importante percorso. L'esperienza svolta in questi mesi mi ha permesso di maturare molto dal punto di vista personale e mi ha aiutato anche a svolgere i primi passi anche dal punto di vista professionale.

Quindi ci terrei a ringraziare in primis il mio relatore, il professor Carlo Rosso, il quale in questi mesi ha saputo sempre aiutarmi in ogni occasione e spronarmi nel modo corretto. Per me è stato importante sapere di poter avere un supporto al mio fianco in grado di potermi dare una linea guida nei momenti di stallo. E ogni suo apprezzamento è stato per me fonte di consapevolezza e autostima e la ringrazio per questo.

Ringrazio anche il mio tutor accademico, l'ingegner Marco Esposito per avermi accolto nel migliore dei modi all'interno dell'azienda sin dal primo momento e avermi dato volta per volta consigli per migliorarmi costantemente.

Ovviamente ringrazio tutte le persone che mi sono state accanto in tutti questi mesi e soprattutto anni. Dalla mia famiglia che mi ha permesso di realizzare ogni mio singolo desiderio fidandosi di me e senza ostacolarmi mai. Ogni singola parola di conforto e di incoraggiamento è una forza per andare avanti e non mollare mai. Tutto questo è stato possibile soprattutto grazie a voi. E per ultimo, ma non per importanza, grazie alle persone che hanno reso questi anni indimenticabili, la mia "seconda" famiglia. Ricorderò con nostalgia ogni singolo momento.

# Chapter 1

## Introduction

### 1.1 Reciprocating compressor: basic knowledge

The aim of this first paragraph is to briefly illustrate the basic knowledge of a reciprocating compressor [1], focusing especially on thermodynamic cycle and crankshaft mechanism.

Fig. 1.1 represents an ideal thermodynamic cycle of a single stage compressor, in a  $p-v$  diagram. This kind of machine works in four phases:

- **Compression (1-2):** in 1, that represents the bottom dead point of the compressor, the volume of gas inside the cylinder is maximum. At this position all of the compressor valves are closed, and the piston is at rest. As the crankshaft rotates the piston will move and the gas volume decreases (from 1 to 2).
- **Discharge phase (2-3):** it is ideally an isobaric transformation. If the pressure equals the delivery pressure, the outlet valve opens and the delivery starts.
- **Pressure reduction (3-4):** in 3, that represents the top dead point of the compressor, the volume of gas inside the cylinder is minimum. This volume is called Clearance volume, and it is generally around 5% of maximum volume. The pressure equals the delivery pressure, the outlet valve closes and the pistons starts going down (from 3 to 4)
- **Suction phase (4-1):** it is ideally an isobaric transformation. The volume in the cylinder is 20-30%. If the pressure equals the suction pressure, the inlet valve opens and the delivery starts. The piston continues to go down.



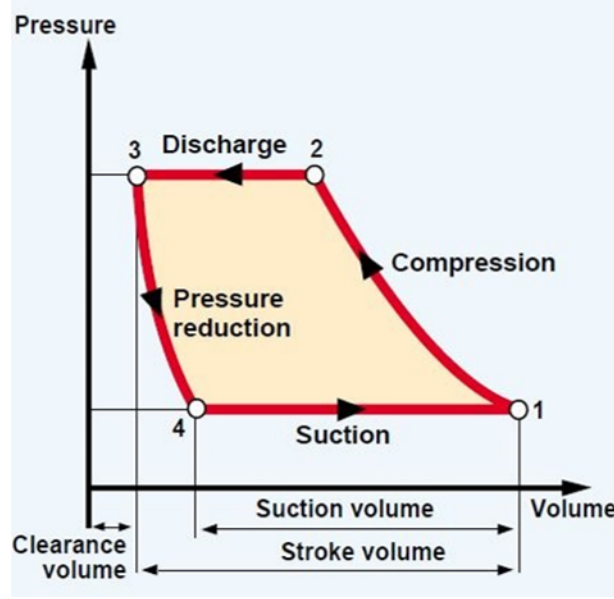


Figure 1.1: Thermodynamic cycle of a single stage compressor

Piston movement, driven by a slider crank mechanism, is shown in Fig. 1.2. It is used to convert circular motion into reciprocating motion, or vice versa. Attached to the end of the crank by a pivot is a rod, usually called **connecting rod**. Instead the other end of the connecting rod is attached to the piston which is displaced inside the cylinder. In this way the rotation of the crank drives the linear movement the slider, or the expansion of gases against a sliding piston in a cylinder can drive the rotation of the crank.

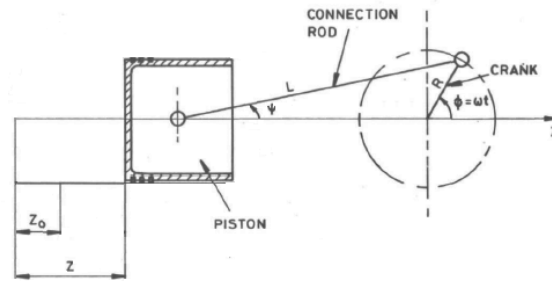


Figure 1.2: Slider crank mechanism

In order to determine in-cylinder thermodynamics conditions, which are depending on variable volume delimited by the head of the piston, it is necessary to identify the displacement of this piston during the motion. Defining it as  $z$ , the following equation can be written:

$$z = z_0 + R + L - R \cos \omega t - \sqrt{L^2 - R^2 \sin^2 \omega t} \quad (1.1)$$

where:

$z_0$  = smallest distance between cylinder and piston (derived from clearance volume);

$R$  = radius of crankshaft;

$L$  = connecting rod length;

$\omega$  = angular velocity of crankshaft.

Hence the velocity of the piston  $w_z$  can be expressed in form of equation by differentiating eq. (1.1):

$$w_z = \frac{dz}{dt} = R\omega \sin \omega t \left( 1 + \frac{R \cos \omega t}{\sqrt{L^2 - R^2 \sin^2 \omega t}} \right) \quad (1.2)$$

## 1.2 Introduction to acoustics principles

In this section a general introduction about acoustics is reported, starting from the definition of it. These preliminary aspects and other further information can be found in [2] and [3]. **Acoustics** is the science of sound, that is the result of pressure variations, or oscillations, in an elastic medium (e.g., air, water, solids), generated by a vibrating surface, or turbulent fluid flow. Sound propagates in the form of longitudinal waves, involving a succession of compressions and rarefactions in the elastic medium.

From the acoustics point of view, **sound** and **noise** represent the same phenomenon that has already been described. The real differentiation between them is subjective. In fact *noise* can be defined as undesired sound or other disturbance: what is sound to one person can be noise to somebody else. Nowadays the recognition of noise is a real health problem, especially in modern industries where the excessive noise could be the cause of important hearing damages.

In the next paragraphs basic definitions and other aspects related to the physics of sound and noise are presented. This is very important to provide the necessary background for the understanding of the topics covered in this dissertation.

### 1.2.1 Quantification of sound

The physical quantities to describe a sound field are presented in this paragraph.

Sound waves can be characterized by **the amplitude of pressure changes**, that can be described by two possible quantities:

- Maximum pressure amplitude  $p_m$ , expressed in Pa;
- Root meansquare amplitude,  $p_{rms}$ , in which the instantaneous sound pressures are squared, averaged and the square root of the average is taken, as in (1.3)

$$p_{rms} = \lim_{t \rightarrow \infty} \sqrt{\frac{1}{T} \int_0^T p^2(t), dt} \quad (1.3)$$

that can be defined also as  $p_{rms} = 0.707 p_m$ .

**Sound intensity** (or Acoustic intensity) is a vector quantity determined as the product of sound pressure and the component of particle velocity in the direction of the intensity vector (see Eq.(1.4)). It is defined as the power carried by sound waves per unit area in a direction

perpendicular to that area and expressed as  $\frac{W}{m^2}$ .

$$I = p\bar{v} \quad (1.4)$$

In a *free-field environment*, i.e., no reflected sound waves and well away from any sound sources, the sound intensity is related to the root mean square acoustic pressure as follows

$$I = \frac{p_{rms}^2}{\rho c} \quad (1.5)$$

where:

$\rho$  is the density of the air ( $kg/m^3$ );

$c$  is the sound speed (343 m/s)

$\rho c$  is also called the "*acoustic impedance*".

**The sound power**,  $W$ , is the total sound energy emitted by a source per unit time and it is expressed in Watt (W). It is obtained by integrating the sound intensity over an imaginary surface surrounding a source.

$$W = \int_A I \cdot \mathbf{n}, dt \quad (1.6)$$

Unlike sound pressure, that is a property of the acoustic field at a point in space, sound power is only a property of a sound source, equal to the total power emitted by that source in all directions. It represents an important property in noise measurement, because in this way it's possible to delete the room and distance dependance of noise source.

The range of sound pressure that can be heard by human ear is very large. Because it's not possible to detect sound pressure in a linear way, all the acoustic quantities are expressed in a logarithmic scale. Thus it is introduced the "*Bel scale*", shown in (1.7)

$$L_q = 10 \log_{10} \frac{Quantity}{Ref.quantity} \quad (1.7)$$

These reference values are related to minimum acoustic pressure audible to a human ear to be in good health.

- $p_0 = 20 \cdot 10^{-6}$  Pa;
- $I_0 = 10^{-12} \frac{W}{m^2}$ ;
- $W_0 = 10^{-12}$  W;

Sound level of acoustics quantities described in this paragraph are reported.

**SOUND PRESSURE LEVEL;**

$$L_p = 10 \log_{10} \frac{p}{p_0} \quad (1.8)$$

**SOUND INTENSITY LEVEL;**

$$L_I = 10 \log_{10} \frac{I}{I_0} \quad (1.9)$$

**SOUND POWER LEVEL;**

$$L_W = 10 \log_{10} \frac{W}{W_0} \quad (1.10)$$

The most simple sound(or noise) propagation way is **free field condition**. The free field is considered as a region in space where sound may propagate free from any form of obstruction. This type of propagation is *spherical*(see 1.3), where sound radiates equally in all directions from the source, and then will diffuse in all directions.

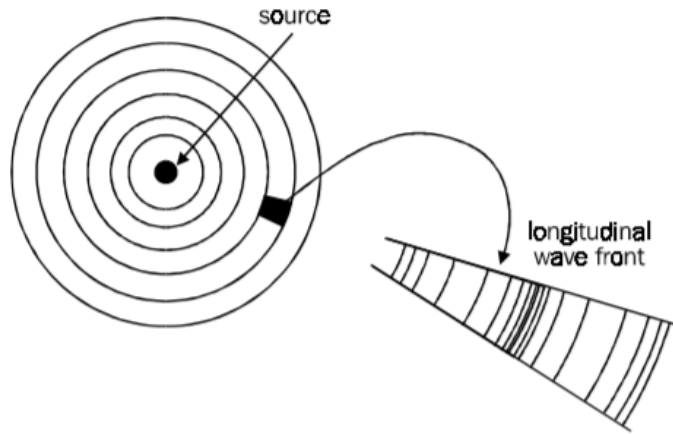


Figure 1.3: Free field condition

In this model sound pressure at a given point, at a distance  $r$  from the source, can be expressed as:

$$p = \rho c I = \rho c \frac{W}{4\pi r^2} \quad (1.11)$$

Thus, in terms of sound pressure:

$$L_p = L_w + 10 \log_{10} \frac{\rho c}{400} - 10 \log_{10} (4\pi r^2) \quad (1.12)$$

which is often approximated as:

$$L_p = L_w - 10 \log_{10} (4\pi r^2) \quad (1.13)$$

Considering two different points, at a respective distance  $r_1$  and  $r_2$  from the source, the difference between two sound level pressure is only dependent on these differents distances.

$$L_{p_2} = L_{p_1} - 20 \log_{10} \frac{r_2}{r_1} \quad (1.14)$$

Starting from Eq.(1.14), it's possible to declare that in a free field there is a reduction of 6dB in sound pressure level if  $r_2=2r_1$ .

### 1.2.2 Frequency analysis

The steady sound analysis can be useful only to describe the phenomena, but frequency analysis is used to make a correct analysis of noise propagation. In fact most sounds in practise have a broadband characteristic and each frequency can affect them in a different way. Thus, noise identification and the evaluation of noise control are done using a frequency analysis, where each signal is decomposed into its spectral component.

The frequency domain used for noise measuring and analysis is divided in set of frequencies called *bands*, that are standardised. The widest band is the **octave band**, in which upper band limit is twice lower band limit and the center band frequency is a geometric mean of these values. However, in noise control and in lots environmental applications is often used an other standardised band, called **octave band**, that provide a further outlook on noise level across the frequency composition. In this case the upper frequency is cube root of two times the lower frequency. The differences between frequency band limit in octave and one third octave bands are shown in Table 1.1. A representation of these two frequency band is shown in Fig. 1.4.

Table 1.1: Band comparison

|                       | OCTAVE BAND            | 1/3 OCTAVE BAND                |
|-----------------------|------------------------|--------------------------------|
| Middle frequency      | $f_o$                  | $f_o$                          |
| Lower frequency bound | $\frac{f_o}{\sqrt{2}}$ | $\frac{f_o}{(\sqrt{2})^{1/3}}$ |
| Upper frequency bound | $f_o \cdot \sqrt{2}$   | $f_o \cdot (\sqrt{2})^{1/3}$   |

| Band number | Octave band center frequency | One-third octave band center frequency | Band limits Lower | Upper |
|-------------|------------------------------|--|-------------------|-------|
| 14 }        | 31.5                         | 25                                     | 22                | 28    |
| 15 }        |                              | 31.5                                   | 28                | 35    |
| 16 }        |                              | 40                                     | 35                | 44    |
| 17 }        | 63                           | 50                                     | 44                | 57    |
| 18 }        |                              | 63                                     | 57                | 71    |
| 19 }        |                              | 80                                     | 71                | 88    |
| 20 }        | 125                          | 100                                    | 88                | 113   |
| 21 }        |                              | 125                                    | 113               | 141   |
| 22 }        |                              | 160                                    | 141               | 176   |
| 23 }        | 250                          | 200                                    | 176               | 225   |
| 24 }        |                              | 250                                    | 225               | 283   |
| 25 }        |                              | 315                                    | 283               | 353   |
| 26 }        | 500                          | 400                                    | 353               | 440   |
| 27 }        |                              | 500                                    | 440               | 565   |
| 28 }        |                              | 630                                    | 565               | 707   |
| 29 }        | 1000                         | 800                                    | 707               | 880   |
| 30 }        |                              | 1000                                   | 880               | 1130  |
| 31 }        |                              | 1250                                   | 1130              | 1414  |
| 32 }        | 2000                         | 1600                                   | 1414              | 1760  |
| 33 }        |                              | 2000                                   | 1760              | 2250  |
| 34 }        |                              | 2500                                   | 2250              | 2825  |
| 35 }        | 4000                         | 3150                                   | 2825              | 3530  |
| 36 }        |                              | 4000                                   | 3530              | 4400  |
| 37 }        |                              | 5000                                   | 4400              | 5650  |
| 38 }        | 8000                         | 6300                                   | 5650              | 7070  |
| 39 }        |                              | 8000                                   | 7070              | 8800  |
| 40 }        |                              | 10000                                  | 8800              | 11300 |

Figure 1.4: Octave band vs one-third octave band

### 1.2.3 Psychoacoustics and filter weighting

The analysis of physical characteristics of acoustics is not sufficient to describe noise criteria because it is also fundamental to consider how the human ear responds to it. This response depends both on sound frequency and sound pressure level. Thus it is introduced the concept of *loudness* for evaluation of noise exposure and to explain how human ear is sensitive in a different way to different frequencies.

Loudness level is expressed in **phons**, defined as the equivalent values of sound pressure level at 1000 Hz. "Equal loudness contours" has been created to rate the loudness of sound, as shown in Fig. 1.5 The curves of this figure has been determined through psycho-acoustical experiment.

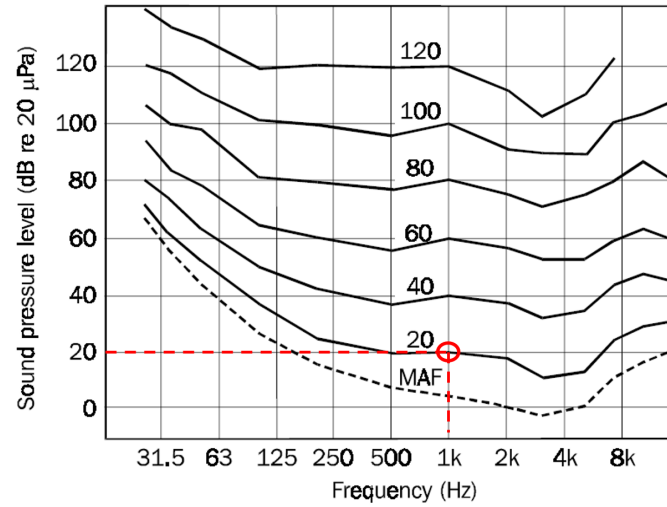


Figure 1.5: Equal loudness contours

Red square indicates the correspondence between loudness values and sound pressure level at 1000Hz (e.g. 20 phons=20dB at 1000 Hz).

It's clear that human ear doesn't react in the same way at all frequencies and also noise measurement has to conform to these different sensitivities. For this reason frequency weighting networks, which are really "*frequency weighting filters*" have been developed. In the following list the most important are reported.

- **A-weighted scale:** modifies the frequency response to follow approximately the equal loudness curve of 40 phons, so it follows the sensitivity human's ears at low levels.
- **C-weighted scale:** modifies the frequency response to follow approximately the equal loudness curve of 100 phons, so it follows the sensitivity human's ears at high levels.

There is also an other weighting network, called "*B*", but it is not important to noise evaluation.

Nowadays in industrial application A-weighted scale is used because it represents the best to describe interior noise environment from the point of view of habitability, community disturbance and hearing damage. In this Thesis all noise criteria are calculated considering A-weighting scale.

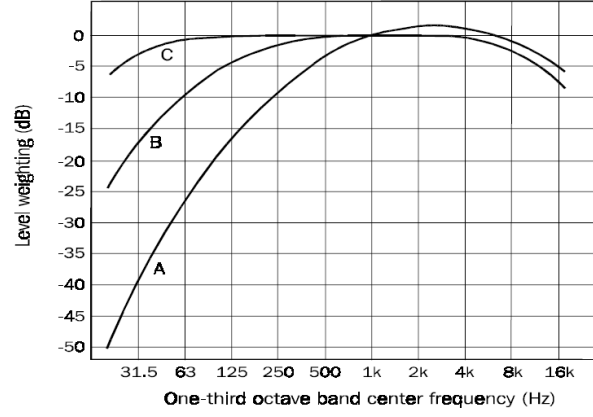


Figure 1.6: A weighting and C weighting networks

A-weighted values attenuation (in dB) is shown in Fig.1.7

| Table of A-weighting Values    |                      |                                |                      |
|--------------------------------|----------------------|--------------------------------|----------------------|
| 1/3 Octave Center Frequency Hz | A-weighting value dB | 1/3 Octave Center Frequency Hz | A-weighting value dB |
| 20                             | -50.5                | 630                            | -1.9                 |
| 25                             | -44.7                | 800                            | -0.8                 |
| 31.5                           | -39.4                | 1000                           | 0                    |
| 40                             | -34.6                | 1250                           | 0.6                  |
| 50                             | -30.2                | 1600                           | 1                    |
| 63                             | -26.2                | 2000                           | 1.2                  |
| 80                             | -22.5                | 2500                           | 1.3                  |
| 100                            | -19.1                | 3150                           | 1.2                  |
| 125                            | -16.1                | 4000                           | 1                    |
| 160                            | -13.4                | 5000                           | 0.5                  |
| 200                            | -10.9                | 6300                           | -0.1                 |
| 250                            | -8.6                 | 8000                           | -1.1                 |
| 315                            | -6.6                 | 10000                          | -2.5                 |
| 400                            | -4.8                 | 12500                          | -4.3                 |
| 500                            | -3.2                 | 16000                          | -6.6                 |

Figure 1.7: A-weighting attenuation

A-weighting network modifies the way to evaluate noise. In fact also noise level is referred to "A-weighted level" and expressed as dB(A). This equivalent sound level is presented in Eq.(1.15)

$$L_{Aeq} = 10 \log_{10} \sum_{i=1}^n 10^{(L_i/10)} \quad (1.15)$$

where:

$L_i$ = sound level at a given frequency in band;

n= number of frequencies considered in noise measurement.

In Thesis project equivalent sound power level  $L_W(A)$  will be used and it can be expressed by:

$$L_w(A) = 10 \log_{10} \sum_{i=1}^n 10^{(L_{w,i}/10)} \quad (1.16)$$

### 1.3 Noise test measurment

The method used to noise measurment follows *ISO 9614*. This normative explains the determination of sound power levels of noise sources using sound intensity and it is divided in three parts:

- **Part 1:** Measurement at discrete points;
- **Part 2:** Measurement by scanning.
- **Part 3:** Precision method for measurement by scanning.

In this paragraph scanning method is reported (ISO 9614-2).

The instrumend used to perform acoustic test is Apollo box, an acoustic analyser shown in Figure 1.8.



Figure 1.8: Apollo box

Apollo box is a flexible 2 or 4 channel data acquisition system with a USB 2.0 interface. It is combined to PC with a software (in this case SAMURAI) and it is used for a wide variety of acoustic and vibration measurement applications. Apollo analyser is connected via cables with the acoustic probe, that measures the sound intensity using two microphones calibrated at 94 dB. Acoustic probe detects a time domain signal, then analyzer converts automatically this signal in its frequency domain by performing a Fast Fourier Transformation (FFT). Thus the output of noise test is sound intensity spectrum, that will be filtered by a low pass filter that cut all frequency that could disturb the signal.

After the presentation of measuring instrument, the method used to perform noise measurment is reported.

- The first step is the definition of external temperature, pressure and wind direction of **surrounding environment**.
- **Definition of the source.** In this case noise source is the pump, thus its dimensions are considered.



- Definition of the box that surrounds the source. In fact the measurement surface shall be defined around the source under test. It is preferably that this box has a parallelepiped shape and each face considered is a rectangle. The number of measurement surfaces are 5, four lateral and one upper. According to the normative, the minimum distance between measurement surface and noise source is 0,25 m. In this case, this distance is equal to 0,5 m in each side.
- Scanning of these surfaces by using acoustic probe. Move the intensity probe continuously along each selected measurement surface, with an uniform velocity (0,5-1 m/s). The duration of the measurements will be not less than 20 s. It needs to scan faces two times, in vertical and horizontal, to improve the grade of accuracy of the measurement. In Table 1.2 errors in the determination of sound power levels are shown. Two-scanning procedure allows to reach *grade 2* that is the limit of acceptability for engineering application.

Table 1.2: Uncertainty in the determination of sound power levels

| Octave band centre frequencies<br>Hz | One- third Octave band centre frequencies<br>Hz | Standard deviation, S       |                        |
|--------------------------------------|---|-----------------------------|------------------------|
|                                      |   | Engineering (grade 2)<br>dB | Survey (grade 3)<br>dB |
| 63 to 125                            | 50 to 160                                       | 3                           | 4                      |
| 250                                  | 200 to 315                                      | 2                           |                        |
| 500 to 4000                          | 400 to 5000                                     | 1,5                         |                        |
| A-weighted                           | 6300  | 2,5                         |                        |

- The output of the measurement is an average value of sound intensity level. It is common to compute sound power level  $L_w$ , only by considering the dimension of measured surface area.

It's possible to define an other hypothetic reference box, having an **hempispherical** shape, as shown in *ISO 3744*. This International Standard explains the method to calculate the sound power level produced by the noise source starting from the measure of the sound pressure levels on a measurement surface that envelop a noise source, under essentially free-field conditions near one or more reflecting planes. Noise source represents the center of this hemisphere and ten microphones are positioned as in the following figure.

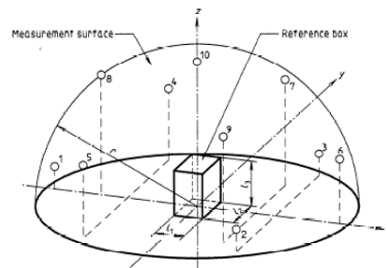


Figure 1.9: Hemispherical box

The positions of microphones are expressed in function of cartesian coordinates x,y,z and radius of hemisphere  $r$ .

Table 1.3: Coordinates of microphones

| Microphone position | $x/r$ | $y/r$ | $z/r$ |
|---------------------|-------|-------|-------|
| 1                   | -0.99 | 0     | 0.15  |
| 2                   | 0.50  | -0.86 | 0.15  |
| 3                   | 0.50  | 0.86  | 0.15  |
| 4                   | -0.45 | 0.77  | 0.45  |
| 5                   | -0.45 | -0.77 | 0.45  |
| 6                   | 0.89  | 0     | 0.45  |
| 7                   | 0.33  | 0.57  | 0.75  |
| 8                   | -0.66 | 0     | 0.75  |
| 9                   | 0.33  | -0.57 | 0.75  |
| 10                  | 0     | 0     | 1     |

Considerations about environmental conditions and uncertainty in measurement are the same than previous test.

Starting from *ISO 3744*, *Directive 2000/14/EC of the European Parliament and of the Council* is presented. The aim of this Directive is to show the method of measurement of airborne noise emitted by equipment for use outdoors. Particularly in addition to the normative, a set of 12 microphones on the hemispherical measurement surface may be used. The radius  $r$  of the hemisphere shall be equal to or greater than twice the largest dimension of the reference parallelepiped, defined as the smallest possible rectangular parallelepiped just enclosing the source. It shall be rounded to the nearest higher of 4, 10 or 16 m.

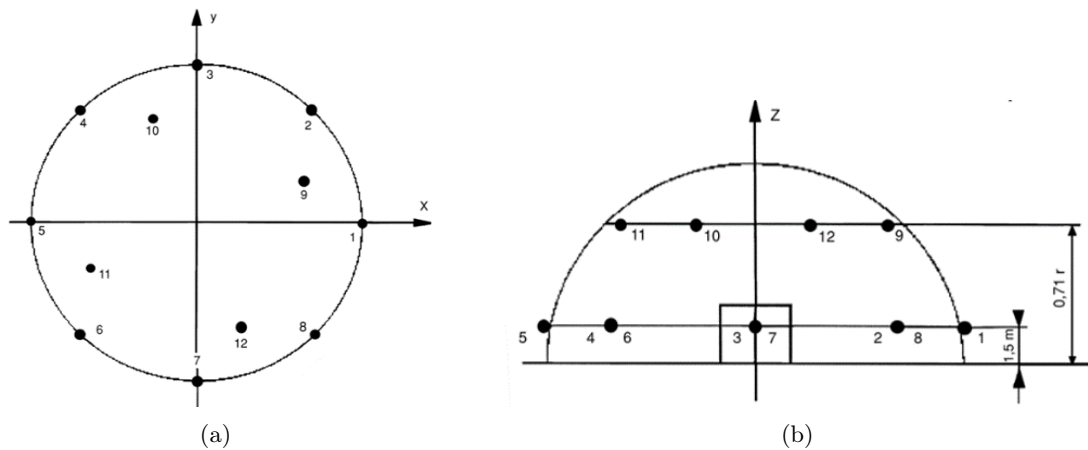


Figure 1.10: Position of microphones according Directive 200/14/EC

The number of point can be reduced at six, chosen only even or odd numbers, when the radiation pattern is shown to be symmetrical (*Section 7.4.2 ISO 3744:1995*).

Noise testing is made three times for each point and the differences between three measurements will be not greater than 1 dB.

Even in this case the duration of each measurements will be not less than 20 s.

Table 1.4: Coordinates of microphones according Directive 200/14/EC

| Microphone position | $x/r$ | $y/r$ | $z$   |
|---------------------|-------|-------|-------|
| 1                   | 1     | 0     | 1.5 m |
| 2                   | 0.7   | 0.7   | 1.5 m |
| 3                   | 0     | 1     | 1.5 m |
| 4                   | -0.7  | 0.7   | 1.5 m |
| 5                   | -1    | 0     | 1.5 m |
| 6                   | -0.7  | -0.7  | 1.5 m |
| 7                   | 0     | -1    | 1.5 m |
| 8                   | 0.7   | -0.7  | 1.5 m |
| 9                   | 0.65  | 0.27  | 0.71r |
| 10                  | -0.27 | 0.65  | 0.71r |
| 11                  | -0.65 | -0.27 | 0.71r |
| 12                  | 0.27  | -0.65 | 0.71r |

## 1.4 Pressure drop in a pipeline

In *Abstract* has been already mentioned that the presence of an intake silencer improves noise performances of the pump, but it could be the cause of high pressure losses. One of the aim of this project is to avoid the risk to increase too much pressure drop down the filter. In this paragraph the theory of pressure drop in a pipeline is presented.[6]

Considering a general pipe, characterized by a lenght  $L_{pipe}$  and an inlet diameter  $D_{pipe}$ , pressure losses through the pipe, called **pressure drop**, are calculated in eq.(1.18).

$$\Delta p_{drop} = \frac{1}{2} \xi \rho u^2 \quad (1.17)$$

where:

$u$ : flow velocity;

$\xi$ : loss coefficient.

This terms  $\xi$  includes both distributed and concentrated losses as shown in the following equation.

$$\xi = f_d \frac{L_{pipe}}{D_{pipe}} + \sum K \quad (1.18)$$

where  $f_d$  is *Darcy factor* (Distributed losses) and  $K$  represents concentrated losses coefficient. Darcy factor depends on Reynolds number  $Re$  and on wall roughness of the pipe  $\epsilon$ , as shown in Moody diagram in Fig. 1.11

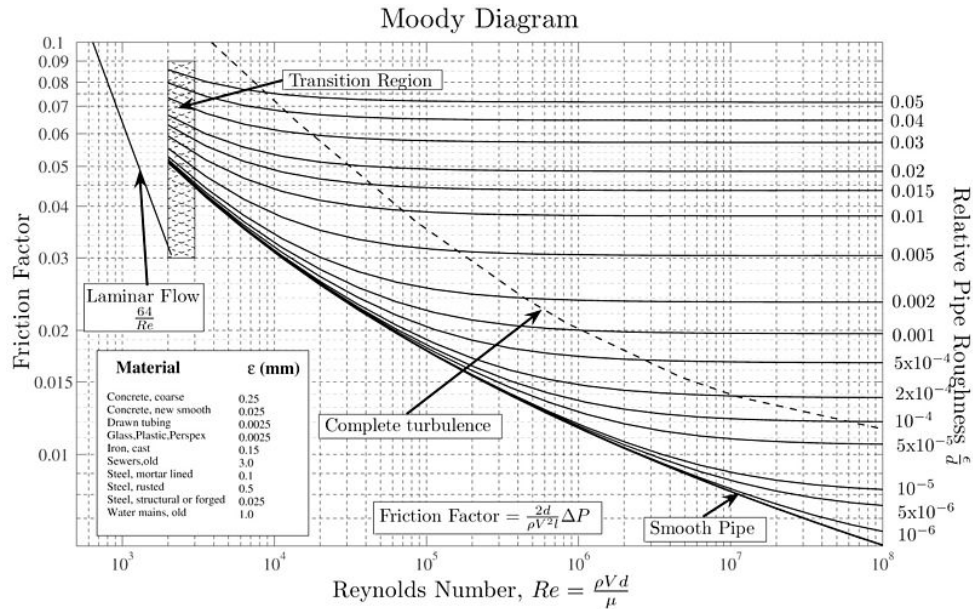


Figure 1.11: Moody diagram

According to Blasius, for values of Reynolds number up to 80,000, the dimensionless friction coefficient can be obtained from:

$$f_d = 0.3164 (Re)^{-\frac{1}{4}} \quad (1.19)$$

$K$  coefficients depends on geometry discontinuities of the pipe(e.g. expansion, reduction or shape) and their values are tabulated [7].

As it will be shown in next paragraphs, in presence of a complex geometry, it could be useful to decompose it in  $n$  parts and applicate to each part this theory. Thus, total pressure drop is calculated as the sum of  $n$  pressure drop, like in eq.(1.20)

$$\Delta p_{drop,tot} = \sum \Delta p_{drop,i} = \sum \frac{1}{2} \xi_i \rho u_i^2 \quad (1.20)$$

In this way it's possible to evaluate parts that present higher pressure losses and, in a design phase, modify them in order to respect pressure losses limits.

In a piston compressor, fluctuating gas velocity  $u_i$  depends on piston movement  $w_z$ , as shown in eq.(1.21)

$$u_i = \frac{A_{piston}}{A_i} w_z \quad (1.21)$$

that represents mass balance equation between pipeline and compressor cylinder without considering valves inertia [8].

## Chapter 2

# PAT Due Project

The aim of this project is the researching of new filter designs that could be reach these goals:

- Improving acoustic performance;
- Not increasing pressure losses down the inlet filter;
- Not increasing too much the size of this filter.

The specific case object of this study is **PAT 49**, commonly called **PAT Due**, shown in Fig. 2.1



Figure 2.1: PAT Due compressor

Table 2.1: PAT Due parameters

| PAT DUE PARAMETERS      |     |
|-------------------------|-----|
| Number of stages [-]    | 2   |
| Number of cylinders [-] | 2   |
| Inlet pressure LP [bar] | 1   |
| Inlet pressure HP [bar] | 3,5 |
| Max pressure Lp [bar]   | 4,5 |
| Max pressure HP [bar]   | 13  |

PAT Due is a two stage-compressor, whose thermodynamic cycle in  $p$ - $v$  diagram is shown in Fig.2.2.

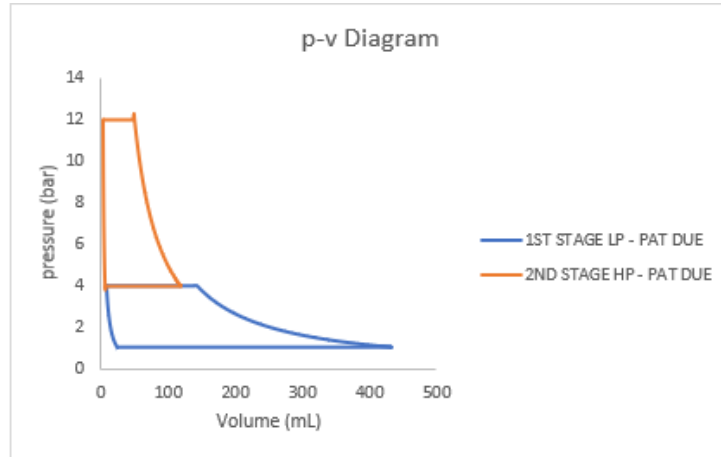


Figure 2.2: PAT Due compressor: P-v diagram

In this chapter pump *PAT Due compressor* input and actual inlet filter characteristics are shown. Moreover, there will be a brief presentation of filter design of previous Thesis about noise performance improvement developed in Abac "*Design of suction filter aimed to noise reduction of reciprocating piston compressor*", called *Noise 1.0 Filter*. All final results will be shown and commented, trying to start new analysis from the further improvements specified at the end of old project.

## 2.1 Air filter

Air filter is an important device, commonly found at air intake of compressor. Air intake filters protect the compressor from any dust and dirt which it might suck in. Dust is a real problem that could be cause wear in compressor element, valves and other parts, deteriorating performance, increasing the maintenance costs and lowering the lifetime of compressor. However, a filtering element could have some positive effects also in noise performance, decreasing noise level respect to a *No filter* situation. One of the purpose of this work is to look for an intake filtering element configuration that combines both cleaning and silencing effects.

*PAT Due Filter* 3D-model is shown in Fig.2.5.

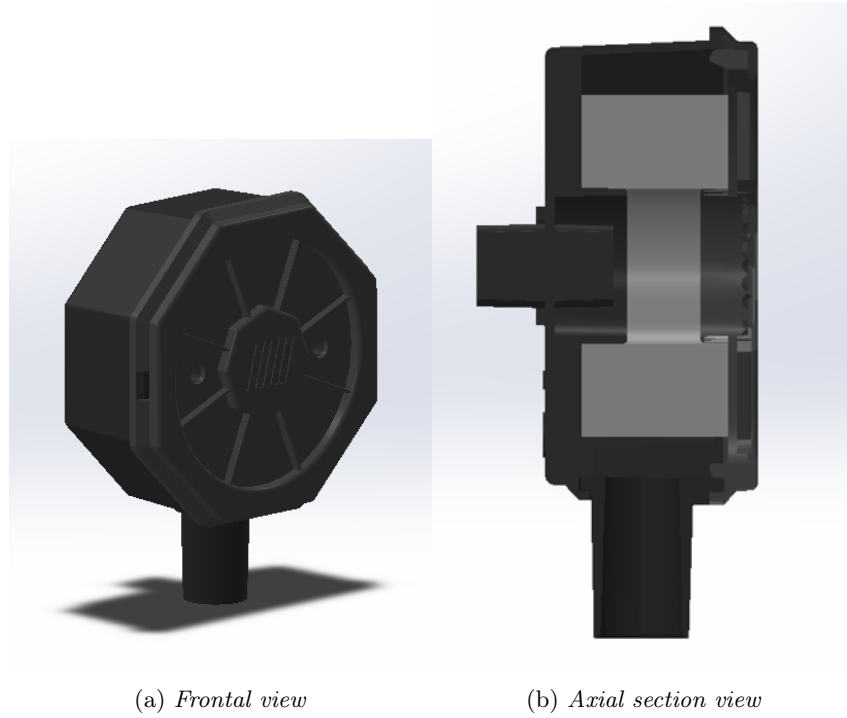


Figure 2.3: Abac Filter: 3D Model

In axial section of *Abac* Filter, there is an absorption element, done in polyester, that has the function to collect impurity and to obstruct its passage inside the compressor chamber. An important problem of filter inserted at air intake is the depression created between environment and compressor, that could affect machine's performance in terms of power and FAD.

**Free air delivery (FAD)** is a common measure of the capacity of an air compressor. It represents the actual quantity of compressed air converted back to the inlet conditions of the compressor and it is expressed in  $m^3/min$ . Considering air delivered and air intake phases:

$$\frac{P_a V_a}{T_a} = \frac{P_1 V_1}{T_1} \quad (2.1)$$

where the subscript  $a$  referred to atmospheric condition, while  $1$  to suction condition.

$$V_a = \frac{P_1}{P_a} \frac{T_a}{T_1} V_1 \quad (2.2)$$



that represent the actual volume of FAD.

FAD is defined in (2.3)

$$FAD = nV_a \quad (2.3)$$

where  $n$  represents compressor running speed in *rpm*. Volumetric efficiency of compressor is computed as the ratio of FAD and volume displacement of pumping group,  $V$

$$\eta_v = \frac{FAD}{V} \quad (2.4)$$

$$V = \frac{\pi D_c^2 s}{4} \frac{N_{stage}}{N_{cylinder}} n \quad (2.5)$$

where:

$D_c$ = Bore diameter;

$s$ = stroke.

Hence an increasing pressure losses in suction cause a reduction of free air delivery and of pump efficiency. The actual filter FAD and pressure drop are shown in Table 2.2.

Table 2.2: Pat Due: Abac Filter

| Parameter     | No filter | Abac filter |
|---------------|-----------|-------------|
| FAD [l/min]   | 531       | 436         |
| Efficiency    | 1         | 0.78        |
| Pressure drop | 0         | 0.24        |

### 2.1.1 Acoustic performance

Two different experimental measurements have done to evaluate noise performance of *Abac* Filter with and without filter. Results of this comparison are reported in the following figure. Lyne markers specify frequencies of one third octave band.

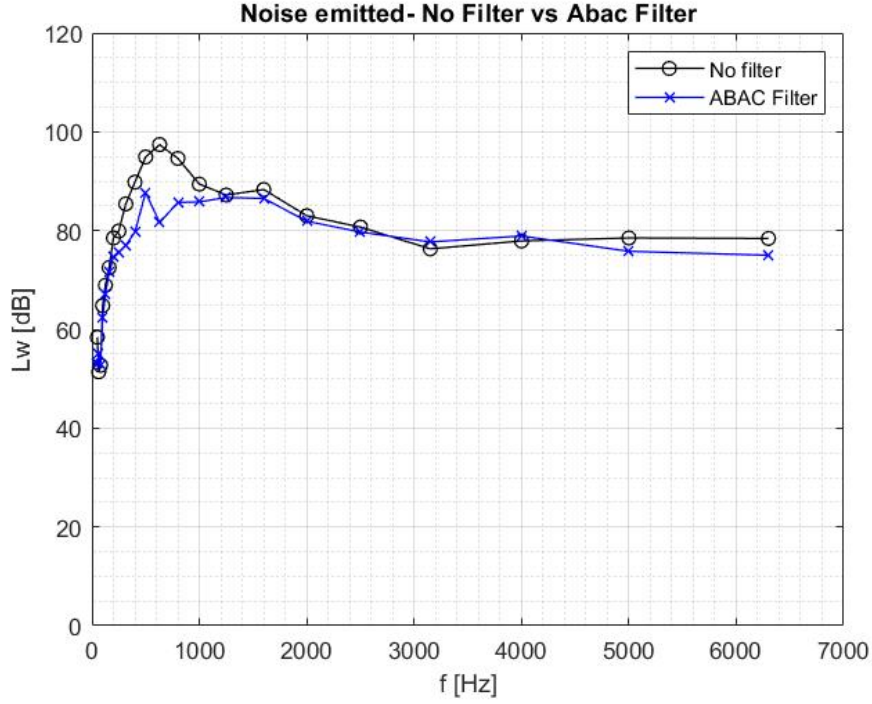


Figure 2.4: No filter vs Abac filter acoustic performance

Thus filtering element is able to decrease noise emitted in a frequency range (500-1000Hz) in which sound power level  $L_w$  is highest in *No filter* configuration. The output of noise analysis, the equivalent sound power level  $L_w(A)$ , shows a reduction of 7.5 dB(A) only inserting an intake filter. This is a great results to indicate the importance of noise reduction at low frequencies.

Table 2.3: Abac Filter: Noise performance

|                 | No Filter | Abac Filter |
|-----------------|-----------|-------------|
| $L_w(A)$ [dBA]  | 101.5     | 94          |
| Reduction [dBA] | -         | -7.5        |

## 2.2 Noise 1.0 Filter

An other important aspect of this Thesis is the comparison between performances of new filters and the filter developed in previous project, *Noise 1.0 Filter*.

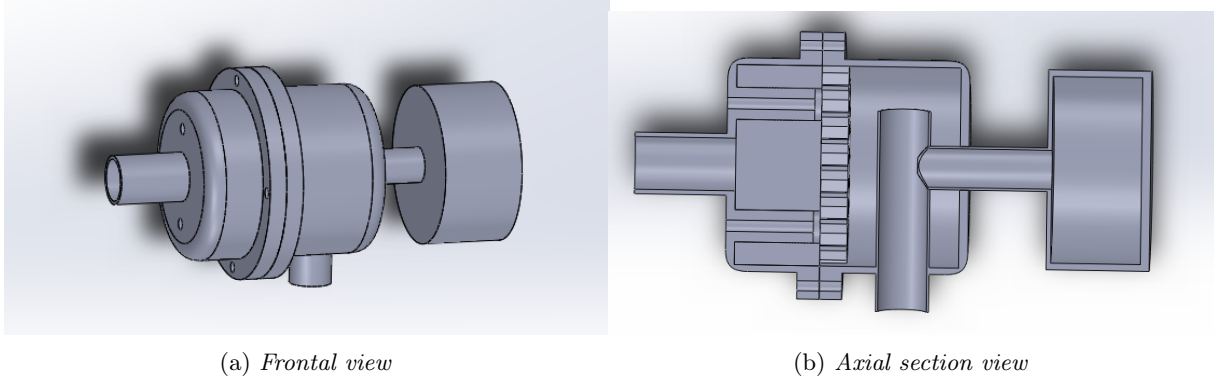


Figure 2.5: Noise 1.0 filter: 3D Model

Experimental results about acoustic performances and pressure losses are reported in the following table.

Table 2.4: Noise 1.0 experimental results

|                     | Noise 1.0 Filter |
|---------------------|------------------|
| $L_W(A)$ [dBA]      | 92.9             |
| Pressure drop (bar) | 0.44             |

- Good acoustic performance because of decreasing of equivalent sound power level respect to Abac Filter. Even if the situation between actual filter and this configuration are similar at high frequencies, this reduction is caused by decreasing of noise in low frequency range (see Fig.2.6)
- Great pressure losses down the filter and consequently bad efficiency of the compressor.

An other aspect to point out is the size of this filter, that is necessary to evaluate if it represents a possible obstruction to structure.

This analysis is made by considering two values: total lenght of the filter  $L_{tot}$  and maximum height  $H$ . In this case this last one corresponds to maximum diameter. A final analysis is reported in Table 2.5. It shows what will be the purpose of new filter configuration, that it would be smaller and have to reduce these great pressure losses, without decreasing the positive effects of noise reduction.

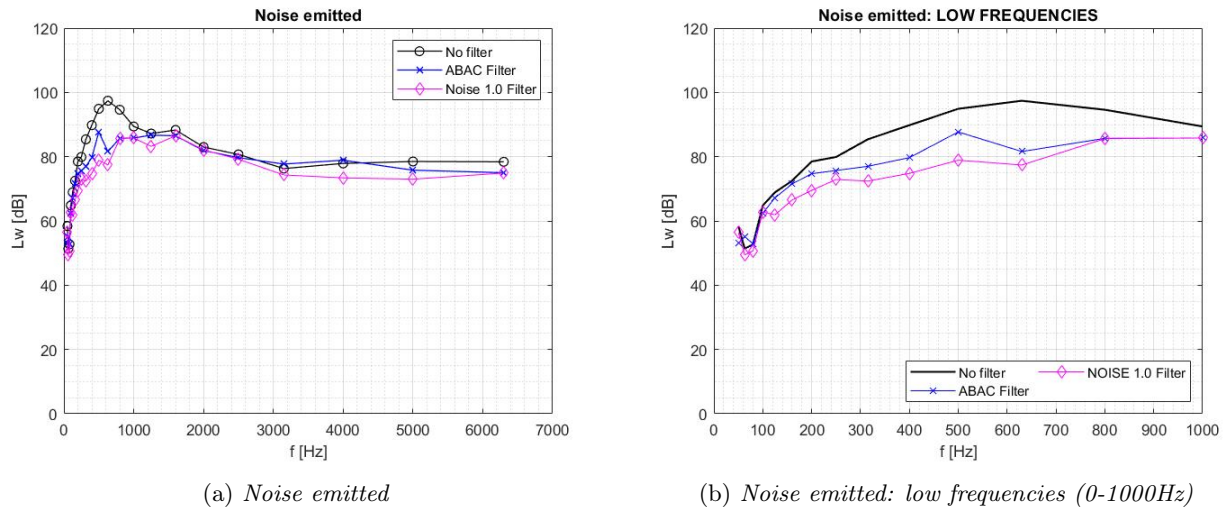


Figure 2.6: Acoustic performances comparison

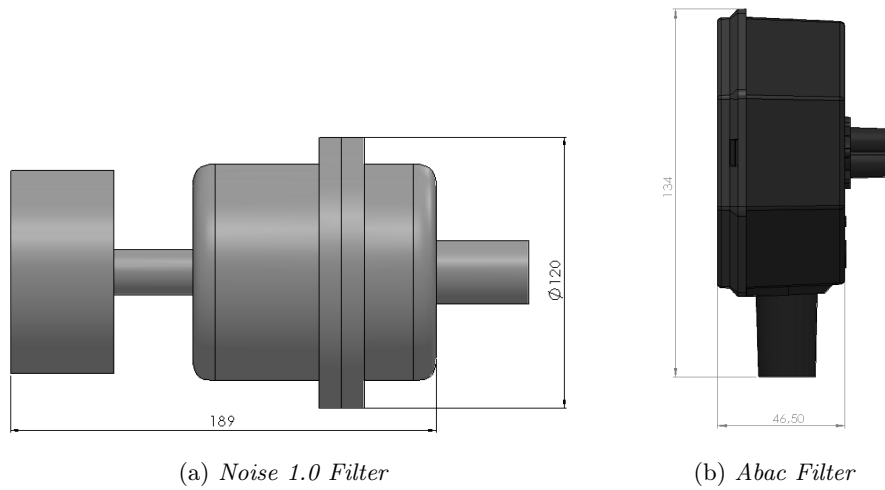


Figure 2.7: Size comparison

Table 2.5: Noise 1.0 filter vs Abac filter

| DESIGN      | NOISE PERFORMANCE | PRESSURE DROP       | SIZE  |                |
|-------------|-------------------|---------------------|-------|----------------|
|             | $L_{w,Aeq}$ [dBA] | Pressure drop (bar) | H(mm) | $L_{tot}$ (mm) |
| Abac filter | 94,9              | 0,24                | 134   | 46,50          |
| Noise 1.0   | 92,9              | 0,44                | 120   | 189            |

## 2.3 Thesis procedure

Before analyzing all mathematical models, it is essential to make a brief summary in which explaining the method that will be used in this dissertation.

More generally it could be distinguish two fundamental steps: **Pressure drop model validation** and **Noise 2.0 Model**.

### 1) Pressure drop model validation

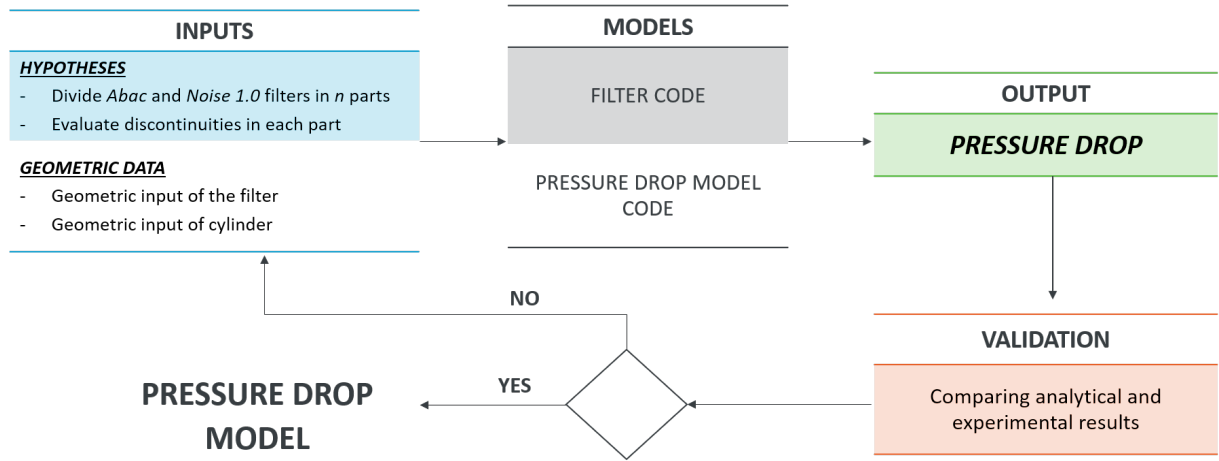


Figure 2.8: Pressure drop model validation

In Fig.2.8 the approach used to reach this first objective is reported. *Inputs* of the model are divided in two subsections: the first represents the hypothesis, while the second the geometric characteristics of filter and pumping group.

*Model part* is also splitted in two different codes: the first calculate local resistance coefficients  $K$  (see (1.18)), which are dependent on geometry of the filter, while the last one gives as output pressure drop diagram, that is dependent on crank angle degree. It is important to point out that model gives others intermediate results as piston velocity  $w_z$  and gas flow velocity  $u_i$ , useful to calculate final pressure drop values. Technically speaking, the model is developed using suite *Matlab/Simulink*.

This model will be applicate to *Abac Filter* and *Noise 1.0 Filter*, because its outputs will be compared to known experimental results. If analytical results will corresponds on experimental results, or if there will be a very little differences between them, so the method could be considered valid. Otherwise, a possible solution could be to modify initial hypotheses.

## 2) Noise 2.0 Model

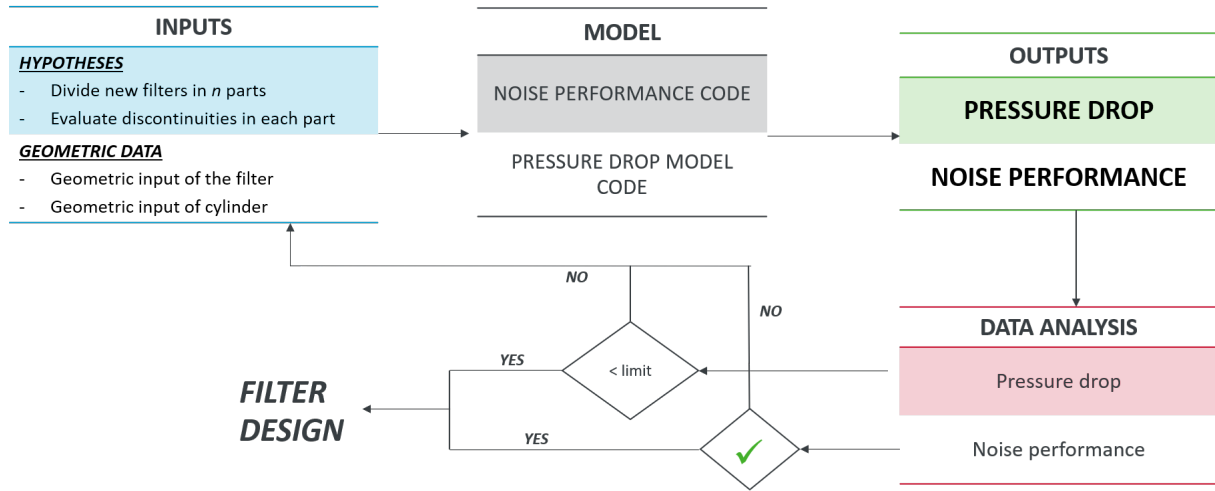


Figure 2.9: Noise 2.0 Model

The second objective of the analysis is the researching of a new model to join acoustical and fluidodynamic performances of new filter configurations.

The inputs of *Noise 2.0 Model* are the same of the previous model. Looking at hypotheses, filter decomposition will be the same both to calculate pressure drop and noise level to ease the correlation of all performances. Two different models to evaluate pressure drop and sound levels have been created. In order to research the best filter solution, output results will be analyze. The limits to accept them are:

- **Noise:** analysis has to guarantee a  $L_w(A)$  reduction respect to previous filters or similar values;
- **Pressure drop:** output has to be less than or equal to a limit, that in this case is in a range between 0,2 and 0,25 bar, like the lowest pressure drop of other filter (Abac and Noise 1.0)

The solution will be considered positive only if both conditions will be respected. Otherwise, a possible solution could be to modify initial hypotheses.

## Chapter 3

# Pressure drop: model validation

Pressure drop model is exposed in the following list.

- Individuate all possible discontinuities in filter geometry and also some cases of different air flow distribution.
- Divide geometry in enough parts  $n$  to best describe filter characteristics. Each part will correspond to a section discontinuity or to a section with a different flow distribution.
- Evaluate flow gas velocity  $u_i$  of each part by using eq. (1.21).

$$u_i = \frac{A_{piston}}{A_i} w_z$$

As mentioned in chapter 1, this velocity depends on piston movement so it will be a time-dependent quantity.

- Calculate Reynold number  $Re$  and then friction coefficient  $f_d$ . In this way *distributed losses* of each filter part are calculated.
- Evaluate all local resistance coefficients  $K$ , depending on geometry. It's possible to import these values from tables, as in example in Fig.3.1. Concentrated losses of each filter part are also known [5].

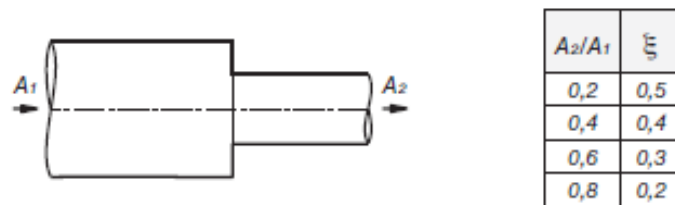


Figure 3.1: Local resistance coefficient

- Total pressure drop is the sum of pressure losses of  $n$  parts (see Eq.(1.20)).

### 3.1 PAT 2: Actual filter

This method is applied to actual filter of *Pat Due* machine, called *Abac Filter*.

Fig.3.2 shows the idea of filter division. A sufficient number of views are used to facilitate the understanding of the characteristics of each part.

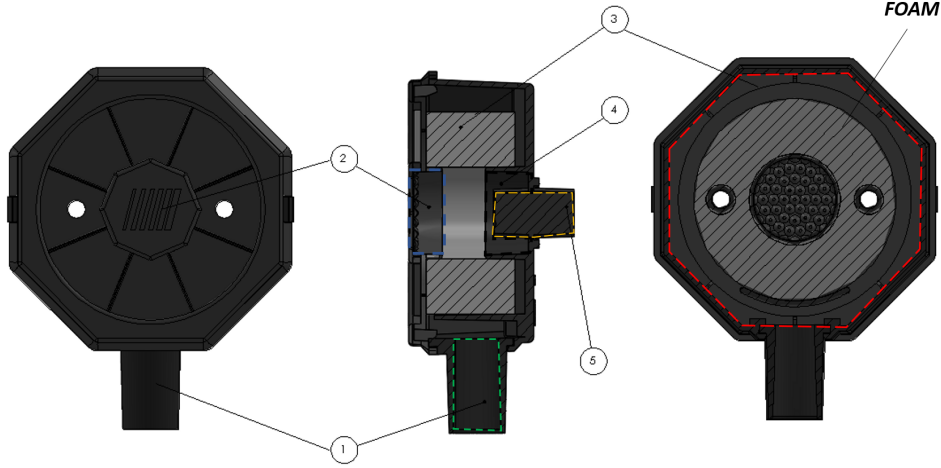


Figure 3.2: Abac filter parts

Flow distribution in *Part 2* is the first aspect to point out before explaining all quantities. In fact, not all air sucked from environment could pass through this sections. To evaluate this distribution the ratio between cross sectional areas  $S_2$  and  $S_3$ , called  $R$ .

The initial hypothesis is the linearity between cross sectional ratio between two inlet parts and mass flow ratio that passes through them. This is possible because it is valid to no consider pressure variation. Hence:

$$R = \frac{S_2}{S_3} = \frac{m_2}{m_3}$$

Filter parts are shown in the following table. The contours of each of them are marked by dotted lines with different colors.

Table 3.1: Description of Abac filter parts

| Part | Color  | Description             | Flow mass         | Balance equation                | Velocity                      |
|------|--------|-------------------------|-------------------|---------------------------------|-------------------------------|
| 1    | Green  | First inlet             | $m_1 = m_{tot}$   | $\rho A_1 u_1 = \rho A_c w_z$   | $u_1 = w_z \frac{A_c}{A_1}$   |
| 2    | Blue   | Pipe                    | $m_2 = R m_{TOT}$ | $\rho A_3 u_3 = R \rho A_c w_z$ | $u_2 = R w_z \frac{A_c}{A_2}$ |
| 3    | Red    | Total optagonal section | $m_3 = m_{tot}$   | $\rho A_3 u_3 = \rho A_c w_z$   | $u_3 = w_z \frac{A_c}{A_3}$   |
| 4    | Black  | Extended pipe           | $m_4 = m_3$       | $\rho A_4 u_4 = \rho A_3 u_3$   | $u_4 = u_3 \frac{A_3}{A_4}$   |
| 5    | Yellow | Outlet pipe             | $m_5 = m_4$       | $\rho A_5 u_5 = \rho A_4 u_4$   | $u_5 = u_4 \frac{A_4}{A_5}$   |

Where  $A_i$  is the cross sectional area of  $i$ -th part.



Instead K-coefficients are reported in Table 3.2

Table 3.2: Local resistance coefficients of Abac Filter

| From..             | To..        | Impedance type |
|--------------------|-------------|----------------|
| <i>Environment</i> | <b>1</b>    | Entrance       |
| <b>1</b>           | <b>3</b>    | Expansion      |
| <i>Environment</i> | <b>2</b>    | Entrance       |
| <b>2</b>           | <b>3</b>    | Porosity       |
|                    |             | Contraction    |
| <b>3</b>           | <b>FOAM</b> | Foam material  |
| <b>3</b>           | <b>4</b>    | Contraction    |
| <b>4</b>           | <b>5</b>    | Contraction    |
|                    |             | Expansion      |
| <b>5</b>           | <b>Head</b> | Expansion      |

### 3.1.1 Foam material

An other important aspect to investigate is the local resistance coefficient of foam material. It may be considered as a porosity material, in which *K-coefficients* depends only on dimensions of the holes.

According to the theory of porosity material, K is defined as:

$$K = [0.707(1 - f)^{0.375} + 1 - f]^2 \frac{1}{f^2} \quad (3.1)$$

where  $f$  represents the porosity of material, that can be evaluate as shown in Fig. 3.3 .

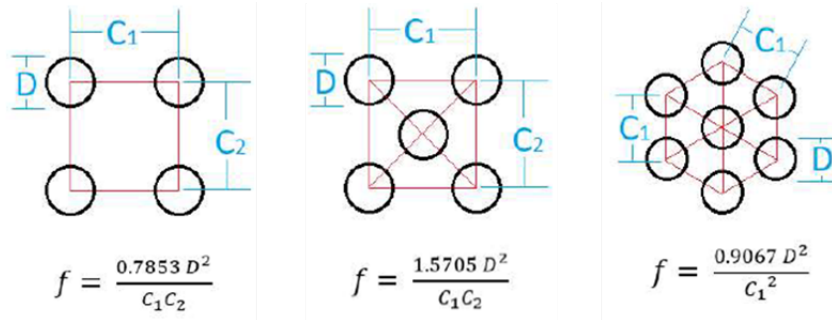


Figure 3.3: Porosity

Thus there two possibilities:

- $f$  represents porosity if porosity of material is known;
- the best hypothesis is that the diameter of each hole is equal to the distance between holes (see right figure in Fig. 3.3):

$$f = \frac{0.9067 D^2}{C_1^2} \approx 0.9067 \approx 0.9$$

### 3.2 Noise 1.0 Filter

Pressure drop model is also applied to *Noise 1.0 Filter*, as shown in Fig.3.4.

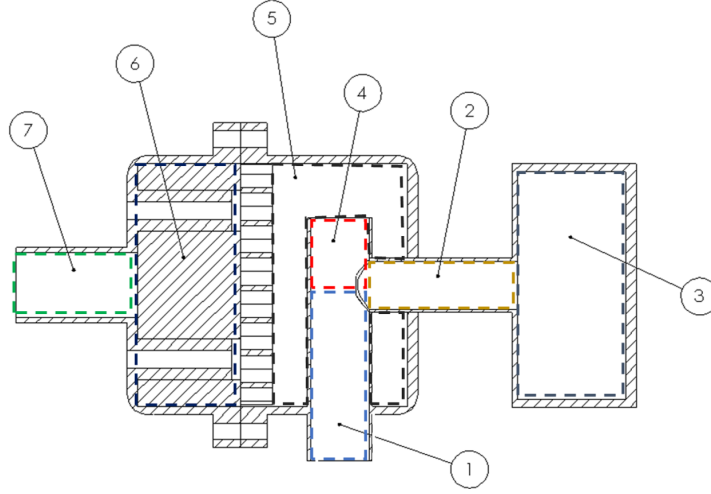
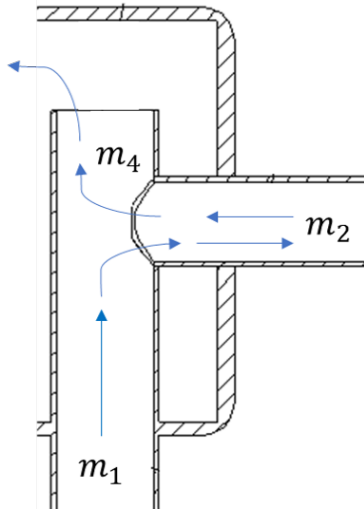


Figure 3.4: Noise 1.0: Filter parts

In this case it's important to point out flow distribution in T-junction between part 4 and part 2 (see Fig 3.5). As explicated in *Abac Filter* the hypotheses of no-pressure changing suggests to consider flow distribution dependent on filter geometry.



X represents the ratio between cross sectional  $S_2$  and  $S_4$ , equal to mass flow ratio in these two parts.

$$X = \frac{S_2}{S_4} = \frac{m_2}{m_4}$$

Y is instead the ratio between total mass and mass of part 2.

$$Y = \frac{m_2}{m_{tot}}$$

$$m_{tot} = m_2 + m_4$$

$$Y = \frac{m_2}{m_2 + m_4} = \frac{m_2}{m_2 + X m_2} = \frac{1}{1 + X}$$

Thus, mass flow distribution is:

$$m_2 = F m_{tot}$$

$$m_4 = (1-F) m_{tot}$$

Figure 3.5: Flow distribution in T-junction

Filter parts are shown in the following table. The contours of each of them are marked by dotted lines with different colors.

Table 3.3: Description of Noise 1.0 filter parts

| Part | Color | Description       | Flow mass                | Balance equation                | Velocity                      |
|------|-------|-------------------|--------------------------|---------------------------------|-------------------------------|
| 1    |       | Inlet pipe        | $m_1 = m_{tot}$          | $\rho A_1 u_1 = F \rho A_c w_z$ | $u_1 = F w_z \frac{A_c}{A_1}$ |
| 2    |       | HR neck           | $m_2 = F m_1$            | $\rho A_2 u_2 = F \rho A_1 u_1$ | $u_2 = F u_1 \frac{A_1}{A_2}$ |
| 3    |       | HR cavity         | $m_3 = m_2$<br>$= F m_1$ | $\rho A_3 u_3 = F \rho A_1 u_1$ | $u_3 = F u_1 \frac{A_1}{A_3}$ |
| 4    |       | Inlet pipe        | $m_4 = m_1$              | $\rho A_4 u_4 = \rho A_1 u_1$   | $u_4 = u_1 \frac{A_1}{A_4}$   |
| 5    |       | Expansion chamber | $m_5 = m_4 = m_1$        | $\rho A_5 u_5 = \rho A_1 u_1$   | $u_5 = u_1 \frac{A_1}{A_5}$   |
| 6    |       |                   | $m_6 = m_5 = m_1$        | $\rho A_6 u_6 = \rho A_1 u_1$   | $u_6 = u_1 \frac{A_1}{A_6}$   |
| 7    |       | Outlet pipe       | $m_7 = m_6 = m_1$        | $\rho A_7 u_7 = \rho A_1 u_1$   | $u_7 = u_1 \frac{A_1}{A_7}$   |

An important filtering element is the **honeycomb stage** between parts 5 and 6, that divides expansion chamber in two different sections. In local resistance calculations it is considered like a porosity material, as *foam material* in part 6.

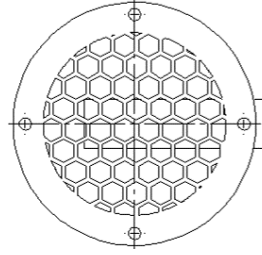


Figure 3.6: Honeycomb stage

Table 3.4: Local resistance coefficients of Noise 1.0 Filter

| From..             | To..             | Impedance type    |
|--------------------|------------------|-------------------|
| <b>Environment</b> | <b>1</b>         | Entrance          |
| <b>1</b>           | <b>2 – 4</b>     | T-junction        |
| <b>2</b>           | <b>3</b>         | Expansion (2-3)   |
|                    |                  | Contraction (3-2) |
| <b>2</b>           | <b>4</b>         | Confluence        |
| <b>4</b>           | <b>5</b>         | Expansion         |
| 5                  | 6                | Honeycomb         |
| 6                  | 7                | Foam material     |
| 6                  | 7                | Contraction       |
| 7                  | Head of cylinder | Expansion         |

### 3.3 Experimental comparison

Analytical and experimental pressure drop values are compared in this section.

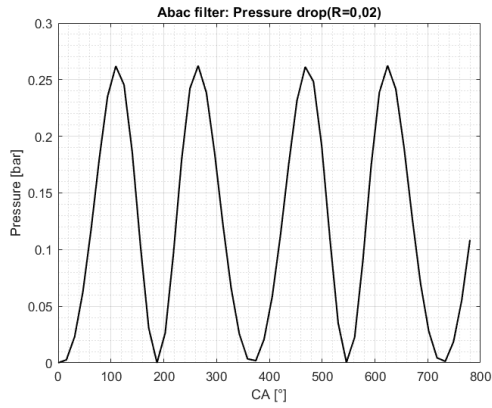
#### Abac Filter

As it has already been mentioned in previous paragraph, pressure model is a time dependent quantity. Particularly, pressure will be dependent on crank angle degree. Moreover, it's possible to have different analysis for different flow distribution in part 2. In this case:

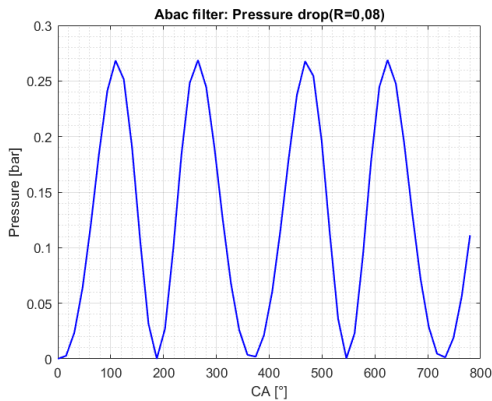
$$R = \frac{S_2}{S_3} = \frac{m_2}{m_3} = 0,08$$

In the following plots analytical results are reported at three values of R:

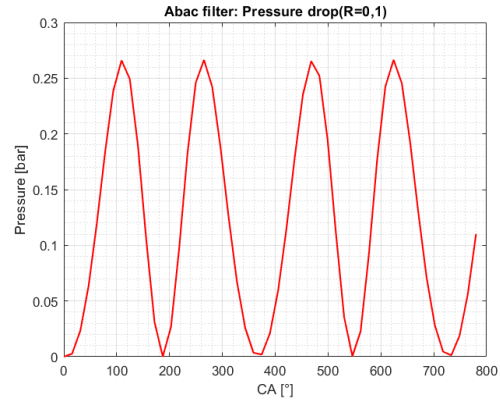
- $R = 0,08$ , that represents the mathematical value calculated;
- $R = 0,02$  and  $R = 0,1$  to evaluate what happens if R increases or decreases.



(a)  $R = 0,02$



(b)  $R = 0,08$



(c)  $R = 0,1$

Figure 3.7: Pressure drop: analytical results

The maximum pressure drop are shown in Table 3.5.

Table 3.5: Maximum pressure drop

| Pressure drop (bar) |        |       |
|---------------------|--------|-------|
| R=0,02              | R=0,08 | R=0,1 |
| 0,26                | 0,27   | 0,27  |

Thus it's possible to evaluate the differences respect to experimental results.

Table 3.6: Experimental vs Analytical results

| CASE                | Pressure drop (bar) | vs Experimental result (%) |
|---------------------|---------------------|----------------------------|
| Experimental result | 0,22                |                            |
| R=0,02              | 0,26                | 15%                        |
| R=0,08              | 0,27                | 18%                        |
| R=0,1               | 0,27                | 18%                        |

### Noise 1.0 Filter

In Noise 1.0 filter there is a flow distribution in T-junction between section 1,2 and 4. X and Y values are:

$$X = \frac{S_2}{S_4} = \frac{m_2}{m_4} \approx 1$$

$$Y = \frac{1}{1 + X} \approx 0.5$$

In the following plots analytical results are reported at two values of Y:

- $Y = 0,5$ , that represents the mathematical value that has been calculated;
- $Y = 0,55$  and to evaluate what happens if Y changes.

The maximum pressure drops are shown in Table 3.7

Table 3.7: Noise 1.0: Maximum pressure drop

| Pressure drop (bar) |        |
|---------------------|--------|
| Y=0,5               | Y=0,55 |
| 0,42                | 0,44   |

Thus it's possible to evaluate the difference to experimental result.

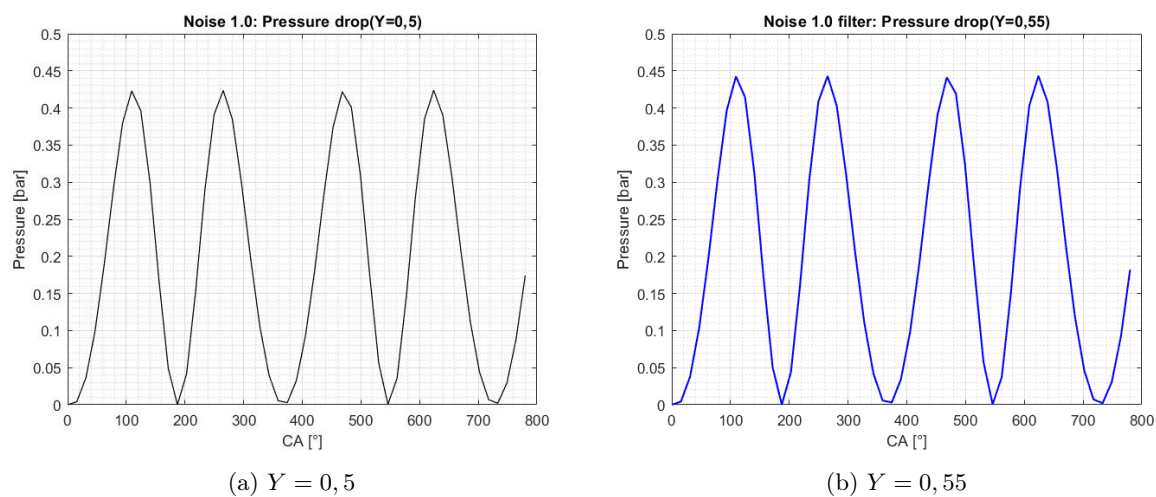


Figure 3.8: Noise 1.0 Filter: Pressure drop

Table 3.8: Noise 1.0: Experimental vs Analytical results

| CASE                 | Pressure drop (bar) | vs Experimental results |
|----------------------|---------------------|-------------------------|
| Experimental results | 0,44                |                         |
| $Y=0,5$              | 0,42                | 4%                      |
| $Y=0,55$             | 0,44                | -                       |

Analytical data are really closed to experimental. It means that the initial hypothesis can be considered acceptable to reach model validation.

### 3.4 Comments

This chapter is fundamental to guarantee that the positive effects of noise attenuation of a silencer correspond also to a no-decreasing of machine's performances. In fact, the principal aim is to create a model that can control pressure losses in each part of the filter.

This model could be considered valid only if its output results are compared positively to experimental results. In this case, it needs to applicate pressure drop model to previous filters, because their experimental data are known.

At the end of this chapter, it's possible to claim that pressure model analysis made in this Thesis project could be used also in the other filter designs that will be developed.

Expecially in *Noise 1.0 Filter* the differences between analytical and experimental data are really small, so the hypotheses of linearity and local coefficients are considered acceptable.

In *Abac Filter*, instead, errors between two analysis are larger. It is an expectative result because flow distribution is more uncertain than the other case and because probably pressure distribution in the considered part is not equal to environment. Moreover, filter geometry is complex, so decomposition and calculation of discontinuities could be not exact. Although, the method gives outputs that are considered positive and not too far from experimental results.

Starting from this conclusion, pressure drop model is considered valid and it will be used also to calculate pressure drop in new designs that will be presented in *Chapter 5*.

## Chapter 4

# Noise performance model

The model and the elements used to noise attenuation are reported in this chapter. Particularly, the following list summarize what it will be studied to evaluate acoustic performance of filters:

- Brief summary of silencers types (reactive or dissipative);
- Explanation of *Transfer Matrix Method*;
- Illustration of each filter parts used in this dissertation.

### 4.1 Silencer general information

A silencer is an important noise control element for reduction of a noise source involving flow of a gas. It may be defined as a device that acts to reduce the sound transmitted along a duct without obstructing gas flow passage [9]. Silencing devices are classified in two different types:

- **Reactive silencers:** consist typically of several pipe segments that interconnect a number of larger diameter chambers. These silencers reduce radiated acoustical power by reflecting back pressure waves, caused by geometry discontinuities. Thus, they permit to control acoustic performance only evaluating noise attenuation level of each filter geometry.
- **Absorptive silencers:** these silencers use an a absorption material. As sound waves pass through the fibers of the absorptive material, the sound energy decreases into small amounts of heat. The noise is absorbed by the packing material, thus others methods to reduce it (as geometry changing) are not very important.

In this Thesis project reactive silencers are considered. The aim is to reach a filter geometry composed by different silencer shapes so that reducing sound power level. For this purpose, the methos used is **Transfer Matrix Method**, which will be explained in next section.



## 4.2 Transfer Matrix Method

**Transfer Matrix Method (TMM)** uses the transfer matrix of a silencer element as a function of the element geometry (diameter, length), state variables of the medium (density, sound velocity), mean flow velocity, and properties of duct liners (if any). The description of TMM can be found in [10].

It's possible to explain this method starting from the theory of plane waves propagation in a rigid straight pipe having length  $L$ , constant cross section  $S$ , where a turbulent incompressible mean flow of velocity  $V$  pass through.

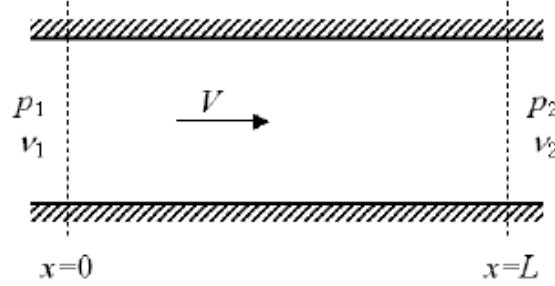


Figure 4.1: Plane wave propagation in straight pipe

Others parameters could influence this method, as higher order modes and temperature gradients. They are neglected in this analysis but they could affect the accuracy of results.

The following is a list of parameters useful to explain TMM:

$p_i$ : acoustical pressure at  $i$  th location;

$c$ : sound velocity

$u$ : flow velocity

$M$ : Mach number defined as  $\frac{u}{c}$  ;

$k_0$ :  $\frac{2\pi f}{c}$ ;

$k_c$ :  $\frac{k_0}{1 - M^2}$ ;

$S_i$ : cross section of  $i$ -th element;

$\rho$ : air density;

Plane waves propagation of Fig.4.1 may be represented as the sum of left and right waves. Using the impedance analogy, the sound pressure  $p$  and volume velocity  $v$  at positions 1 ( $x=0$ ) and 2 ( $x=L$ ) can be related by:

$$p_1 = Ap_2 + Bv_2 \quad (4.1)$$

$$v_1 = Cp_2 + Dv_2 \quad (4.2)$$

where  $A, B, C, D$  are the four **pole constants**, that in the case of a straight pipe are defined as in [11]:

$$A = \exp(-jMk_cL) \cos(k_cL) \quad (4.3)$$

$$B = -j(\rho c/S) \exp(-jMk_cL) \sin(k_cL) \quad (4.4)$$

$$C = -j(S/\rho c) \exp(-jMk_c L) \sin(k_c L) \quad (4.5)$$

$$D = \exp(-jMk_c L) \cos(k_c L) \quad (4.6)$$

Eq. (4.1) and (4.2) can be represented in matrix form as:

$$\begin{bmatrix} p_2 \\ v_2 \end{bmatrix} = \begin{bmatrix} A & B \\ C & D \end{bmatrix} \begin{bmatrix} p_1 \\ v_1 \end{bmatrix}$$

This matrix can be expressed also in the form:

$$\begin{bmatrix} p_2 \\ \rho_0 S_2 \end{bmatrix} = \begin{bmatrix} T_{11} & T_{12} \\ T_{21} & T_{22} \end{bmatrix} \begin{bmatrix} p_1 \\ \rho_0 S_1 \end{bmatrix} \quad (4.7)$$

where  $\begin{bmatrix} T_{11} & T_{12} \\ T_{21} & T_{22} \end{bmatrix}$  represent the **Transfer Matrix**.

Referring to example of Fig. 4.1, the transfer matrix of a straight pipe is:

$$T_{pipe} = \exp(-jMk_c L) \begin{bmatrix} \cos(k_c L) & Y_i \sin(k_c L) \\ \frac{1}{Y_i} \sin(k_c L) & \cos(k_c L) \end{bmatrix}$$

where:

$$Y_i = \frac{c}{S_i}$$

The importance of this method is that it depends only on geometry and flow conditions, so each element may be described by its transfer matrix. Thus the idea is to decompose each complex geometry in some simple elements and applicate Transfer Matrix Method.

In general, matrix in eq. (4.7) may be expressed in this form:

$$\begin{bmatrix} p_{i+1} \\ \rho_0 S_{i+1} \end{bmatrix} = \begin{bmatrix} T_{11} & T_{12} \\ T_{21} & T_{22} \end{bmatrix} \begin{bmatrix} p_i \\ \rho_0 S_i \end{bmatrix} \quad (4.8)$$

And it could be applied to multiple sections, as in Fig. 4.2

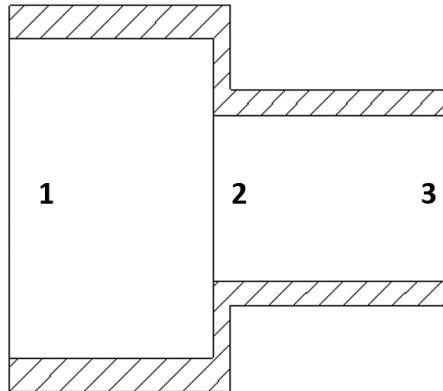


Figure 4.2: Plane wave propagation in more elements

In fact, considering Transfer Matrices of 2 and 3

$$\begin{bmatrix} p_2 \\ \rho_0 S_2 \end{bmatrix} = \begin{bmatrix} T_{11} & T_{12} \\ T_{21} & T_{22} \end{bmatrix} \begin{bmatrix} p_1 \\ \rho_0 S_1 \end{bmatrix} = T^{(1)} \begin{bmatrix} p_1 \\ \rho_0 S_1 \end{bmatrix}$$

$$\begin{bmatrix} p_3 \\ \rho_0 S_3 \end{bmatrix} = \begin{bmatrix} T_{11} & T_{12} \\ T_{21} & T_{22} \end{bmatrix} \begin{bmatrix} p_2 \\ \rho_0 S_2 \end{bmatrix} = T^{(2)} \begin{bmatrix} p_2 \\ \rho_0 S_2 \end{bmatrix} = T^{(1)} T^{(2)} \begin{bmatrix} p_1 \\ \rho_0 S_1 \end{bmatrix}$$

Thus Transfer Matrix is a **linear** method. In fact,

$$T = T^{(1)} T^{(2)} \dots T^{(n)} = \prod_{i=1}^n T^{(i)} \quad (4.9)$$

where  $n$  represents the number of elements of the geometry.

Then Transfer Matrix of two subsystems useful in this Thesis can be represented analytically as follow.

- **Continuities sections:**

$$T_{pipe} = \exp(-jMk_c L) \begin{bmatrix} \cos(k_c L) & Y_i \sin(k_c L) \\ \frac{1}{Y_i} \sin(k_c L) & \cos(k_c L) \end{bmatrix}$$

- **Discontinuities sections:**

$$T_{disc} = \exp(-jMk_c L) \begin{bmatrix} 1 & 0 \\ \frac{j}{Y_i \cot(k_c L)} & 1 \end{bmatrix}$$

In this case  $Y_i = \frac{c}{S_i - S_{i-1}}$

#### 4.2.1 Transmission loss

Transmission loss is the parameter chosen to evaluate acoustics performance of the filter.

**Transmission loss (TL)** in acoustics is defined as the difference between the power incident on a acoustic device (silencer) and that transmitted downstream into an anechoic termination. It is a quantity independent of the source and requires an anechoic termination at the end. Transmission loss is expressed in dB

$$TL(dB) = L_{w,in} - L_{w,out} = 10 \log_{10} \frac{S_i p_i^2}{S_o p_o^2} \quad (4.10)$$

In lot of applications, inlet and outlet pipes have the same cross sectional areas, so eq. (4.10) can be reduced in:

$$TL(dB) = 20 \log_{10} \frac{p_i}{p_o} \quad (4.11)$$

Each system can be described by its transmission matrix (or four-pole matrix), as in eq. (4.7). With this representation it can prove that Transmission loss of each subsystem can be calculated

as:

$$TL(dB) = 20 \log_{10} \left| \frac{T_{11} + T_{12}/Y_i + T_{12}Y_o + T_{22}}{2} \right| \quad (4.12)$$

or alternatively using four pole matrix the equivalent TL is:

$$TL(dB) = 10 \log_{10} \left| \frac{1}{4}A + B \frac{S_i}{\rho c} + C \frac{\rho c}{S_o} + D \right| \quad (4.13)$$

where pedix  $i$ ,  $o$  are referred to inlet and outlet pipe.

### 4.3 Helmholtz Resonator

Theory of Helmholtz resonator is shown in [12] and [13].

Helmholtz resonance is widely known as the phenomenon of air resonance in the cavity or chamber that contains a gas. The name comes from a device created in the 1850s by Hermann Ludwig Ferdinand von Helmholtz. The **Helmholtz resonator** consists of an enclosed volume of air, called **cavity**, communicating with the outside (noise source) through a small opening, called **neck** of the resonator. The schematic simple Helmholtz resonator geometry is shown in Fig. 4.3

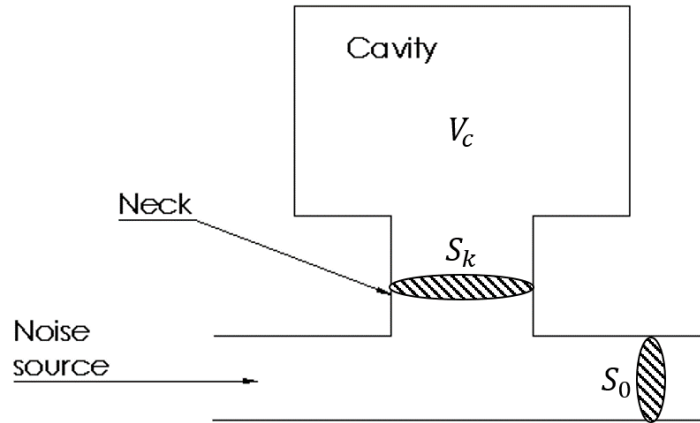


Figure 4.3: Helmholtz resonator

At a specific frequency, called **resonance frequency**  $f_r$  the cavity will resonate and the waves in the exhaust pipe are reflected back towards the source. It depends on the volume of the cavity and the geometry of neck, properly sized to tune this frequency to a specified value.

A Helmholtz resonator produces sound frequencies by a method analogous to the oscillation of a mass-spring oscillator. In fact, when air is forced into the cavity, the pressure in the cavity is increased and more air will be expelled out of the resonator than necessary. Hence, the pressure inside the resonator  $p$  will now be less than the pressure outside  $p_0$  and in order to compensate the pressure differences, more air will be sucked into the cavity. In this way gas within the volume of the resonator is alternately compressed and expanded and this process repeats until the system finally reaches pressure equilibrium. This movement of air into and out

of the resonator is identical to the movement of a spring along the vertical axis, where air in neck behaves as a discrete mass, while the air in the cavity has the role of a spring.

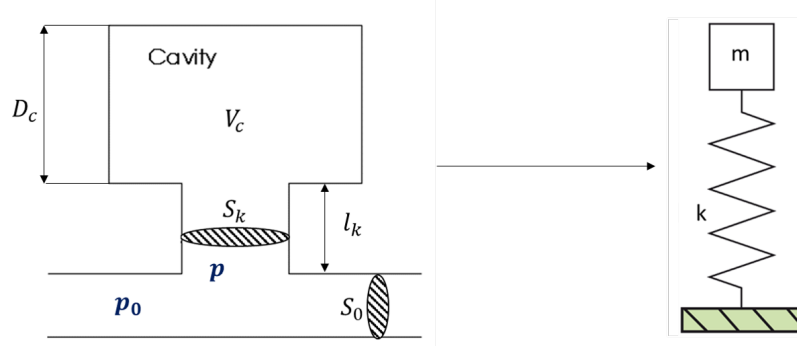


Figure 4.4: HR and mass-spring oscillation

The correspondence between sound frequency and mass-spring oscillator is evident in frequency resonance definition. Considering a mass balance  $F = ma$ :

$$a = \frac{dx^2}{dt^2} = \frac{F}{m} \quad (4.14)$$

where  $m$  is the mass,  $a$  the acceleration and  $x$  the displacement of the spring.

Using the hypothesis of adiabatic system with air as an ideal gas:

$$\frac{p}{p_0} = \gamma \frac{\Delta V_c}{V_c} \quad (4.15)$$

where  $p$  is the pressure of resonator,  $p_0$  is the output pressure and  $V_c$  the volume of cavity. The change in volume of cavity is:

$$\Delta V_c = -S_k x \quad (4.16)$$

where  $S_k$  is the neck cross section of cavity and  $x$  is the displacement.

The force can be expressed as a product of pressure  $P$  and cross sectional area  $S_k$ . Considering eq. (4.14), (4.15) and (4.16):

$$F = P S_k = \gamma \frac{S_k^2 x p_0}{V_c} \quad (4.17)$$

Referring to the solution of (4.14) and the definition of  $\omega$ :

$$x(t) = e^{-i\omega t} \quad (4.18)$$

$$\omega = 2\pi f \quad (4.19)$$

It is calculated the force in the following form:

$$F = \gamma \frac{S_k^2 p_0}{V_c} e^{-i\omega t} \quad (4.20)$$

The mass of resonator  $m$  is instead dependent on the geometry of the neck

$$m = \rho S_k l_k \quad (4.21)$$

where  $l_k$  is the length of the neck  $F$  and  $m$  equation are substituted in (4.14).

$$\frac{dx^2}{dt^2} = (i\omega^2)e^{-i\omega t} = \gamma \frac{S_k^2 p_0}{V_c \rho S_k l_k} e^{-i\omega t} = \gamma \frac{S_k p_0}{V_c \rho l_k} e^{-i\omega t} \quad (4.22)$$

$$\omega^2 = \gamma \frac{S_k p_0}{V_c \rho l_k} \quad (4.23)$$

The sound velocity  $c$  is defined as:

$$c = \sqrt{\gamma \frac{p_0}{\rho}} \quad (4.24)$$

And eq. (4.23) can be expressed as:

$$\omega^2 = c^2 \frac{S_k}{V_c l_k} \quad (4.25)$$

That can be compared to  $\omega^2$  of mass-spring oscillation

$$\omega^2 = \frac{k}{m} \quad (4.26)$$

to evaluate the equivalent parameters of sound frequency analysis

$$m = \rho S_k l_k$$

$$k = \frac{\rho c^2 S_k^2}{V_c} \quad (4.27)$$

Combining (4.25) and (4.19)

$$f_r = \frac{c}{2\pi} \sqrt{\frac{S_k}{V_c l_k}} \quad (4.28)$$

$f_r$  represents the **resonance frequency** of Helmotz resonator.

### 4.3.1 Transmission loss: Helmotz resonator

Transfer Matrix Method is used to calculated Transmission Loss of an Helmotz resonator between point 1 and 2 in Fig. 4.5

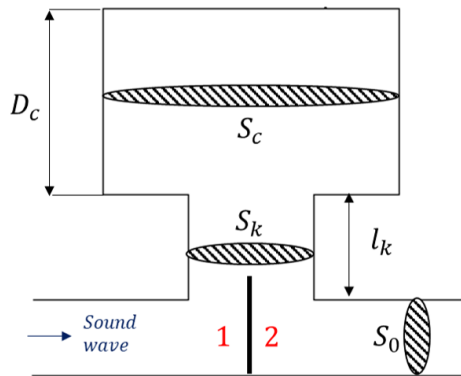


Figure 4.5: Helmotz resonator: sound wave propagation

In terms of acoustic impedance, the Transfer Matrix of a simple Helmotz resonator is expressed in following matrix equation:

$$\begin{bmatrix} p_2 \\ V_2 \end{bmatrix} = \begin{bmatrix} 1 & 0 \\ \frac{1}{-jZ_c \cot(kl_c) + Z_h} & 1 \end{bmatrix} \begin{bmatrix} p_1 \\ V_1 \end{bmatrix} \quad (4.29)$$

where:

$Z_c = \frac{\rho c}{S_c}$  represents acoustic impedance of a resonator's cavity;

$Z_h$  = impedance of the hole (experimental results)

And TL can be calculated as:

$$TL(dB) = 20 \log_{10} \left| \frac{T_{11} + T_{12}/Z + T_{12}Z + T_{22}}{2} \right| \quad (4.30)$$

where  $Z = \frac{\rho c}{S_0}$  is the tube impedance.

In a more simple way, it is demonstrated that Transmission Loss of an Helmotz resonator could be calculated as:

$$TL(dB) = 10 \log_{10} \frac{1 + \frac{\sqrt{\frac{V_c S_k}{l_k}}}{2S_0}}{\left(\frac{f}{f_r} - \frac{f_r}{f}\right)^2} \quad (4.31)$$

which it will be used in noise analysis in this dissertation.

A common TL plot is reported in the following figure, where the peak of TL amplitude is at resonance frequency.

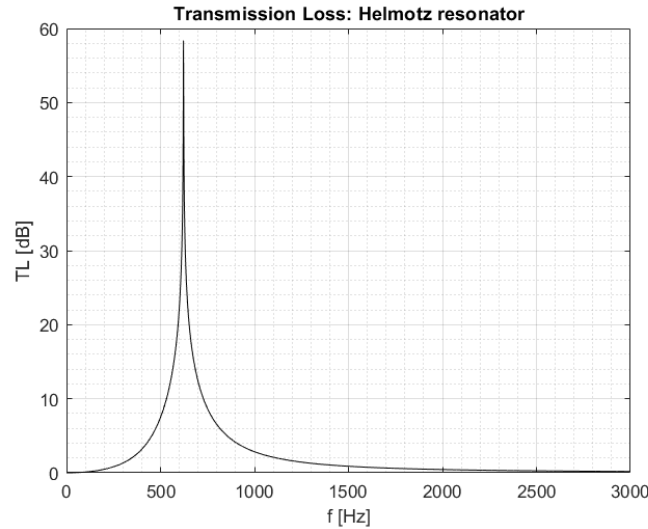


Figure 4.6: Transmissison loss of Helmotz resonator

Helmholtz resonators are typically used to attenuate sound pressure when the system is originally at resonance. Thus it could be interesting to make a sensitivity analysis on Helmotz resonator parameters when resonance frequency  $f_r$  is fixed.

These parameters are:  $V_c$ ,  $S_k$  and  $l_k$  and each time one of them is fixed, while the others change.

### Lenght of neck $l_k=\text{constant}$

In this first case,  $l_k$  is constant,  $S_k$  and  $V_c$  are variables. Particularly the parameter that changes is the cross sectional area of the neck and consequently changes also the volume of cavity to guarantee  $f_r$  constant.

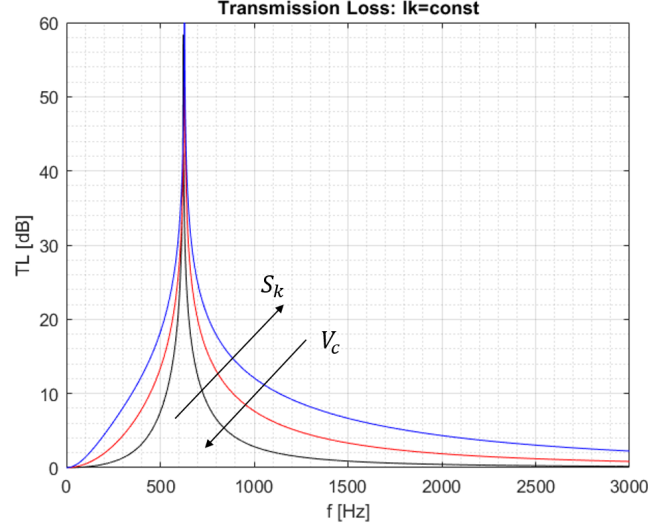


Figure 4.7: Influence of HR parameters:  $l_k=\text{const}$

Thus if  $S_k$  increases, TL curve become "wider" and then noise attenuation is higher also at frequency that precede or succeed resonance frequency.

### Cross sectional area of the neck $S_k=\text{constant}$

The parameter that changes is the lenght of the neck  $l_k$  and consequently changes the volume of the cavity  $V_c$  to guarantee  $f_r$  constant.

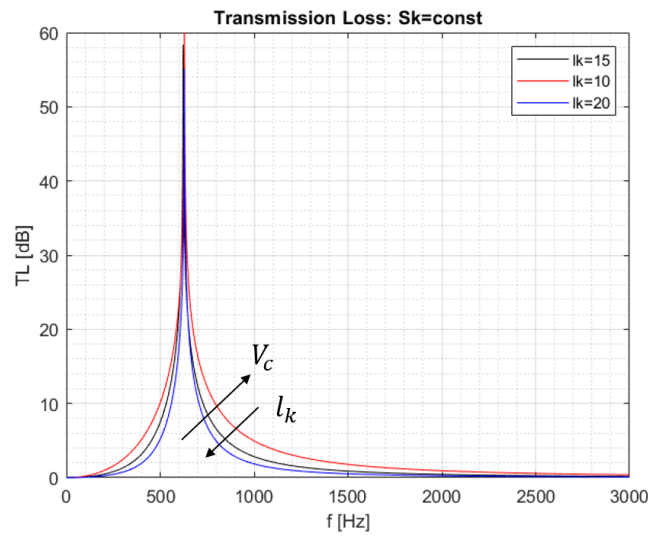


Figure 4.8: Influence of HR parameters:  $S_k=\text{const}$



### Volume of the cavity $V_c = \text{constant}$

The parameter that changes is the length of the neck  $l_k$  and consequently changes the cross sectional area of the neck  $S_k$  to guarantee  $f_r$  constant.

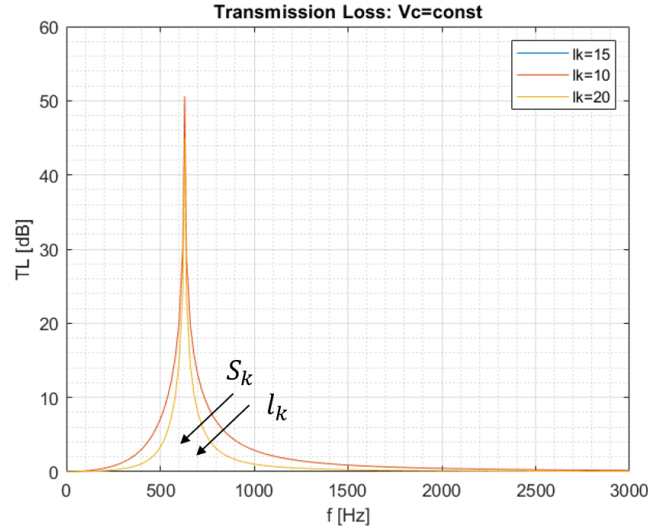


Figure 4.9: Influence of HR parameters:  $V_c = \text{const}$

The influence of  $l_k$  is evident in analytical model only if the variation is high. In the example of Fig. 4.9 there are difference in TL amplitude only if  $l_k$  is twice than an other. Thus, this case is not interesting as the other that it has been reported.

These sensitivity results will be very important to choose the correct combination of all parameters in design phase, reported in next chapters.

### 4.3.2 From Helmholtz resonator to perforated tube

In some cases, for low duct porosity, Helmholtz resonator model can be applied also to a perforated tube. The perforations and the outer chamber can be considered as a neck and a cavity, respectively. Instead, the length of the neck  $l_k$  is the perforated duct wall thickness  $t_w$ .

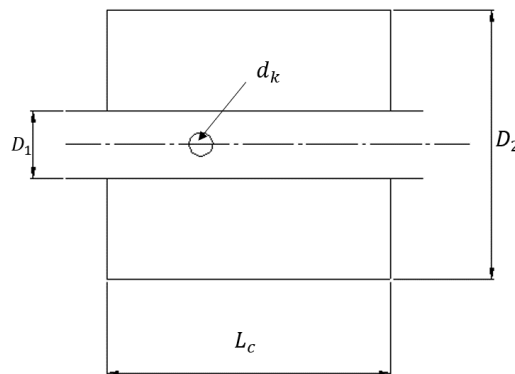


Figure 4.10: Perforated tube

A brief summary of connections between Helmotz model and perforated tube is reported in the following table.

Table 4.1: Helmotz resonator vs Perforated tube

| Helmotz resonator | Perforated tube                     |
|-------------------|-------------------------------------|
| $V_c$             | $\pi \frac{(D_2^2 - D_1^2)}{4} L_c$ |
| $l_k$             | $t_w$                               |

where:

$D_2$ : outer diameter;

$D_1$ : inner diameter.

And then, the equivalent resonance frequency of a perforated tube.

$$f_{r,p} = \frac{c}{2\pi} \sqrt{\frac{S_k}{(\frac{\pi(D_2^2 - D_1^2)}{4})t_w}} \quad (4.32)$$

The use of a perforated pipe as silencer element could be interesting in some applications in which a resonator is connected to an expansion chamber having the same outer diameter  $D_2$  and an inner pipe having the same diameter  $D_1$ . In this way size of silencer is more compact and a small porosity of the pipe reduces flow distribution and pressure drop inside the neck of the resonator.

## 4.4 Expansion chamber

The most simple reactive silencer is the single **expansion chamber** (cross-sectional area  $S_2$  and length  $L$ ) with an inlet and outlet pipe both having cross-sectional area  $S_1$ .

A schematic single expansion chamber geometry is shown in Fig. 4.11

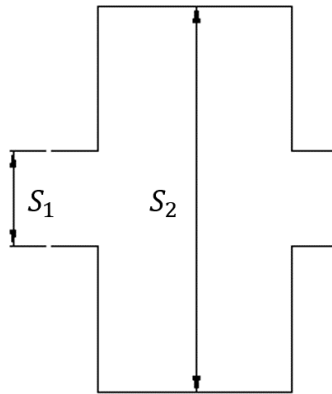


Figure 4.11: Single expansion chamber

The chamber is considered as a tube having a cross sectional area  $S_2$ , so its transfer matrix is defined as:

$$T_{EC} = \exp(-jMk_cL) \begin{bmatrix} \cos(k_cL) & Y_2 \sin(k_cL) \\ \frac{1}{Y_2} \sin(k_cL) & \cos(k_cL) \end{bmatrix} \quad (4.33)$$

where  $Y_2 = \frac{c}{\pi R_2^2}$ .

According to eq. (4.12), Transmission Loss of a single expansion chamber is calculated as follow:

$$TL(dB) = 20 \log_{10} \left| \frac{\cos(k_cL) + \frac{Y_2}{Y_1} \sin(k_cL) + \frac{Y_1}{Y_2} \sin(k_cL) + \cos(k_cL)}{2} \right| \quad (4.34)$$

Substituting to the above equation TL of this simple reactive silencer is also expressed by:

$$\begin{aligned} TL(dB) &= 10 \log_{10} \left( \frac{\cos(k_cL) + \frac{Y_2}{Y_1} \sin(k_cL) + \frac{Y_1}{Y_2} \sin(k_cL) + \cos(k_cL)}{4} \right)^2 \\ &= 10 \log_{10} \left( \cos^2(k_cL) + \frac{1}{4} \left( m + \frac{1}{m} \right) \sin^2(k_cL) \right) \end{aligned} \quad (4.35)$$

where  $m = \frac{S_2}{S_1}$  is the ratio between chamber and inlet(or outlet) pipe cross sectional areas.

Eq. (4.34) and (4.35) doesn't consider effects of flow velocity ( $M=0$ ).

TL amplitude graphic is shown in Fig. 4.12.

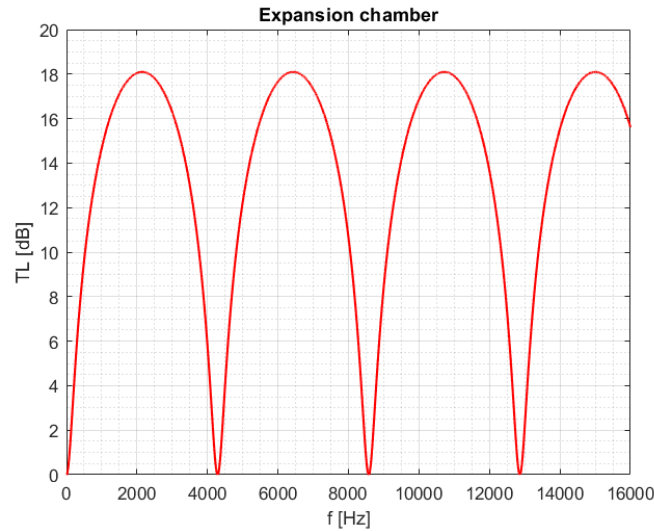


Figure 4.12: Transmission loss: single expansion chamber

Results are reported in a very high frequency range(0-16000Hz) to evaluate better all expansion chamber parameters. Geometric input of this example are:

Table 4.2: Example: Expansion chamber parameters

| Expansion chamber parameters |    |
|------------------------------|----|
| $D_2(\text{mm})$             | 80 |
| $L(\text{mm})$               | 40 |

Considering the above figure, it's important to point out:

- **Cut off frequency  $f_c$** , that represents the frequency in which TL amplitude is zero. It is defined consider (4.35) equal to zero.

$$f_c = \frac{nc}{2L} \quad (4.36)$$

where  $n$  is an integer number to evaluate the multiple of first cut off frequency.

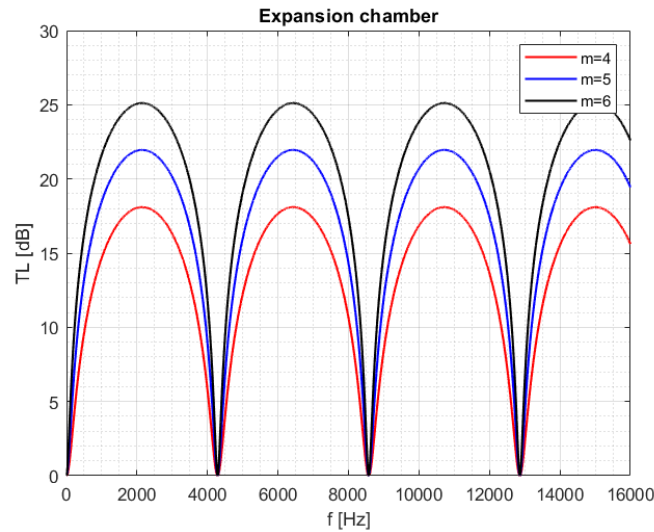
- **Frequency of TL peaks  $f(TL_{max})$** , that represents the frequency in which TL amplitude is maximum. It is defined considering the derivative of eq. (4.35) equal to zero.

$$f(TL_{max}) = \frac{c}{4L} + \frac{nc}{2L} \quad (4.37)$$

Even in this case it could be interesting make a sensitivity analysis on parameters of Expansion chamber:  $m$  and  $L$ .

### Influence of $m$

From the example in Fig.4.12, TL amplitude of various  $m$  are shown.


 Figure 4.13: Influence of  $m$ 

The peak of TL amplitude increases if  $m$  increases, while cut off frequency  $f_c$  doesn't depend on this parameter.

### Influence of L

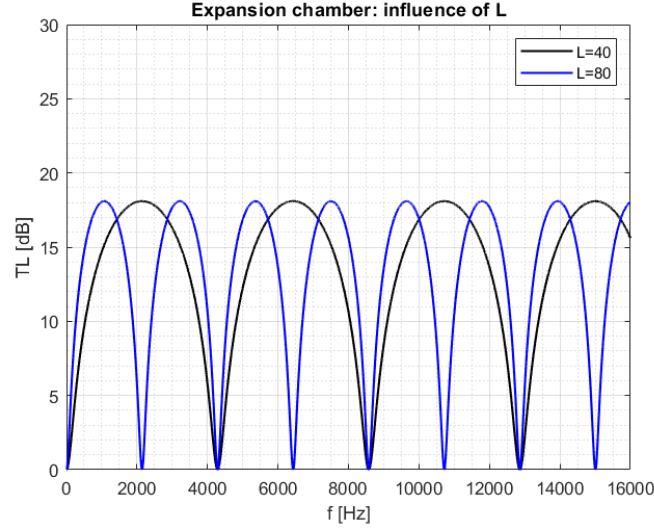


Figure 4.14: Influence of L

First cut off frequency of silencer decreases if total length of the chamber increases, according to eq.(4.36), while peak of TL amplitude doesn't depend on this parameter. Considering the same graphic of Fig.4.14 in a smaller frequency range (0-4500Hz) an other important aspect is highlighted through a geometric consideration.

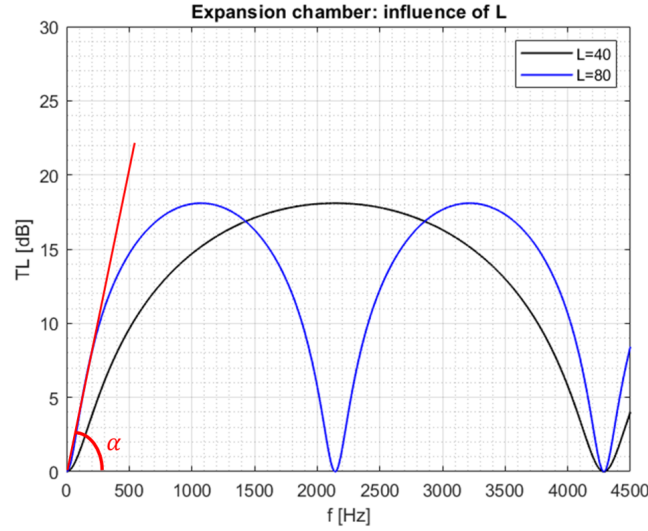


Figure 4.15: Influence of L (0-4500 Hz)

$\alpha$ , the angle between x-axis and the tangent to the TL curve, increases if the length of the chamber decreases. It means that a longer silencer influences more noise attenuation at low frequencies. This consideration is very important considering the sensibility of human ear at low frequencies (see A-weighted scale in Fig. 1.7). Even in design phase of this Thesis project, it will be a fundamental parameter to consider.

The most significant results of this sensitivity analysis are:

- $m = \frac{S_2}{S_1}$  influences only the maximum value of Transmission Loss amplitude;
- $L$  instead influences the first cut off frequency  $f_c$  and the frequency at which the amplitude is maximum  $f(TL_{max})$ .

#### 4.4.1 Extended pipes

The simple geometry of a one chamber silencer could be modified considering extended pipes in inner and outer parts, as in Fig.4.16.

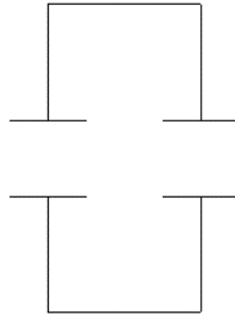


Figure 4.16: Single expansion chamber with extended pipes

As it has already be mentioned, a more complex geometry can be decomposed in some simple elements and then Transfer matrix method TMM may be applicate. In this case:

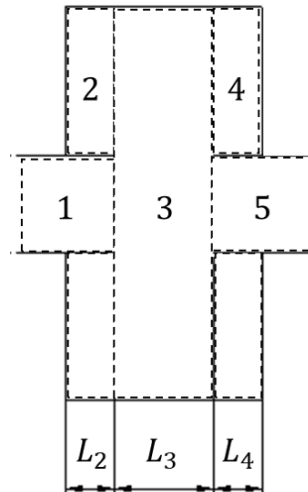


Figure 4.17: Decomposition of silencer

For the continuos section 1,3,5 Transfer matrix is:

$$T_i = \begin{bmatrix} \cos(kL_i) & Y_i \sin(kL_i) \\ \frac{1}{Y_i} \sin(kL_i) & \cos(kL_i) \end{bmatrix}$$

where:

$L_i$  is the lenght of each considered part;

$$Y_i = \frac{c}{\pi R_i^2};$$

$R_i$  is the radius of pipes.

Instead for the discontinuos section 2,4 Transfer matrix is:

$$T_i = \begin{bmatrix} 1 & 0 \\ \frac{j}{Y_i \cot(kL_i)} & 1 \end{bmatrix}$$

where:

$$Y_i = \frac{c}{\pi(R_i^2 - R_{i-1}^2)}$$

$R_{i-1}$  is the radius of pipe before discontinuity.

Total transfer matrix is the product of each Transfer matrix;

$$T = T^{(1)}T^{(2)}T^{(3)}T^{(4)}T^{(5)}$$

A comparison between a single expansion chamber with extended pipes and a simple one-chamber silencer is made to evaluate what is the effect of a more complex geometry. In order to make this analysis the total lenght of extended pipes model is equal to the lenght of simple expansion chamber. Thus:

$$L_2 + L_3 + L_4 = L_{EC}$$

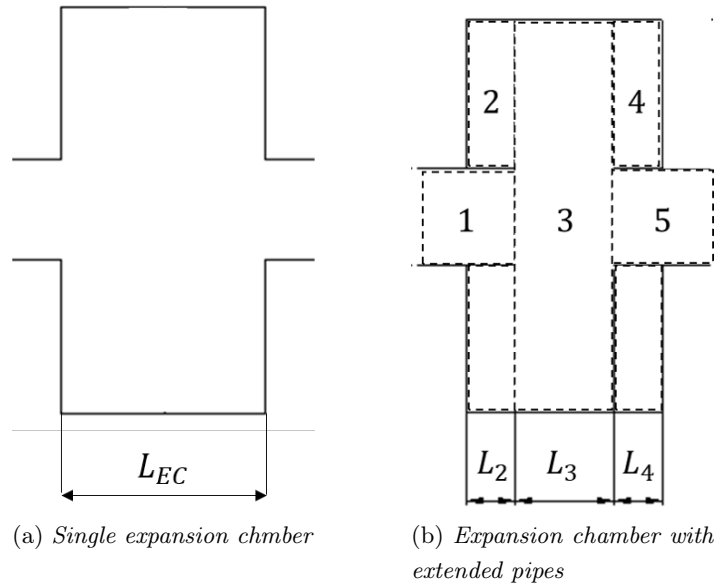


Figure 4.18: Comparison between single EC model and extended model

In this section some possible cases of expansion chambers with extendend pipes are reported.

**Case 1:**  $L_3=L_4$   $L_2=2L_3$ 

In this first case, the extended pipe in inlet is twice of extended pipe in outlet and the length of expansion part is equal to outlet, as shown in following figure.

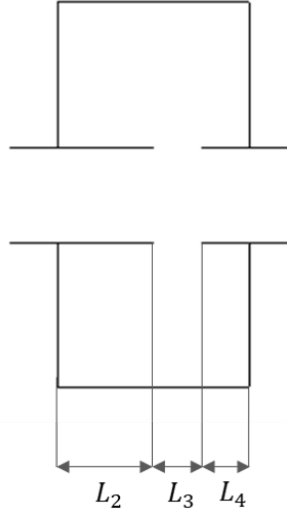


Figure 4.19: Case 1

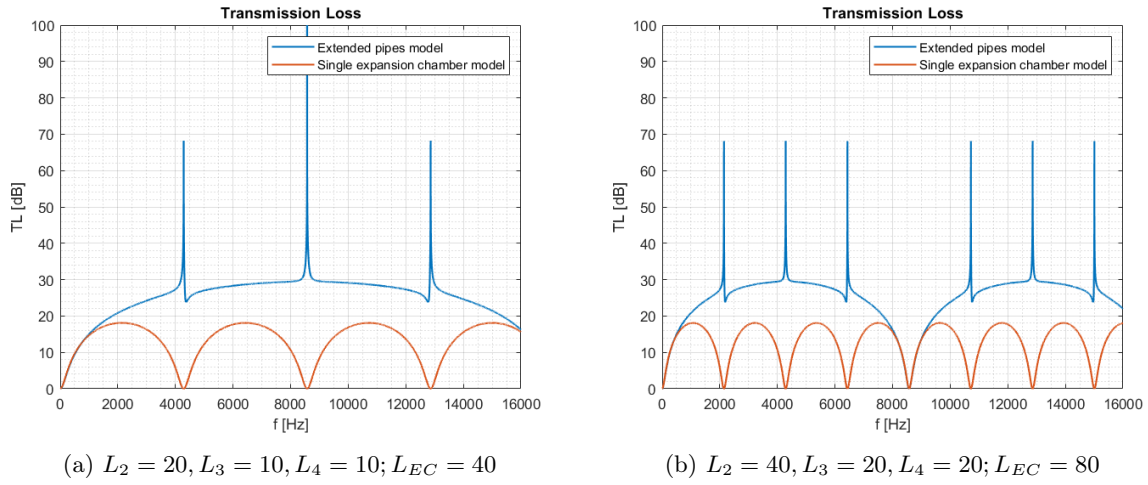


Figure 4.20: Case 1: Analytical results

The most interesting results are reported in the following list:

- Comparing two types of silencers having the same total length, initial tangent of the curve has the same inclination, so the noise attenuation is the same at low frequencies. Instead, comparing case a) and b) an increasing length causes an higher inclination of the curve and consequently better performance at low frequencies. It is in accord to **influence of L** discussed in previous pages.
- First cut off frequency of extended pipes model corresponds to fourth  $f_c$  of the single chamber model.

$$f_{c,EXT1} = 4n \frac{c}{2L} = n \frac{2c}{L} \quad (4.38)$$



- The maximum amplitude is bigger than EC case. Moreover, the model presents some peaks in the first three cut off frequencies of single chamber silencer.

$$f_{peaks1} = i \frac{c}{2L} \quad \text{if } i \neq 4n$$

Similar results are obtained if  $L_3=L_2$  and  $L_4=2L_3$ .

**Case 2:**  $L_2=L_3=L_4$

In this case three parts of silencer have the same length.

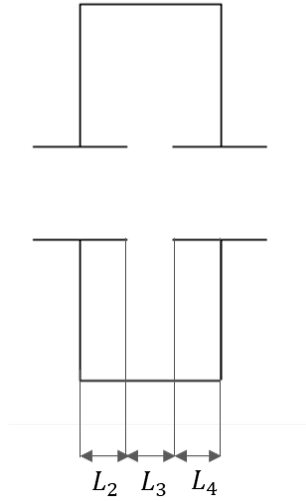


Figure 4.21: Case 2

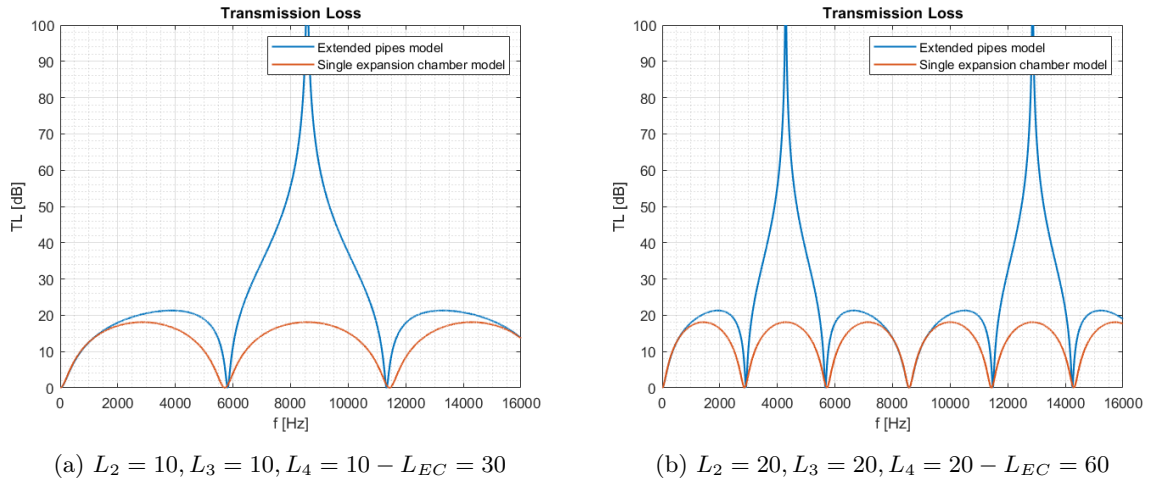


Figure 4.22: Case 2: Analytical results

- Considerations about length are the same of previous case.
- First cut off frequency corresponds to  $f_c$  of the single chamber model.

$$f_{c,EXT1} = n \frac{c}{2L} \quad (4.39)$$

- The model presents peaks in some frequencies, as shown.

$$f_{peaks,2} = f(TL_{max}) = \frac{c}{4L} + (3n - 2) \frac{c}{2L}$$

**Case 3:**  $L_2=L_4$   $L_3=2L_2$

Inner and outer parts have the same length, while expansion part is twice of them.

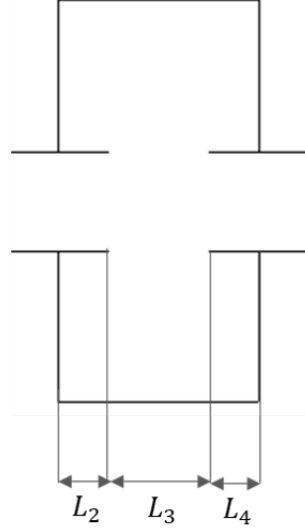


Figure 4.23: Case 3

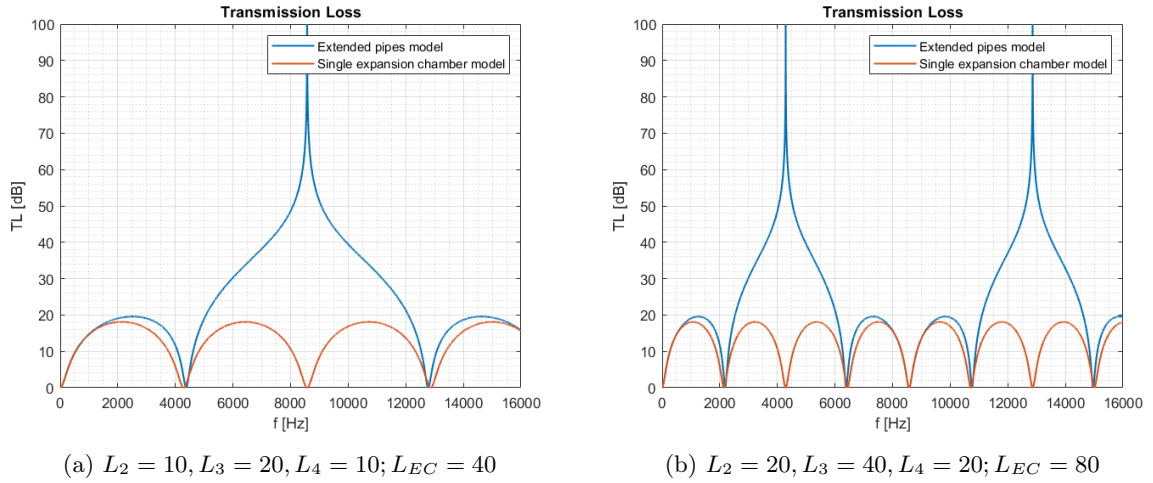


Figure 4.24: Case 3: Analytical results

- Considerations about length are the same of previous case.
- Looking to fig.4.24(a) there are two possible cut off frequencies:
  - 1) The first corresponds to first cut off frequency of single chamber model.

$$f_{c1,EXT3} = \frac{c}{2L}$$

2) The second corresponds to third cut off frequency of single chamber model.

$$f_{c2,EXT3} = 3 \frac{c}{2L} = \frac{3}{2} \frac{c}{L}$$

Considering fig. 4.24(b) and the periodicity of the function, cut off frequency of case 3 can be expressed by:

$$f_{c,EXT3} = i \frac{c}{2L} \quad \text{if } i \neq (4n-2)$$

- The model presents peaks in some frequencies, as shown.

$$f_{peaks3} = i \frac{c}{2L} \quad \text{if } i = (4n-2)$$

#### Case 4: $L_2=0$ $L_3=L_4$

There isn't an extended inlet pipe, while expansion part and outlet pipe have the same length.

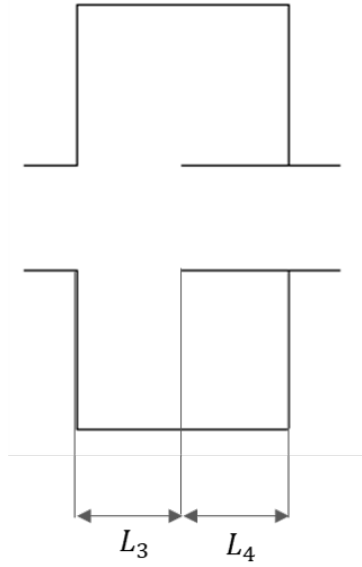


Figure 4.25: Case 4

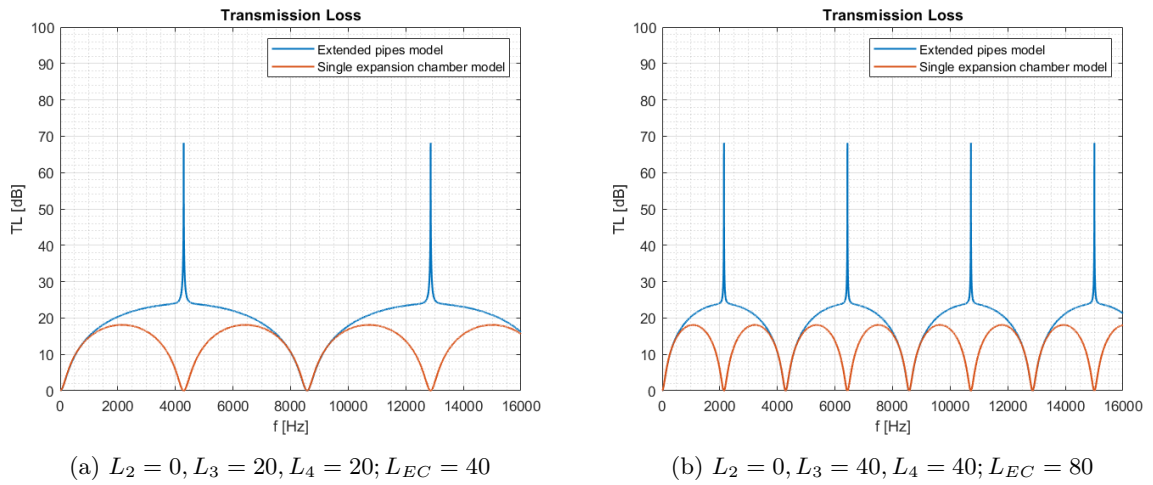


Figure 4.26: Case 4: Analytical results

- Considerations about length are the same of previous case.
- First cut off frequency corresponds to second  $f_c$  of the single chamber model:

$$f_{c,EXT4} = i \frac{c}{2L} \quad \text{if } i=2n.$$

- The model presents peaks in some frequencies, as shown.

$$f_{peaks4} = i \frac{c}{2L} \quad \text{if } i=(2n-1)$$

#### Case 5: $L_2=0$ $L_4=2L_3$

There isn't an extended inlet pipe, while expansion part has a length twice of outlet pipe

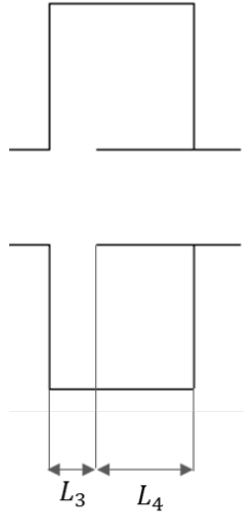


Figure 4.27: Case 5

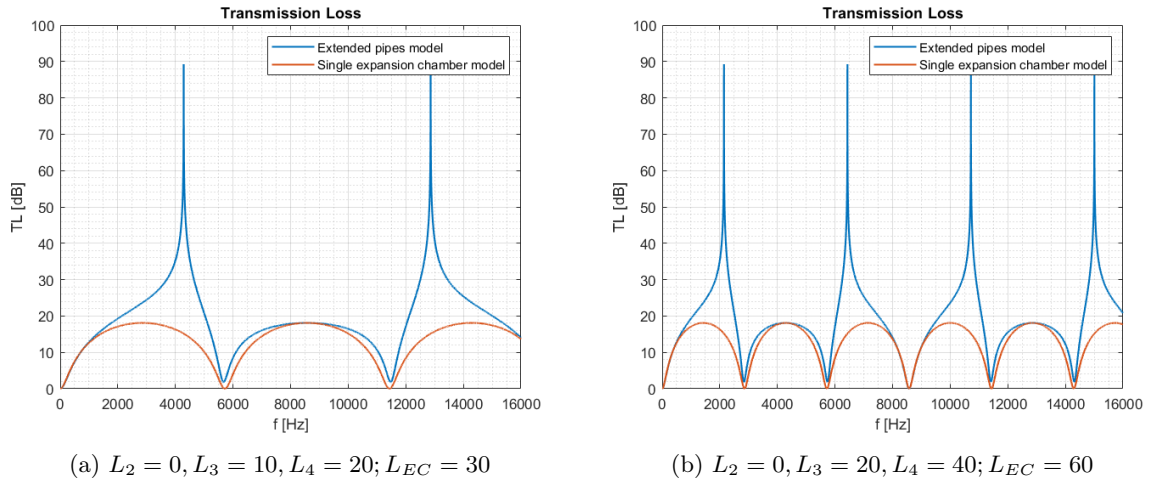


Figure 4.28: Case 5: Analytical results

- Considerations about length are the same of previous case.
- First cut off frequencies corresponds to  $f_c$  of the single chamber model:

## 4.5 From Transmission Loss to Sound power level $L_w$

So far the output chosen for acoustics analysis is Transmission Loss. The application of all criteria and all sensitivity analyses described in this chapter (e.g. Transfer Method Matrix) are not sufficient to evaluate noise attenuation of the silencer.

For example, it has been considered a very high frequency range (0-16000 Hz), in order to understand in great detail the influence of each parameter of the geometry on noise performances. But not each frequency affects noise attenuation in the same way, as it has been mentioned in the first chapter of this dissertation talking about psychoacoustics and filter weighting network. For this reason, the final output of noise model is the equivalent sound power level  $L_W(A)$ , measured in dB(A), that may approximate the sensitivity of human ear to different frequency ranges.

This quantity is calculated as follow:

$$L_W(A) = 10 \log_{10} \sum_{i=1}^n 10^{(L_{W,i}/10)}$$

where  $L_{W,i}$  is the sound power level of each frequency considered.

Frequency band used in Noise measurement in *ABAC* is the **one-third octave band**.

The logical way to pass from Transmission Loss model to  $L_w(A)$  derives from the definition of Transmission Loss. In fact:

$$TL(dB) = L_{w0} - L_W$$

Thus, for each frequency of the band, sound level power is defined as:

$$L_{W,i} = L_{w0,i} - TL_i$$

$L_{w0,i}$  is the initial level of noise emitted at each frequency, that in this project represents sound power level of the pump without any silencer.

Only in this way it's possible to compare the effects of different silencer geometries. In the following scheme this method is summarized.

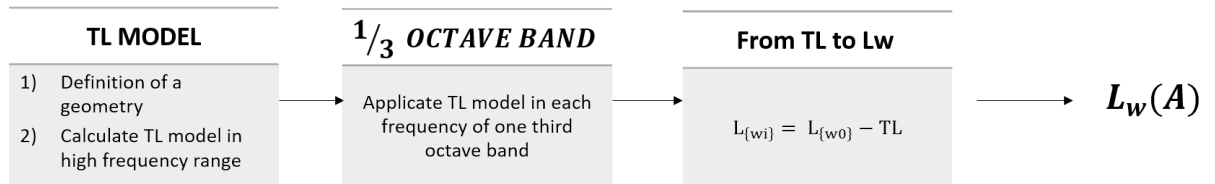


Figure 4.29: Noise analysis

## 4.6 Comments

The principal aim of this chapter is to research a general method to evaluate noise performance of each silencer geometry. For this reason, the application of Transfer Matrix Method to acoustics can be considered an important result to calculate noise level in each condition. It may be described in some steps:

- 1) Decomposition of a complex geometry in  $n$  simple elements;
- 2) Application of TMM to each one;
- 3) Total Transfer Matrix, using the linearity of this method;
- 4) Calculation of TRANSMISSION LOSS.

This theory is valid for reactive silencer considered in this Thesis, in which the research of the best geometry is fundamental to reduce noise effects.

The most important silencer types, **Helmotz resonator** and **expansion chamber** are presented. The explication of Trasmission Loss results permits to understand which is their area of application. In next chapter, when it will be proposed some possible new designs, a combination of both geometries will be also considered.

Moreover, it's really important to point out on sensivity analysis of Helmotz resonator and expansion chamber parameters. In fact, this kind of study requires a particular attention on each detail of the geometry. Therefore the assessment of this changes is really interesting to reach a correct design and to be able to compare how they affect noise performances. For example, extended pipes in a single expansion chamber represent a great results, expecially considering *case 1* (see *subsection 4.4.1: Extended pipes*). In this case the plot of Transmission loss shows the same amplitude at low frequencies, but very greater at high frequencies. Even if the most important contribute is at low frequencies, as indicated previously, increasing also the amplitude at high frequencies could have positive effects on  $L_w(A)$  and then on noise attenuation. In fact, this configuration will be one of the parts of new filter designs.

Next chapter (*chapter 5*) will be dedicated to design phase of new filters and to all consideration about them.

## Chapter 5

# Filter design

In this chapter, new filter designs will be proposed. In order to research the best solution, an iterative method is used, as it has already been shown in Fig. 2.9.

The starting point of the analysis is represented by noise experimental results of the machine without filter. In this way it's possible to evaluate which are the critical frequencies. Remembering that Helmotz resonator is typically used to attenuate noise if a system is at resonance, the first idea is to insert it centering its resonance frequency on the one that presents high noise level.

$L_w$  of *Pat Due machine* without filter is shown in Fig. 5.1.

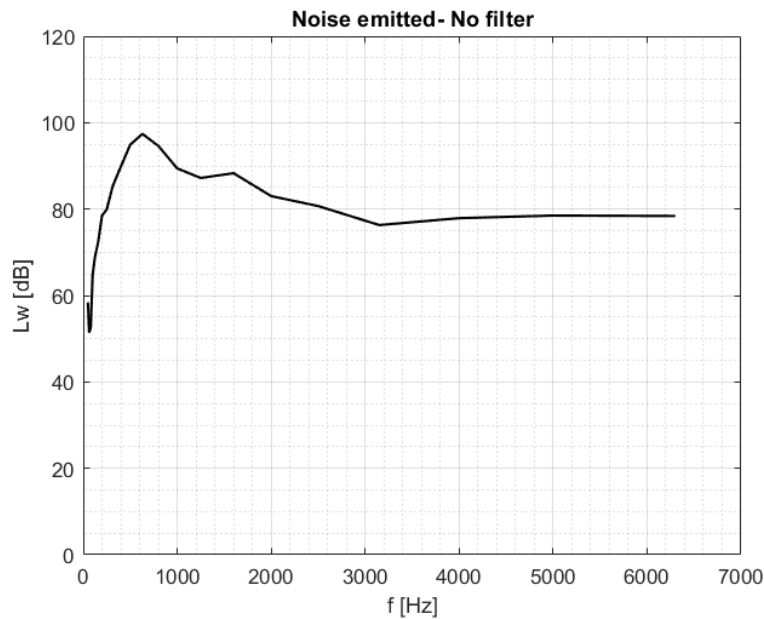


Figure 5.1: PAT 2: Sound power level without filter

Highest noise emitted is at  $f=630\text{Hz}$ , thus geometric value of Helmotz resonator have been chosen to center  $f_r$  at this frequency.

The second idea is to combine the resonator to an other type of silencer, an expansion chamber to improve acoustics attenuation. As mentioned in *Comments* part of previous chapter, the most interesting shape is the single expansion chamber with two extended pipes, both in inlet and outlet, where the lenght of one of the extended pipes is twice of the other and the lenght of

extension part is equal to the smaller (see Fig.4.19).

To facilitate the junction of this two silencers and to create a compact geometry, a perforated pipe is used as resonator (see subsection 4.10).

The next step is the decomposition of this new filter in  $n$  simple elements and applicate acoustics model described in Chapter 4. This method is shown in Figure 5.2

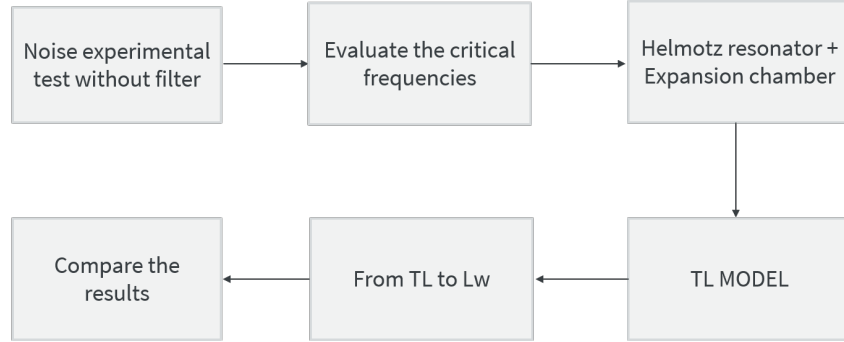


Figure 5.2: Acoustics model

This decomposition is valid both to acoustics and pressure analysis. This is really useful to create only a single analytical model in which it's possible to join two macro-arguments discussed in this dissertation.

Then, after evaluation of noise performances of new filter, the next step is the calculation of pressure losses inside the filter. It is possible by using the analytical method reported in *Chapter 3*. Full analysis is positive only if both acoustics and fluidodynamic aspects are respected. The required limits are as follows:

- *Acoustic analysis*:  $L_w(A)$  of new configuration less than actual filter or Noise 1.0 filter.
- *Pressure losses*: pressure drop similar or less than the minimum of previous filter ( $\simeq 0,25$  bar)

Total number of new configurations that will be considered is 5. The motivations to consider more designs will be shown in a different subsection, after the explication of initial design (Design 1). At the end of the chapter CAD 3D representations and final assemblies are reported.



## 5.1 Design 1

The schematic geometry and the decomposition of *Design 1* is shown in Fig. 5.3. Geometric values in Fig.5.3(a) are referred only to the parts of the filter in which air flows, without considering thickness of the pipe.

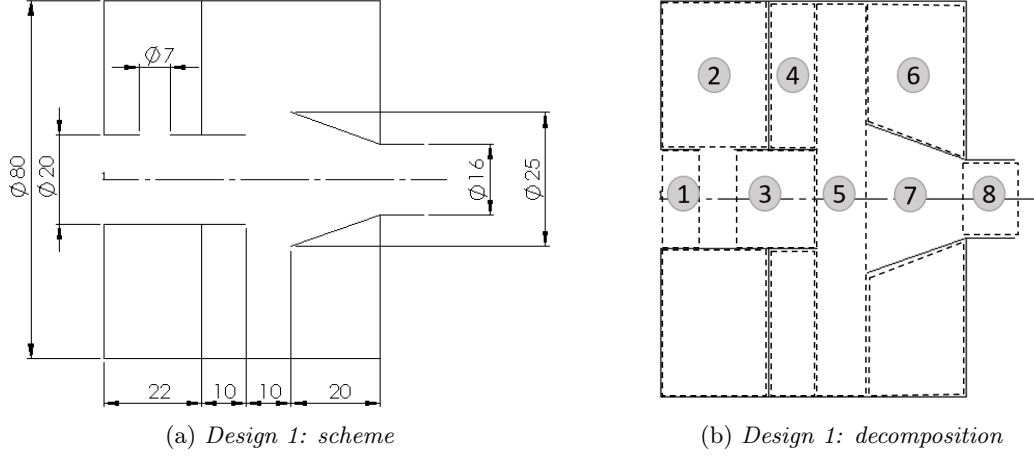


Figure 5.3: Design 1

All filter parts are reported in the following table.

Table 5.1: Design 1: filter parts

| DESIGN 1 |                                     |
|----------|-------------------------------------|
| Part     | Description                         |
| 1        | Inlet pipe                          |
| 2        | Annulus (Helmoltz resonator cavity) |
| 3        | Extended inlet pipe                 |
| 4        | Annulus                             |
| 5        | Expansion part                      |
| 6        | Annulus                             |
| 7        | Extended outlet pipe                |
| 8        | Outlet pipe                         |

The extended outlet pipe of the expansion chamber (Part 7) is represented by a truncated cone, instead of a simple cylindrical pipe. That because this different shape could reduce the local resistance in the contraction of cross sectional area between expansion part 5 and outlet pipe 8. In analytical code this truncated cone is considered as an equivalent cylinder having its same volume. Hence:

$$V_{tr} = V_{cyl}$$

$$\frac{1}{3}\pi(R_{7,max}^2 + R_{7,min}^2 + R_{7,max}R_{7,min})L_7 = \pi R_{7,eq}L_7$$

$$R_{7,eq} = \sqrt{\frac{1}{3}\pi(R_{7,max}^2 + R_{7,min}^2 + R_{7,max}R_{7,min})}$$

where:

$R_{7,max}$ = maximum radius of truncated cone;

$R_{7,min}$ = minimum radius of truncated cone;

$R_{7,eq}$ = equivalent radius of cylinder.

### Noise performance

Each part of the filter represents a simple element of the silencer, as shown in Table 5.2.

Table 5.2: Design 1: Acoustic element

| DESIGN 1 |                                     |                    |
|----------|-------------------------------------|--------------------|
| Part     | Description                         | Element            |
| 1        | Inlet pipe                          | HELMOLTZ RESONATOR |
| 2        | Annulus (Helmoltz resonator cavity) |                    |
| 3        | Extended inlet pipe                 | PIPE               |
| 4        | Annulus                             | DISCONTINUITY      |
| 5        | Expansion part                      | PIPE               |
| 6        | Annulus                             | DISCONTINUITY      |
| 7        | Extended outlet pipe                | PIPE               |
| 8        | Outlet pipe                         | PIPE               |

Therefore, the first two elements represent Helmotz resonator and eq. (4.28) and eq.(4.31) can be applied. The neck of the resonator is represented by the hole between part 1 and part 2 and its lenght is the thickness of the inlet pipe (3 mm).

Instead, the rest of the filter is analyzed by using *TRANSFER MATRIX METHOD*, where:

$$T_i = \begin{bmatrix} \cos(kL_i) & Y_i \sin(kL_i) \\ \frac{1}{Y_i} \sin(kL_i) & \cos(kL_i) \end{bmatrix}$$

for i=3,5,7,8.

$$T_i = \begin{bmatrix} 1 & 0 \\ \frac{j}{Y_i \cot(kL_i)} & 1 \end{bmatrix}$$

for i=4,6.

In this way it is possible to calculate equivalent Transmission Loss as in eq. (4.34).

Two silencer effects may be added and then can be expressed in sound power level by considering the frequencies of one-third octave band and the definition of Transmission Loss (see subsection 4.5). Final results are shown in the following plot.

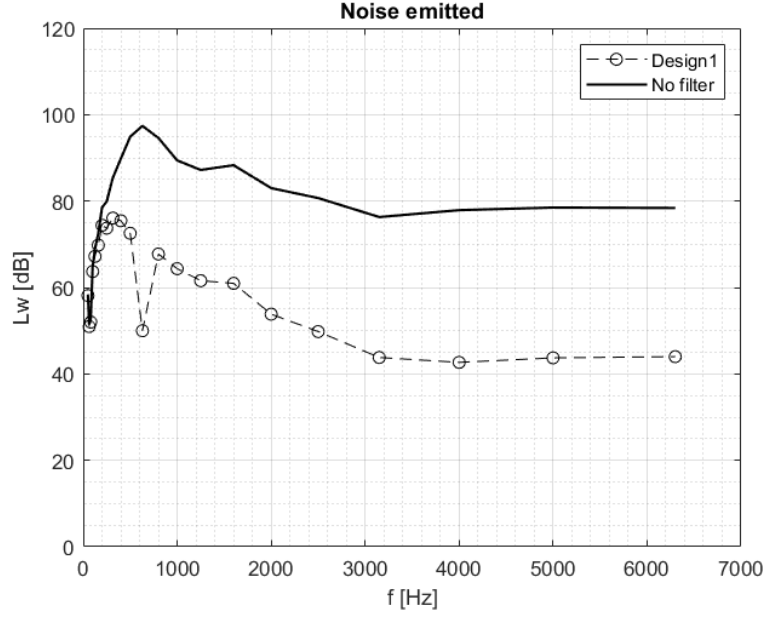


Figure 5.4: Sound power level- Design 1

In this Thesis project each design in  $L_w$  representation is compared to initial situation without filter, like in Fig. 5.4. To facilitate a final comparison between all designs that will be reported in this chapter, each one is represented by a different line type (e.g different color, or different line or different markers) while *No Filter* situation by a black continuous line. Final output,  $L_w(A)$ , is in the following table.

Table 5.3: Equivalent sound power level- Design 1

| DESIGN 1       |       |
|----------------|-------|
| $L_w(A)$ [dBA] | 82,42 |

### Pressure drop analysis

The other important aspect to point out in this dissertation is the calculation of pressure drop down the filter. Even in this case the initial consideration is about flow distribution in some critical parts of the filter.

Design 1, as the other designs in this chapter, have a single part in which it needs some comments, the hole that ideally represents the neck of Helmotz resonator.

As it has already desribed in *Chapter 3*, the hypoteses of no variation of pressure and linearity between discontinuities in geometry and flow distribution are considered acceptable.

In Fig. 5.5 the first three parts of the filter are highlited to evaluate flow distribution inside the hole having cross sectional are  $S_k$ .

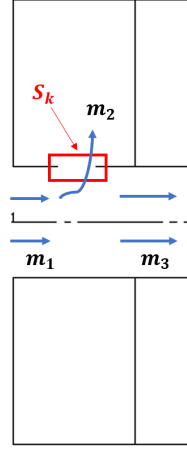


Figure 5.5: Flow distribution- Design 1

The dimensionless coefficient  $Z$  is defined as the ratio between air flow that passes through the hole,  $m_2$  and air flow in inlet pipe  $m_1$ .

$$Z = \frac{m_2}{m_1} = \frac{S_k}{S_1} \quad (5.1)$$

In Design 1, according to the dimensions in Fig. 5.3, this value is:

$$Z = \left(\frac{7}{20}\right)^2 = 0,12$$

Mass flow and then velocity of each part are computed by a simple mass balance equation. As shown in Table 5.4 velocity of part 1  $u_1$  is the only one that is referred to piston velocity  $w_z$ , while the other are expressed as a function of inlet velocity.

Table 5.4: Design 1: mass flow and velocity

| Part | Flow mass           | Balance equation                      | Velocity                                 |
|------|---------------------|---------------------------------------|--|
| 1    | $m_1 = m_{tot}$     | $\rho A_1 u_1 = \rho A_c w_z$         | $u_1 = w_z \frac{A_c}{A_1}$              |
| 2    | $m_2 = Z m_1$       | $\rho A_2 u_2 = Z \rho A_1 u_1$       | $u_2 = Z u_1 \frac{A_1}{A_2}$            |
| 3    | $m_3 = (1 - Z) m_1$ | $\rho A_3 u_3 = (1 - Z) \rho A_1 u_1$ | $u_3 = (1 - Z) u_1 \frac{A_1}{A_3}$      |
| 4    | $m_4 = m_3$         | $\rho A_4 u_4 = (1 - Z) \rho A_1 u_1$ | $u_4 = (1 - Z) u_1 \frac{A_1}{A_4}$      |
| 5    | $m_5 = m_4 = m_1$   | $\rho A_5 u_5 = (1 - Z) \rho A_1 u_1$ | $u_5 = (1 - Z) u_1 \frac{A_1}{A_5}$      |
| 6    | $m_6 = m_5 = m_1$   | $\rho A_6 u_6 = (1 - Z) \rho A_1 u_1$ | $u_6 = (1 - Z) u_1 \frac{A_1}{A_6}$      |
| 7    | $m_7 = m_6 = m_1$   | $\rho A_7 u_7 = (1 - Z) \rho A_1 u_1$ | $u_7 = (1 - Z) u_1 \frac{A_1}{A_{7,eq}}$ |
| 8    | $m_8 = m_7 = m_1$   | $\rho A_8 u_8 = (1 - Z) \rho A_1 u_1$ | $u_8 = (1 - Z) u_1 \frac{A_1}{A_7}$      |

In this way, by using definition of Reynold's number and Darcy's friction coefficient  $f_d$ , distributed pressure losses are computed.

Instead, local resistance (concentrated pressure losses) are computed by considering impedance types reported in the following table.

Table 5.5: Design 1: local resistance

| From..             | To..     | Impedance type |
|--------------------|----------|----------------|
| <i>Environment</i> | <b>1</b> | Entrance       |
| <b>1</b>           | <b>2</b> | Contraction    |
|                    |          | Expansion      |
| <b>3</b>           | <b>5</b> | Expansion      |
| <b>5</b>           | <b>4</b> | Contraction    |
| <b>5</b>           | <b>6</b> | Contraction    |
| <b>5</b>           | <b>7</b> | Contraction    |
| <b>7</b>           | <b>8</b> | Contraction    |
| <b>8</b>           | Head     | Expansion      |

Hence, it's possible to evaluate final pressure drop of Design 1.

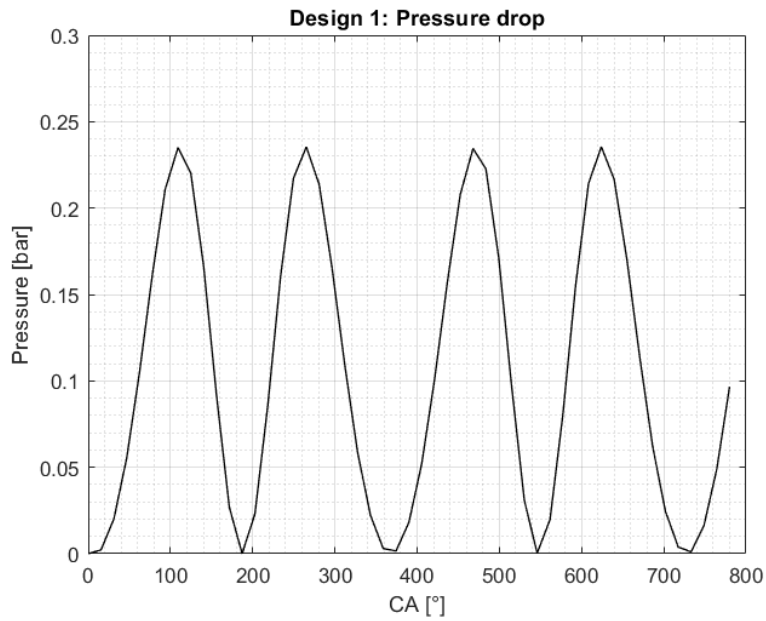


Figure 5.6: Pressure drop-Design 1

The maximum pressure drop value respects the limits imposed.

Table 5.6: Design 1: maximum pressure drop

| DESIGN 1                       |      |
|--------------------------------|------|
| <i>Max pressure drop [bar]</i> | 0,23 |

### 5.1.1 Choice of other designs

Design 1 is only the starting point of full analysis made in this Chapter. It is important to understand the geometry chosen for the filter and the method used to obtain both acoustics and fluidodynamics results.

The reason to consider other possible designs is linked to sensitivity analysis explained in Chapter 4. In fact, it's possible to understand how geometry parameters could influence both results.

Total number of designs considered are 5. In the following list reasons to consider other cases are reported. To help the comprehension, the part of the filter that represents Helmotz resonator is called **PART A**, while the other one that represents Expansion chamber **PART B**.

- **Design 2:** the difference between this case and *Design 1* is about the maximum diameter of PART A and PART B, that is bigger than the first one. The lenght of PART A is less to center again resonance frequency to  $f=630\text{Hz}$ . Hence, study of *Design 2* is important to understand how increasing of maximum diameter could influence final results.
- **Design 3:** in this case the difference is in PART B. In fact, while PART A doesn't change, the lenght of PART B decreases.
- **Design 4:** the difference is also in PART B, but in this case its lenght increases.
- **Design 5:** this time PART A changes while PART B is unchanged. Its lenght increases and in this way resonance frequency  $f_r$  doesn't correspond to frequency in which there is maximum noise level.

In Table 5.7 is reported a brief summary about the reasons of the choice of these designs.

Table 5.7: Reasons of the choice

| INITIAL DESIGN | FINAL DESIGN | REASON OF THE CHOICE   |
|----------------|--------------|--|
| 1              | 2            | Evaluate the differences between two designs with different size |
| 1              | 3            | Evaluate the differences decreasing the lenght of PART B         |
| 1              | 4            | Evaluate the differences increasing the lenght of PART B         |
| 1              | 5            | Evaluate the differences increasing the lenght of PART A         |

Noise performances of each design is represented in different ways. Particularly:

- Designs having the same PART A of Design 1 (3 and 4) are reported using the same color line (Black), but different types of lines and markers.
- Design 2 having different size than 1 is represented by a red line.
- Design 5 having the same PART B than 1 is represented by a blue line.

## 5.2 Design 2

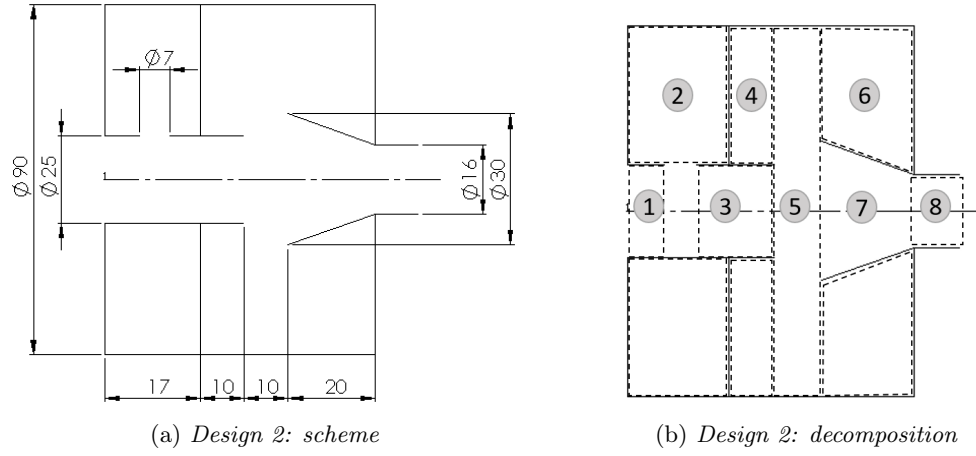


Figure 5.7: Design 2

Filter is decomposed in the same way of Design 1, so all parts are represented in Table 5.1. As it has already introduced in the previous paragraph, the differences between this design and the first are maximum diameter ( $\phi=90\text{mm}$ ), inlet pipe diameter ( $\phi=25\text{mm}$ ) and consequently (to have same  $f_r$ ) length of PART A. Thus, all acoustics element and all impedance types doesn't change.

### Noise performance

Sound power level results are shown in the following plot.

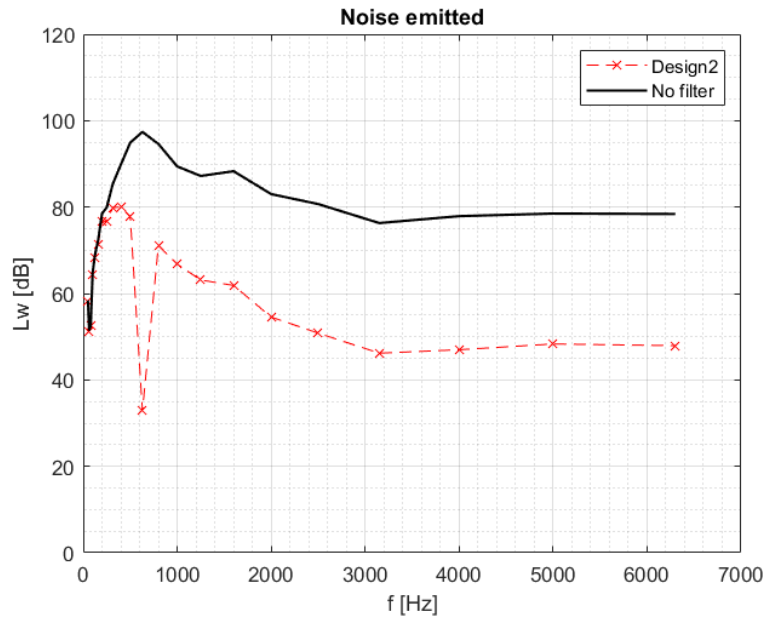


Figure 5.8: Sound power level- Design 2

Final output,  $L_w(A)$ , is in the following table.

Table 5.8: Equivalent sound power level- Design 2

| DESIGN 2       |    |
|----------------|----|
| $L_w(A)$ [dBA] | 86 |

### Pressure drop analysis

Because of variation in PART A, even flow distribution between inlet pipe and hole changes. In fact, in this case, the dimensionless coefficient is:

$$Z = 0,08$$

In Fig. 5.9 final pressure drop is shown.

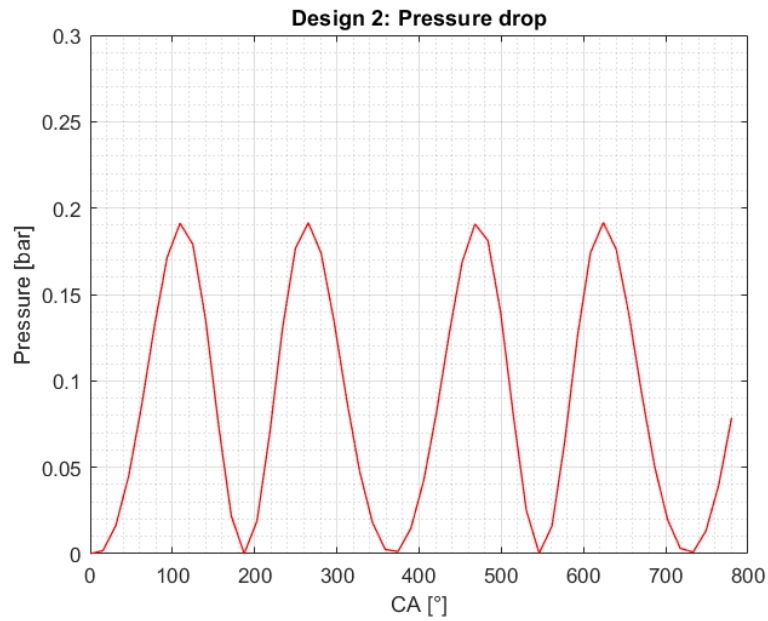


Figure 5.9: Pressure drop-Design 2

The maximum pressure drop value respects the limits imposed.

Table 5.9: Design 2: maximum pressure drop

| DESIGN 2                       |      |
|--------------------------------|------|
| <i>Max pressure drop</i> [bar] | 0,19 |



### 5.3 Design 3

Design 3 has the same composition of Design 1 (Helmholtz resonator+ expansion chamber with extended pipes), but different lengths in PART B. In fact lengths of extended pipes and expansion part are halved. Hence, even if there are these differences, Design 3 presents also same decomposition and same local resistances of Design 1. Thus, in this section only results will be reported.

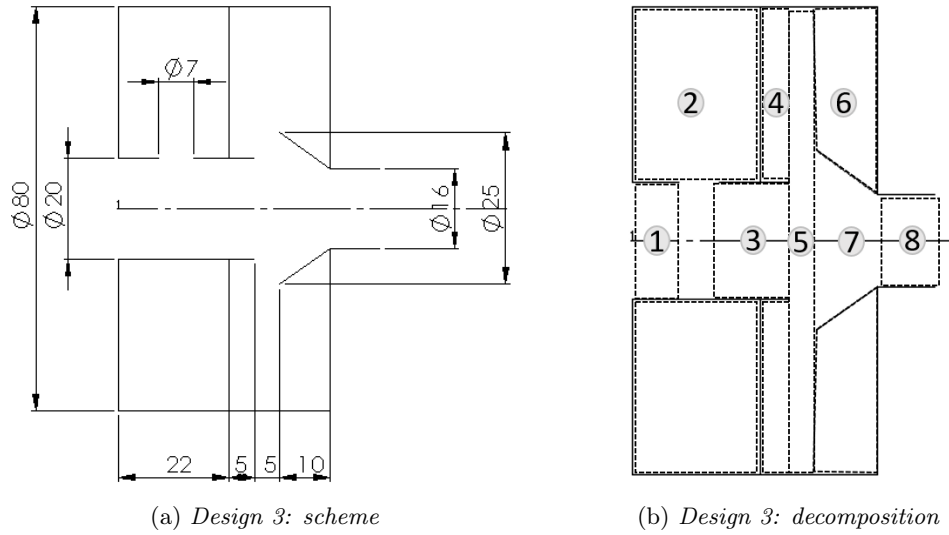


Figure 5.10: Design 3

#### Noise performance

Sound power level results are shown in the following plot.

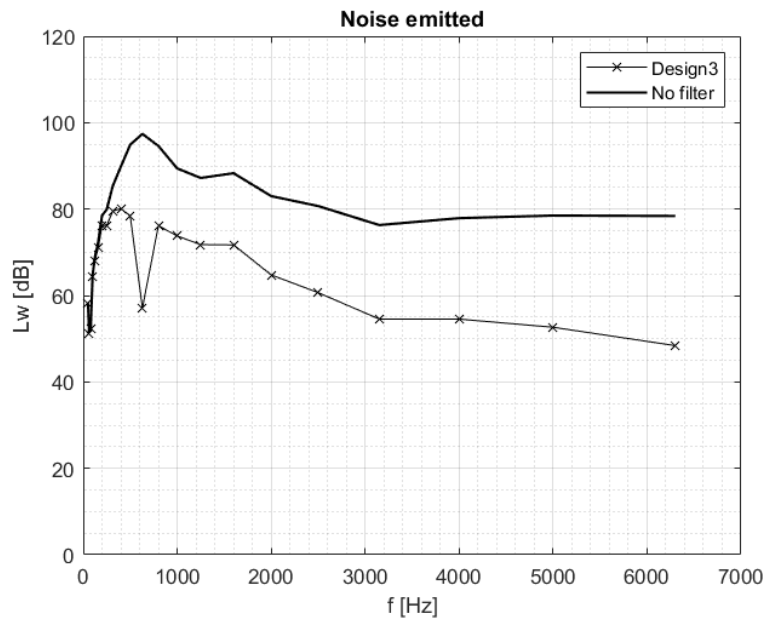


Figure 5.11: Sound power level- Design 3

Final output,  $L_w(A)$ , is in the following table.

Table 5.10: Equivalent sound power level- Design 3

| DESIGN 3       |      |
|----------------|------|
| $L_w(A)$ [dBA] | 86,7 |

### Pressure drop analysis

There is no variation in PART A than Design 1, so the dimensionless coefficient Z is:

$$Z = 0,12$$

In Fig. 5.12 final pressure drop is shown.

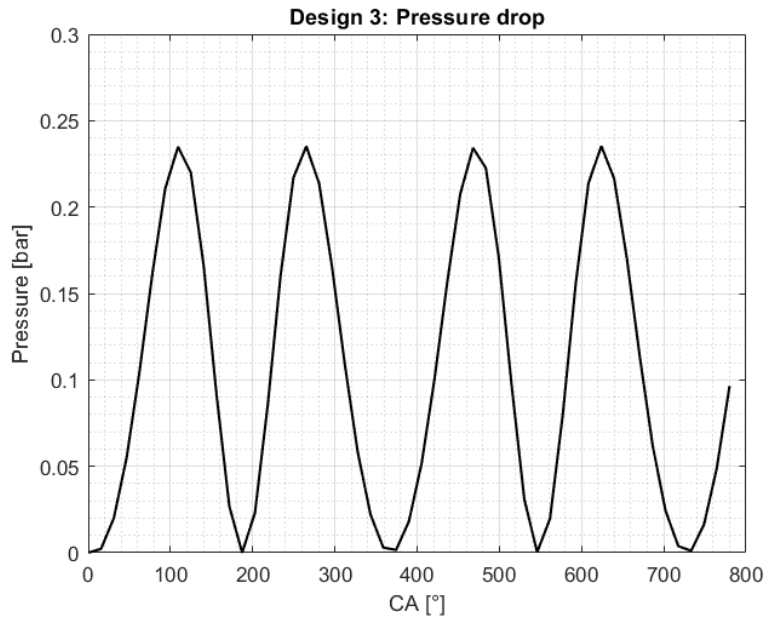


Figure 5.12: Pressure drop-Design 3

The maximum pressure drop value respects the limits imposed.

Table 5.11: Design 3: maximum pressure drop

| DESIGN 3                       |      |
|--------------------------------|------|
| <i>Max pressure drop</i> [bar] | 0,23 |

## 5.4 Design 4

Design 4 has on opposite concept than Design 3. In fact in this case lengths of extended pipes and expansion part are doubled.

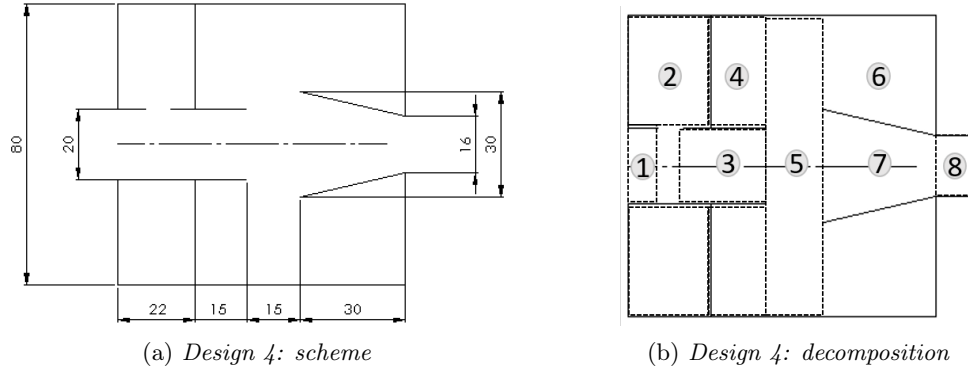


Figure 5.13: Design 4

### Noise performance

Sound power level results are shown in the following plot.

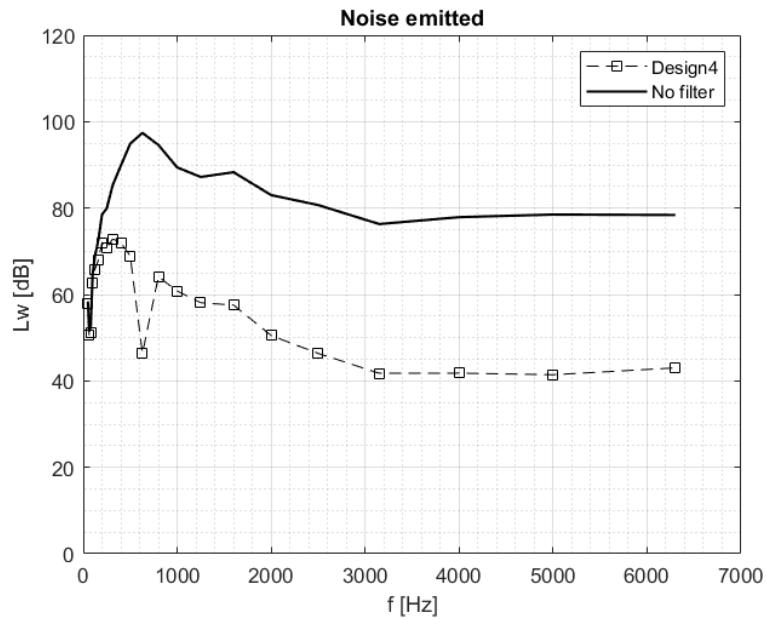


Figure 5.14: Sound power level- Design 4

Final output,  $L_w(A)$ , is in the following table.

Table 5.12: Equivalent sound power level- Design 4

| DESIGN 4       |      |
|----------------|------|
| $L_w(A)$ [dBA] | 79,5 |

### Pressure drop analysis

There is no variation in PART A than Design 1, so the dimensionless coefficient Z is:

$$Z = 0,12$$

In Fig. 5.15 final pressure drop is shown.

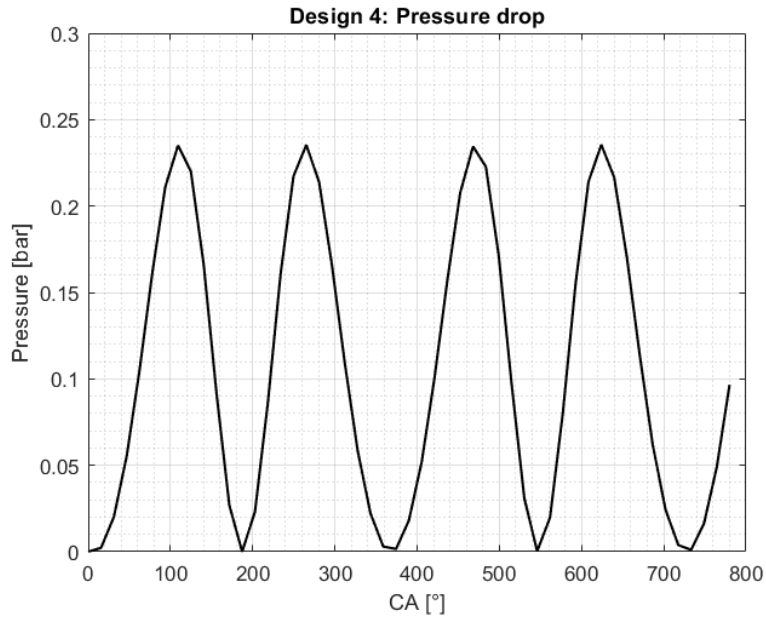


Figure 5.15: Pressure drop-Design 4

The maximum pressure drop value respects the limits imposed.

Table 5.13: Design 4: maximum pressure drop

| DESIGN 4                       |      |
|--------------------------------|------|
| <i>Max pressure drop</i> [bar] | 0,24 |

## 5.5 Design 5

Respect to the others designs, Design 5 has a different lenght of PART A. Because of this variation, frequency  $f_r$  is not centered in frequency that have higher noise level. Particularly, an increasing of this lenght causes a smaller resonance frequency. In this way it's possible to have a decreasing of noise emitted at low frequencies.

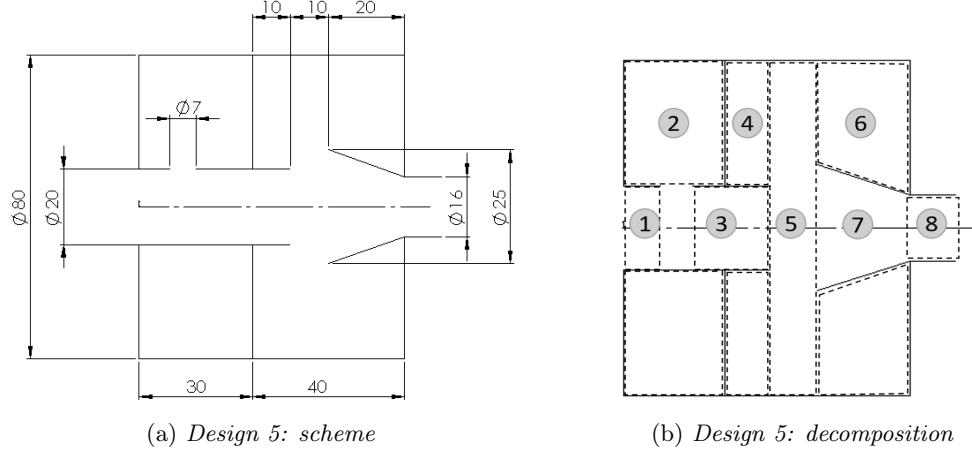


Figure 5.16: Design 5

### Noise performance

Sound power level results are shown in the following plot.

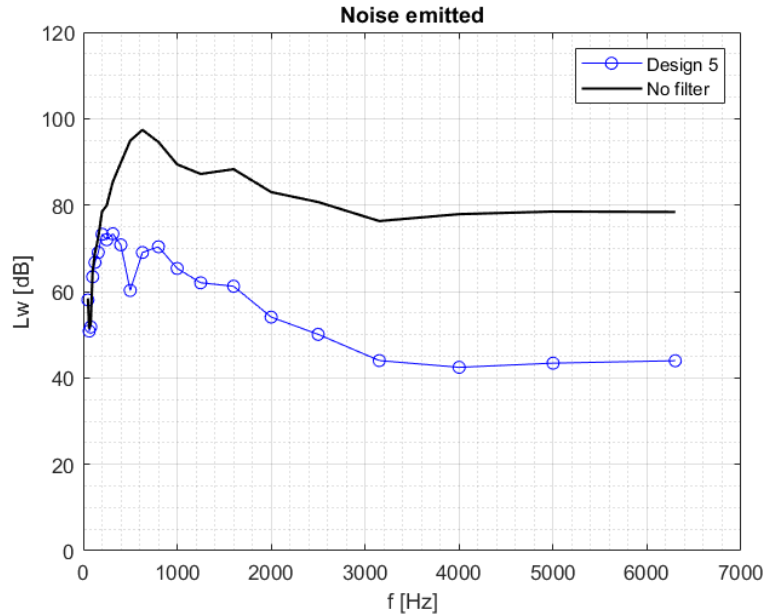


Figure 5.17: Sound power level- Design 5

Final output,  $L_w(A)$ , is in the following table.

Table 5.14: Equivalent sound power level- Design 5

| DESIGN 5       |      |
|----------------|------|
| $L_w(A)$ [dBA] | 80,5 |

### Pressure drop analysis

There is no variation in PART A than Design 1, so the dimensionless coefficient  $Z$  is:

$$Z = 0,12$$

In Fig. 5.18 final pressure drop is shown.

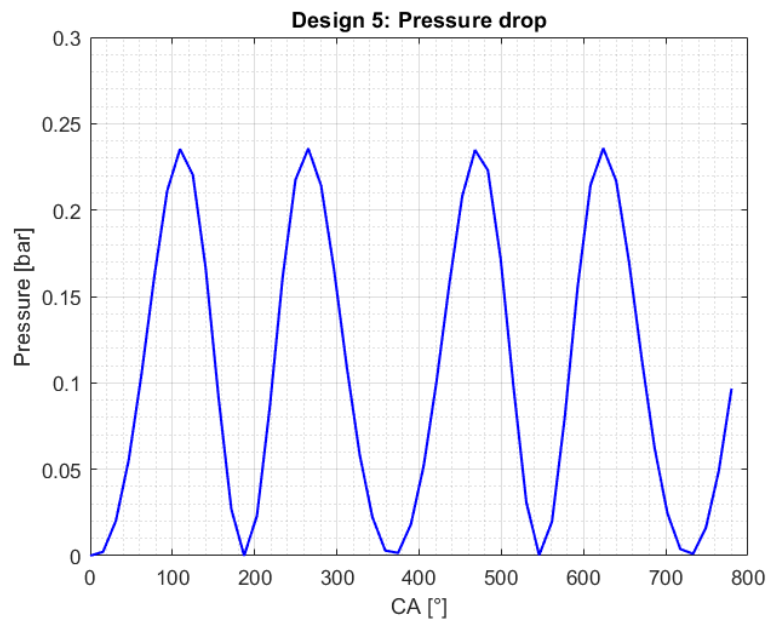


Figure 5.18: Pressure drop-Design 5

The maximum pressure drop value respects the limits imposed.

Table 5.15: Design 5: maximum pressure drop

| DESIGN 5                       |      |
|--------------------------------|------|
| <i>Max pressure drop</i> [bar] | 0,23 |

## 5.6 CAD 3D and assembly

In order to carry out new experimental tests on *PAT 2* machine, all designs proposed has been printed using a 3D-technique. The material chosen for each component is **ABS**, which allows to have lots of advantages in impact resistance, toughness, and heat resistance.

CAD 3D of desings is shown in this section. The model that it will be reported is valid for each design, because the decomposition of the filter is similar for each one. Thus, the analysis is done considering only one configuration (e.g. Design 1).

Generally new filters are composed by three parts, as described in the following list.

- **PART A:** it represents that part of filter geometry that simulate the behaviour of an Helmotz resonator, considered as a perforated tube. An isometric view is shown in Fig. 5.19. The elements indicated in the above figure are explained in the following table.

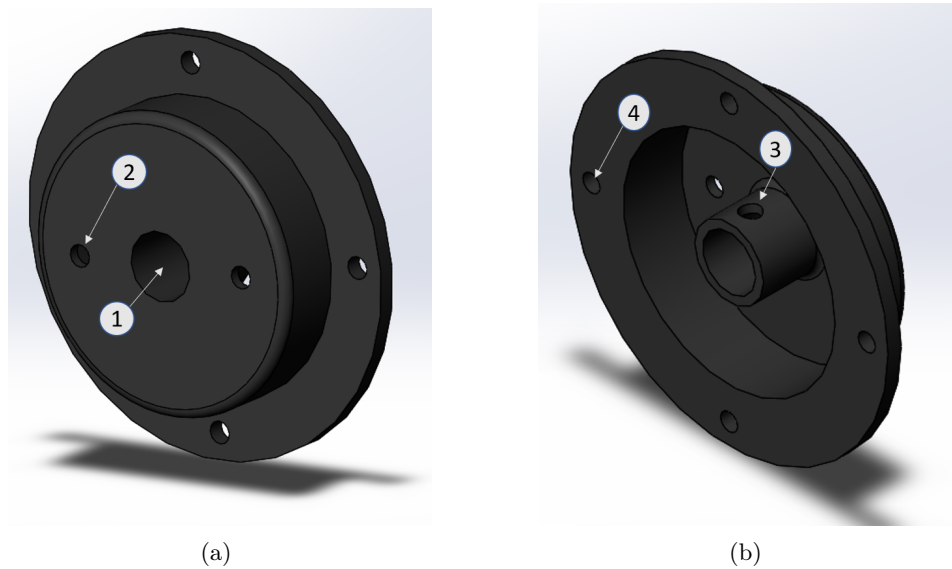


Figure 5.19: PART A: isometric view

Table 5.16: PART A: details

| PART A: DETAILS |   |
|-----------------|---|
| 1               | Air inlet   |
| 2               | Holes (2x) to insert M6 screw to join filter and head of cylinder |
| 3               | Hole that simulate neck of Helmotz resonator                      |
| 4               | Holes (4x) to insert M6 screw to join filter parts                |

- **PART B:** it represents that part of filter geometry that simulate the behaviour of the expansion chamber. An isometric view is shown in Fig. 5.20.

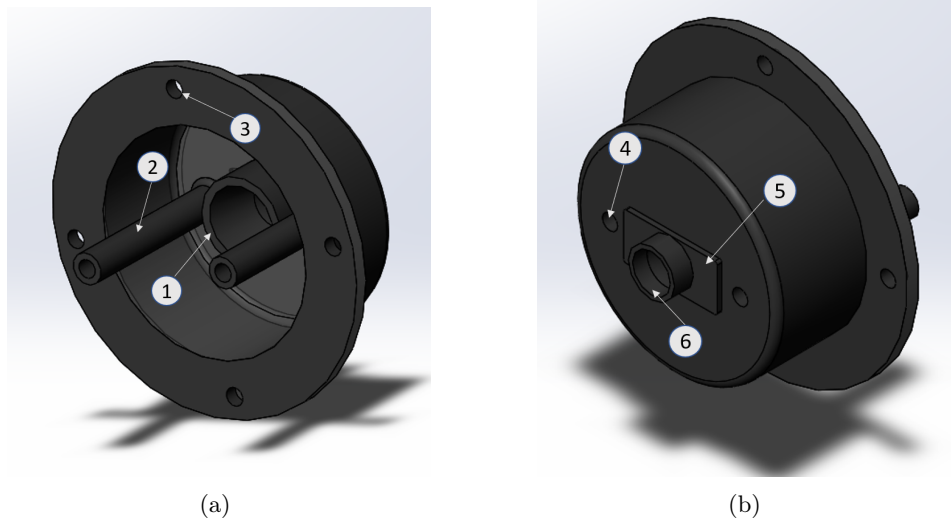


Figure 5.20: PART B: isometric view

The elements indicated in the above figure are explained in the following table.

Table 5.17: PART B: details

| PART B: DETAILS |   |
|-----------------|---|
| 1               | Extended outlet pipe  |
| 2               | Pipes (2x) to insert M6 screw to join filter and head of cylinder   |
| 3               | Holes (4x) to insert M6 screw to join filter parts                  |
| 4               | Holes (2x) to insert M6 screw to join filter and head of cylinder   |
| 5               | Geometry to facilitate junction between filter and head of cylinder |
| 6               | Outlet pipe   |

The length of pipes where M6 screws pass through (number 2 in Table 5.17) is equal to total length of the filter. The below figure shows a section of the axial view of PART B, where it's possible to indicate truncated cone shape of extended outlet pipe.

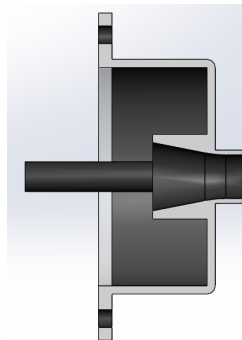


Figure 5.21: PART B- Axial view



- **CONNECTION PART:** It is a fundamental part of the filter because allows the connection and division of two parts that has been described. In fact, in this way, it makes possible to investigate on each of these two parts and moreover to remove and change foam material when it is necessary. It is represented as a disc with an extended pipe that simulate inlet extended pipe of expansion chamber.

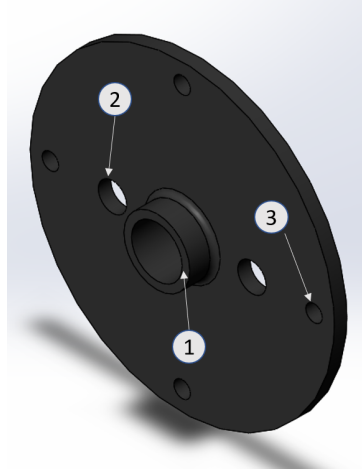


Figure 5.22: CONNECTION PART- Isometric view

The elements indicated in the above figure are explained in the following table.

Table 5.18: CONNECTION PART: details

| CONNECTION PART : DETAILS |   |
|---------------------------|---|
| 1                         | Extended pipe   |
| 2                         | Holes (2x) to insert pipes where M6 screws pass through |
| 3                         | Holes (4x) to insert M6 screw to join filter parts      |

An other important element of filter is the foam material, in *Polyurethane*. Its scope is to collect dust and other impurity that could flow inside the pump. An isometric view of foam material is shown in Fig.5.23

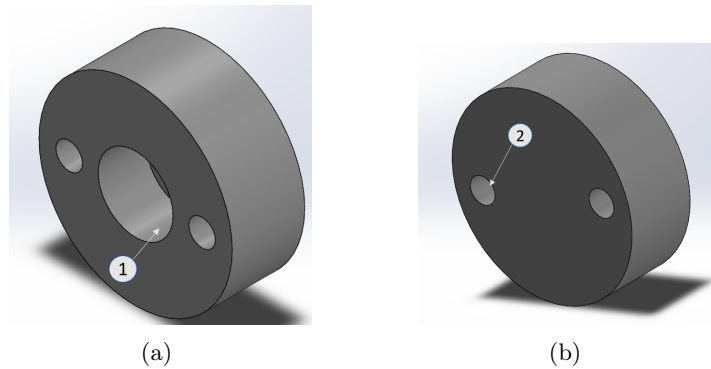


Figure 5.23: FOAM MATERIAL: isometric view

The elements indicated in the above figure are explained in the following table.

Table 5.19: FOAM MATERIAL: details

| FOAM MATERIAL : DETAILS |   |
|-------------------------|---|
| 1                       | Hole for extended pipe                                  |
| 2                       | Holes (2x) to insert pipes where M6 screws pass through |

Foam material is inserted in PART B of the filter. Thus, as indicated in Table 5.19, there is an hole for the outlet extended pipe and two holes to insert pipes of M6 screws. The lenght of foam material is equal to total lenght of PART B without considering the lenght of extended inlet pipe. An assembly of PART B and foam material is shown in this figure.

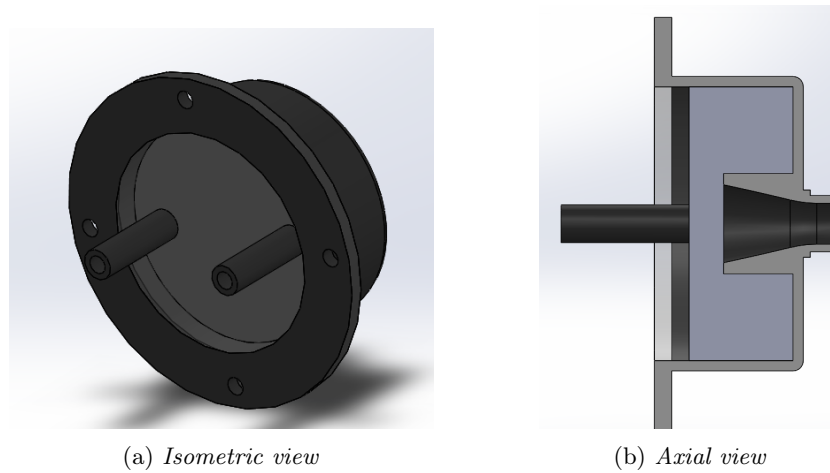


Figure 5.24: FOAM MATERIAL and PART B

The **assembly method** is reported in the following list.

- 1) Firstly join PART B (with foam material) and connection part, inserting small tubes in which the screws pass in the appropriate holes.

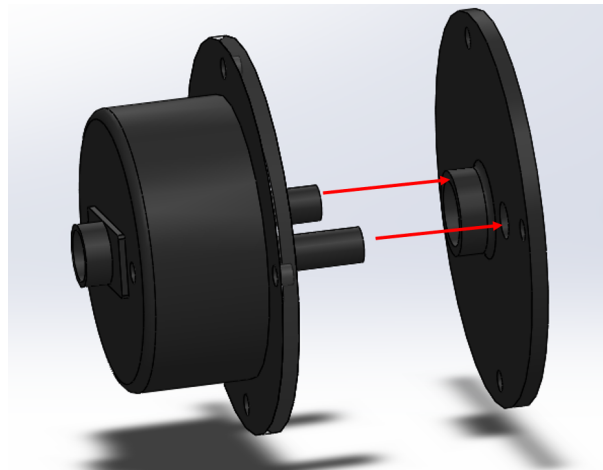


Figure 5.25: PART B and CONNECTION PART

- 2) Join this equivalent part and PART A, by using M6 screws and M6 nuts.

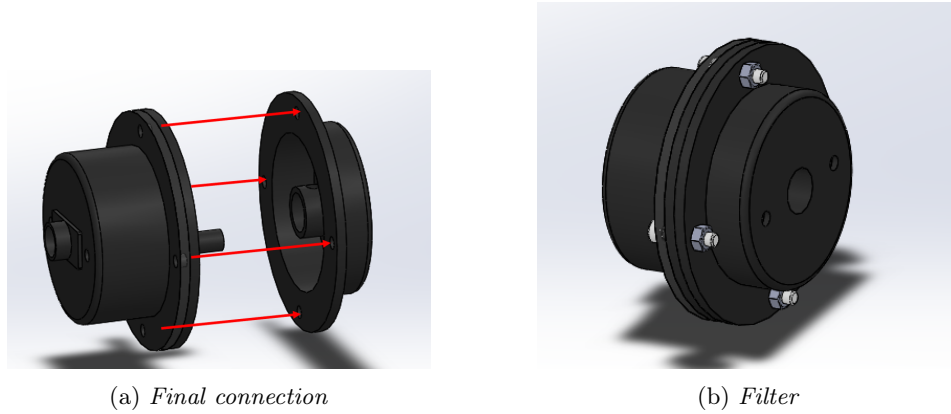


Figure 5.26: Filter representation

- 3) Connect total filter to the head of the cylinder, by using M6 screws. 3D model of head of cylinder is shown in this figure.

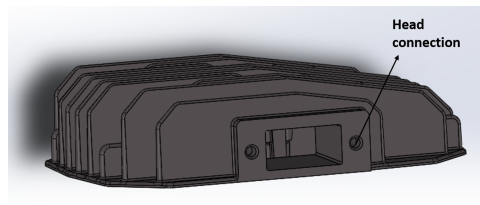


Figure 5.27: Head of cylinder

In the above figure is indicated the filter's head connection assembly, represented by two holes having diameter 6,5mm.

Thus, total assembly is shown in Fig. 5.28

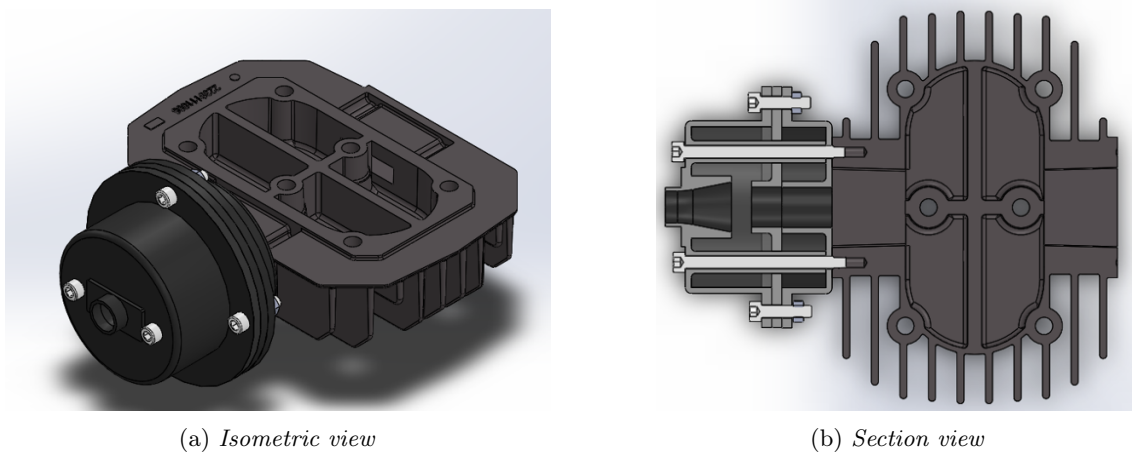


Figure 5.28: Total assembly

One of the aim in CAD modeling is to realize more number of designs using the smallest number of components. At the end, the number of parts realized to assembly 5 final designs are 10, to which to add also 4 foam materials.

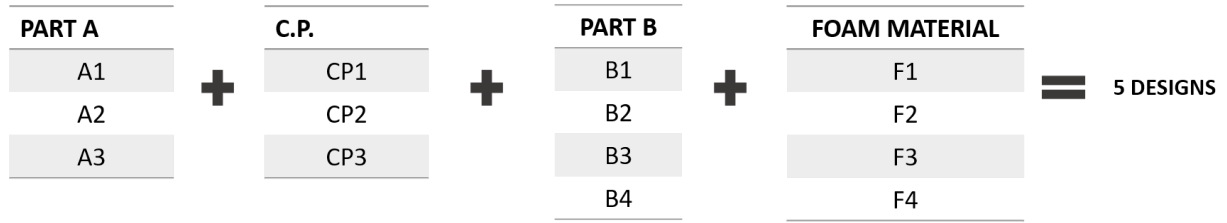


Figure 5.29: Total number of components

In the following table the decomposition of each filter design.

Table 5.20: Decomposition of each filter

| FILTER PARTS |    |    |     |    |
|--------------|----|----|-----|----|
| DESIGN       | A  | B  | CP  | F  |
| 1            | A1 | B1 | CP1 | F1 |
| 2            | A2 | B2 | CP2 | F2 |
| 3            | A1 | B3 | CP1 | F3 |
| 4            | A1 | B4 | CP3 | F4 |
| 5            | A3 | B1 | CP1 | F1 |

## 5.7 Final comparisons

Final comparisons between all designs proposed is reported in this section. It concerns the assessment of three different parameters:

- Noise performances;
- Pressure drop;
- Size of the filter, considering the biggest diameter (H) and total length (L) as shown in Fig. 5.30.

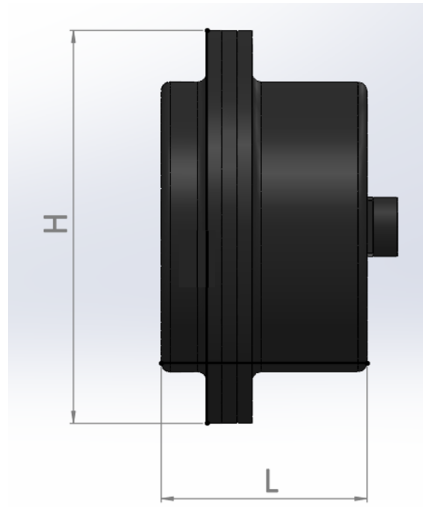


Figure 5.30: Size

A brief summary of all results is shown in the following table.

Table 5.21: Analytical results

|              | NOISE<br>PERFORMANCE | PRESSURE<br>DROP       | SIZE  |       |
|--------------|----------------------|------------------------|-------|-------|
| DESIGN       | $L_{w,Aeq}$ [dBA]    | Pressure drop<br>(bar) | H(mm) | L(mm) |
| Abac         | 94,9                 | 0,24                   | 135   | 50    |
| Noise<br>1.0 | 92,9                 | 0,44                   | 130   | 176   |
| 1            | 82,42                | 0,23                   | 120   | 73    |
| 2            | 85,98                | 0,18                   | 130   | 68    |
| 3            | 86,73                | 0,23                   | 120   | 53    |
| 4            | 79,5                 | 0,23                   | 120   | 93    |
| 5            | 80,5                 | 0,23                   | 120   | 81    |

The results of ABAC and Noise 1.0 filters are experimental.

The first important results is about **pressure drop**. In fact, as shown in *Analytical results*, all designs except Design 2 present similar values of pressure losses inside the filter. Design 2, unlike the others, has different cross sectional areas and different values of local resistance  $K$ . Instead Design 1 differs from others (3,4,5) only about lengths of one of the parts. It follows that pressure drop down the filter is more influenced by concentrated losses and not by distributed. Thus, it's possible to control this parameters only choosing the best combination of all geometrical discontinuities.

Results about noise performances are shown in next figures.

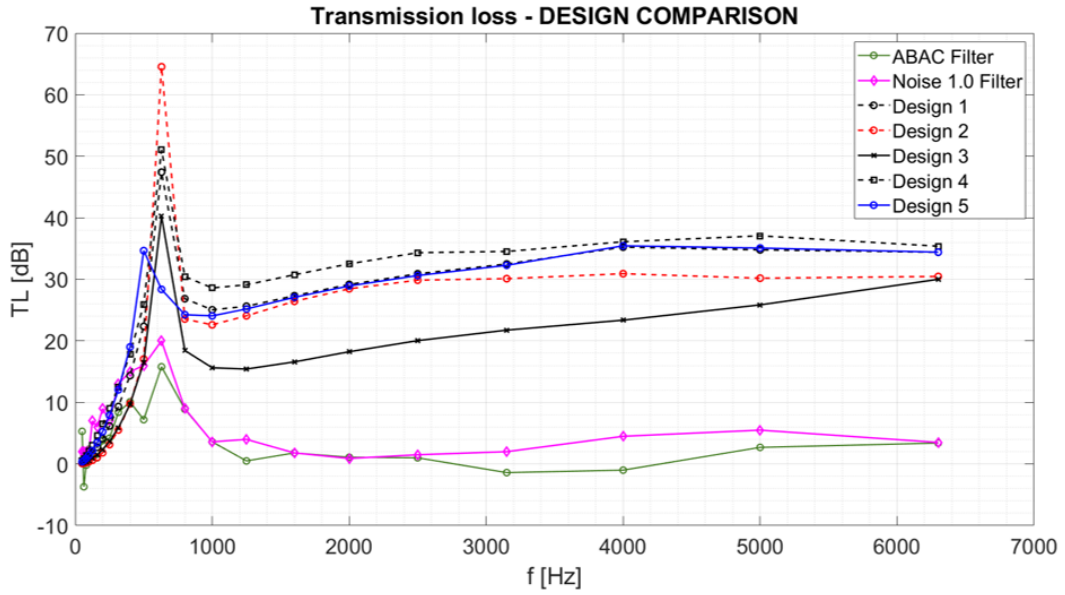


Figure 5.31: Transmission loss

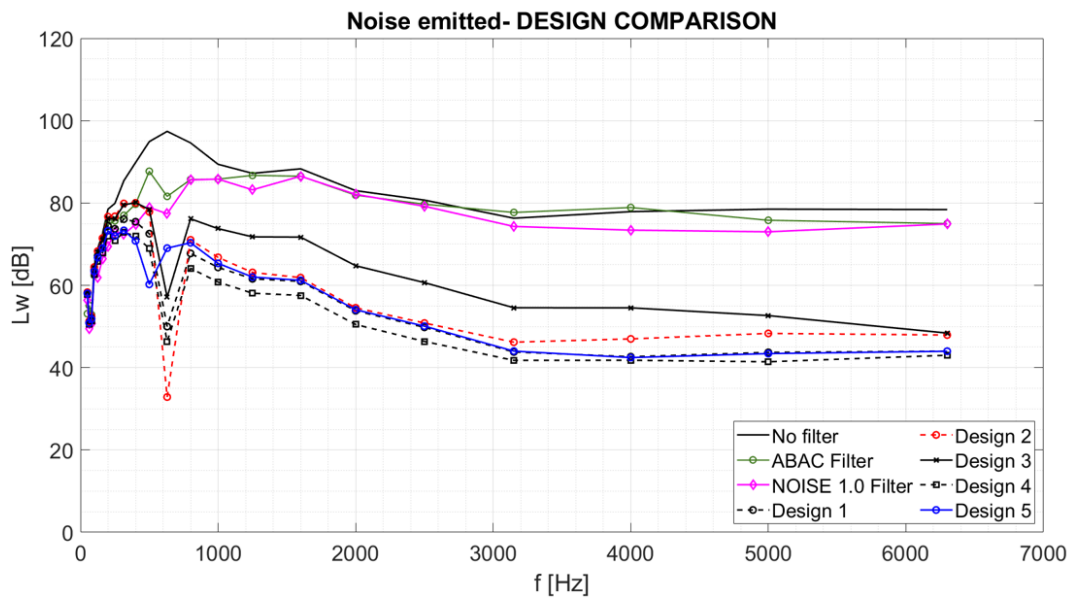


Figure 5.32: Sound power level

Transmission loss and consequently sound power level of all designs are shown in the above figures. It's clear that analytical model attenuates noise in all frequency range considered (0-6300Hz). It could be very interesting show the same results of noise emitted both in low and high frequencies, as in Fig. 5.33 and 5.34.

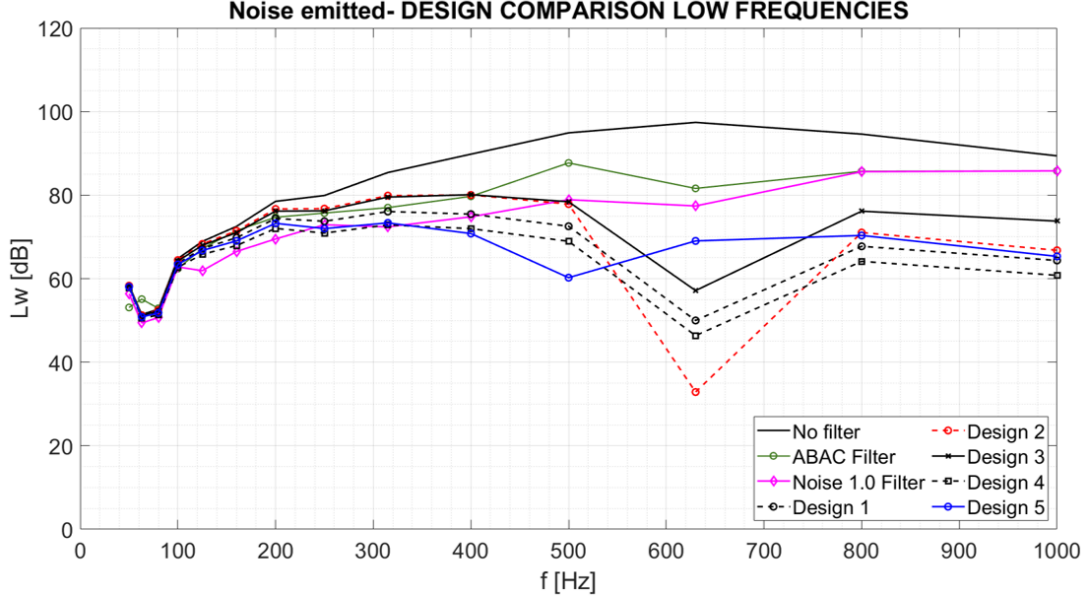


Figure 5.33: Sound power level: Low frequencies

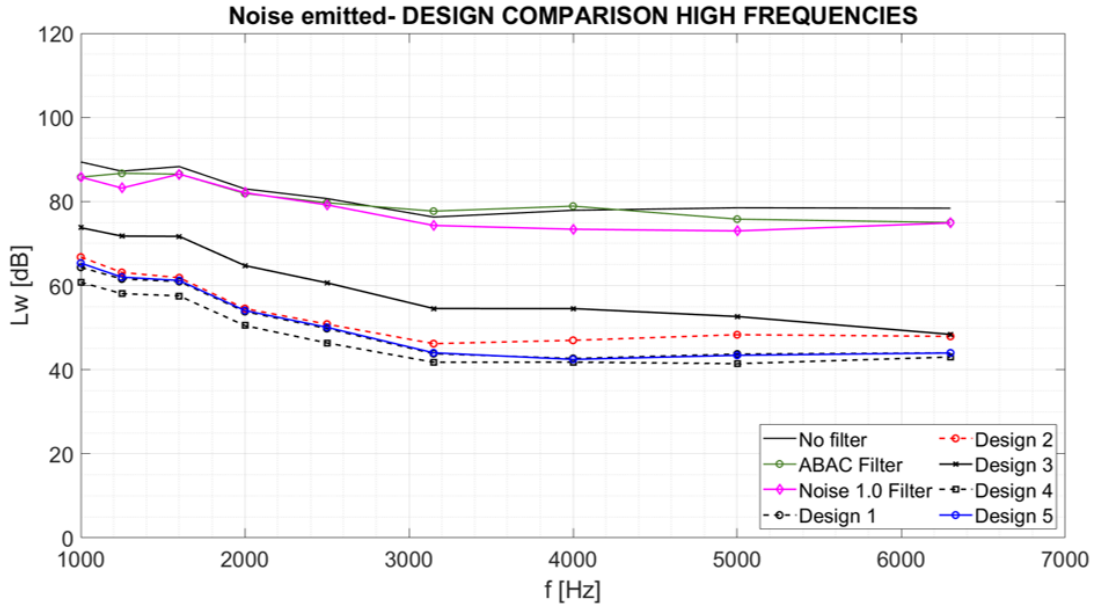


Figure 5.34: Sound power level: High frequencies

*Low frequency range* considered is between 0-1000 Hz, because according to *A-weighted* network in this range there is an attenuation (see Fig.1.7). In fact, frequency 1000 Hz corresponds to attenuation equal to zero. The others frequencies considered are in *High* range. Respect to experimental results of *Abac Filter* and *Noise 1.0 Filter*, new designs present a similar curve shape in frequencies between 0-400 Hz. In this range the differences are caused by total length of

the filter, that could modify the amplitude of noise attenuation in low frequencies, as it will be explained in next lines. Near resonance frequency of the silencer the attenuation is really higher than the others, and it could be caused both by the geometry of the filter but also to a peak of analytical model. In High frequencies, instead, noise attenuation of analytical model is very high (about 30-40dB). Even if human ear is more sensitive to low frequencies, a strong attenuation also in high range could reduce the equivalent  $L_w(A)$  and improve acoustic performances. A good idea to investigate about  $L_w(A)$  of each design described is to compare each design to another one that have a geometric parameter in common. In this way it's easy to understand how a variable parameter could affect noise property of the filter. For this purpose these comparisons will be proposed:

- Designs 1,3,4 having the same PART A and different lenghts of PART B;
- Designs 1,2 having different diameter of expansion chamber;
- Designs 1,5 having the same PART B and different lenghts of PART A;

These comparisons correspond to the reason because of choise of filter configurations, as it has described in previous chapter.

### Design 1,3,4

Transmission loss and noise emitted of these three designs is shown in the belowing figures.

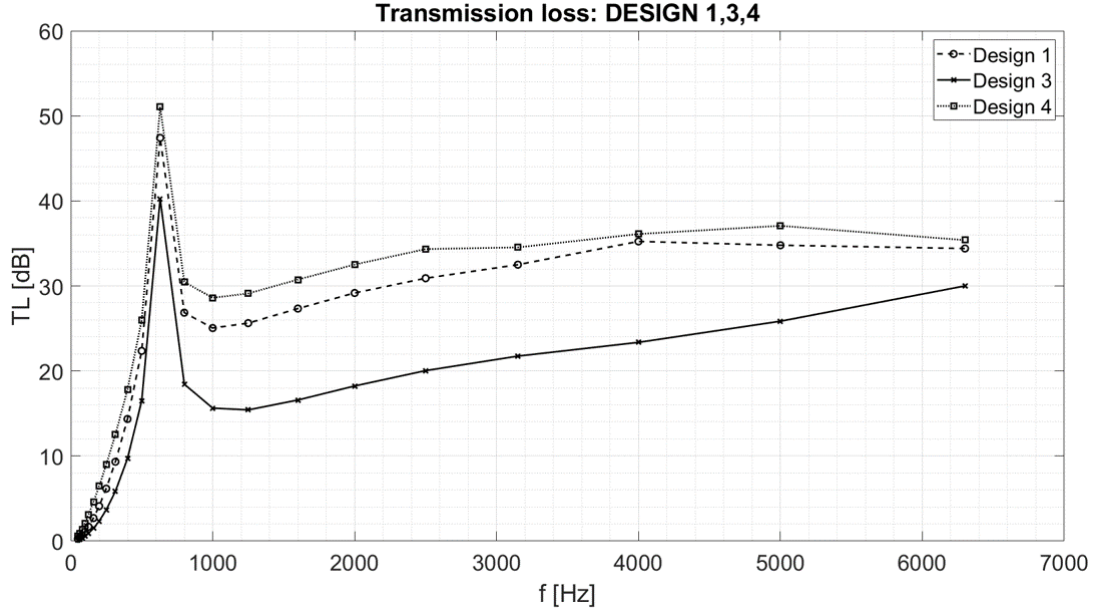


Figure 5.35: Transmission Loss 1,3,4



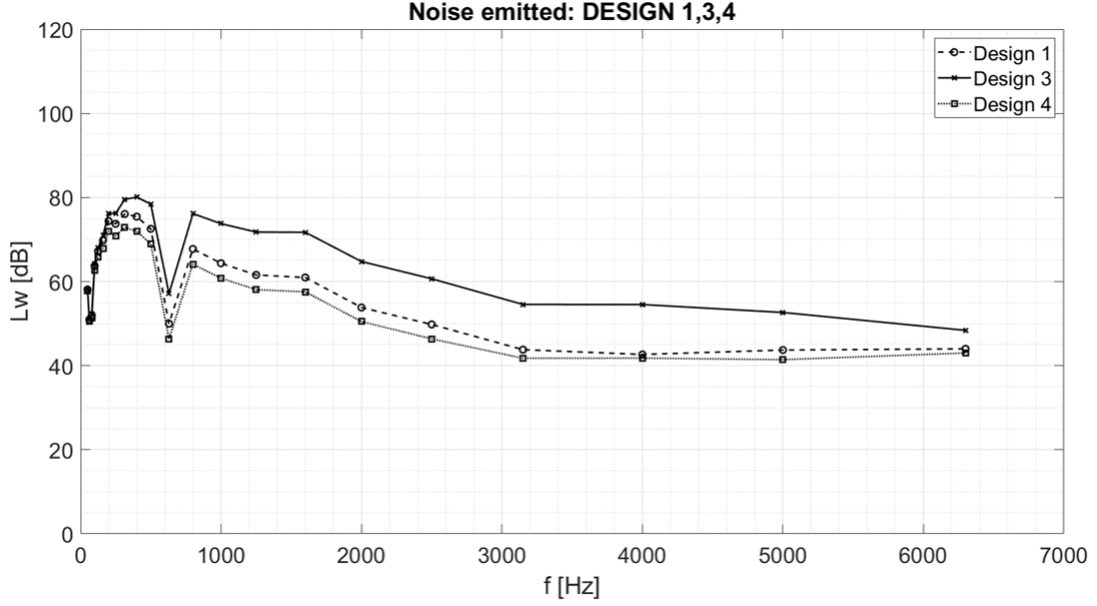


Figure 5.36: Sound power level 1,3,4

It's important to evaluate these plots considering the final outputs of the analysis,  $L_w(A)$ .

Table 5.22: Design 1,3,4

| DESIGN | $L_{w,Aeq}$ [dBA] |
|--------|-------------------|
| 1      | 82,42             |
| 3      | 86,73             |
| 4      | 79,5              |

These results depend on length of expansion chamber (PART B). As indicated in sensitivity analysis in Chapter 4, an increasing of length of expansion chamber decreases both cut off frequency and frequency at which noise attenuation is highest. In this way Transmission Loss curve (and consequently  $L_w$ ) is more "fletted" and thus amplitude of noise attenuation is higher at low frequencies. Remembering the importance of low frequencies in loudness, in theory a longer silencer should have better noise performance. And these expectative results could be observed also in Fig. 5.35 and they can explain that Design 4, that is the longest of all configurations, presents the lowest  $L_w(A)$ . Unlike Design 3, the shortest design, has the worst performance.

### Design 1,2

Design 2 is the only filter solution of this Thesis project that has different diameter of chamber and different inlet pipe diameter. Thus it is interesting to evaluate the importance of this changing in acoustics performances, by comparing it to Design 1 which has same length of PART B and similar total length.

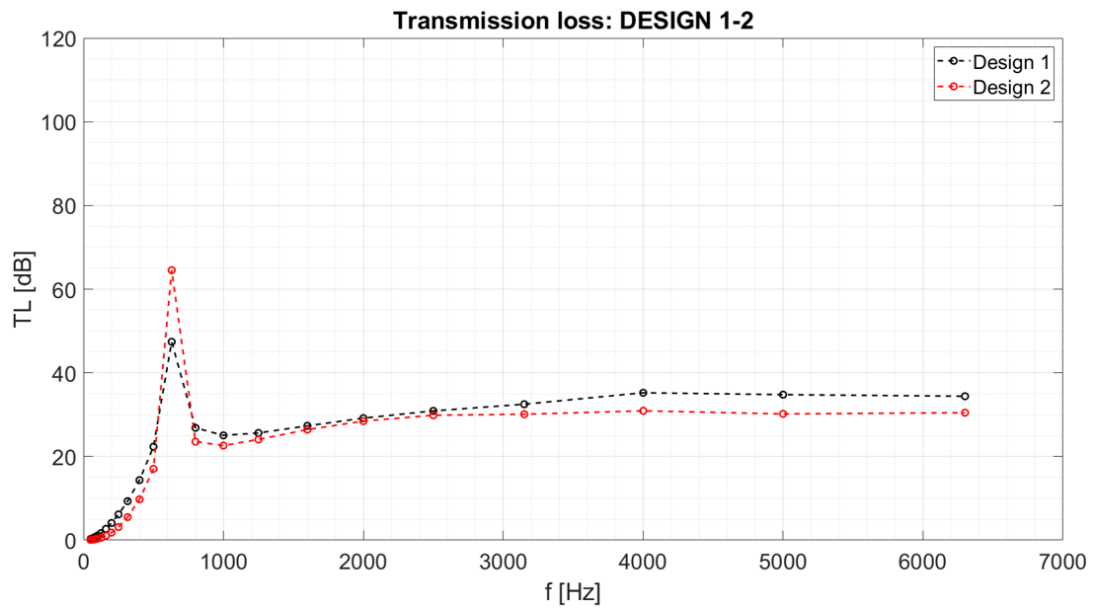


Figure 5.37: Transmission Loss 1,2

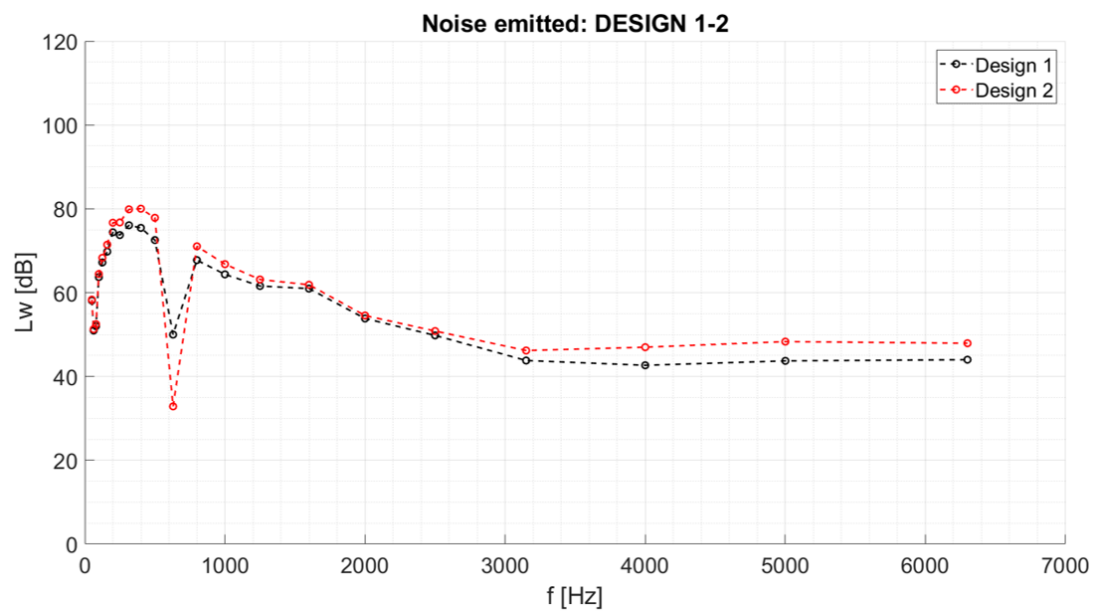


Figure 5.38: Sound power level 1,2

Table 5.23: Design 1,2

| DESIGN | $L_{w,Aeq}$ [dBA] |
|--------|-------------------|
| 1      | 82,42             |
| 2      | 85,98             |

The differences in output results are caused by two different effects, the different geometry of PART A and the different cross sectional ratio between inlet pipe and maximum diameter of expansion chamber. The first is caused by the idea to change geometry quantities of the filter to center its resonance at 630 Hz (higher noise level without filter). Thus it's clear that the peak of TL is at the same frequency, but not the shape of the curve. In fact in Design 1, considering the same frequency range between 0-500Hz, amplitude is bigger and this aspect influences the difference in attenuation between two cases. The high peak in Design 2 probably depends only on analytical model. The second effect is more visible at high frequency, especially between 3000-6300 Hz. As described in sensitivity analysis of expansion chamber in Chapter 4, the maximum amplitude of Transmission Loss depends on ratio  $m$  between inlet pipe and expansion chamber diameters. In this case,  $m$  value of Design 1 ( $m=4$ ) is higher than that one of Design 2 ( $m=3,6$ ), so it explains the difference of some dB between black and red lines in Fig. 5.37 and 5.38.

### Design 1,5

Design 5 is the only filter solution of this Thesis project that has different resonance frequency. The reason of this Design starts to a consideration about *A-weighted scale*. In fact, if noise attenuation is an increasing curve between 0-1000 Hz, it could be a good idea to center resonance frequency lower than 630 Hz. According to the definition of  $f_r$  it's possible to decrease it by increasing total length of Helmotz resonator, PART A of the filter.

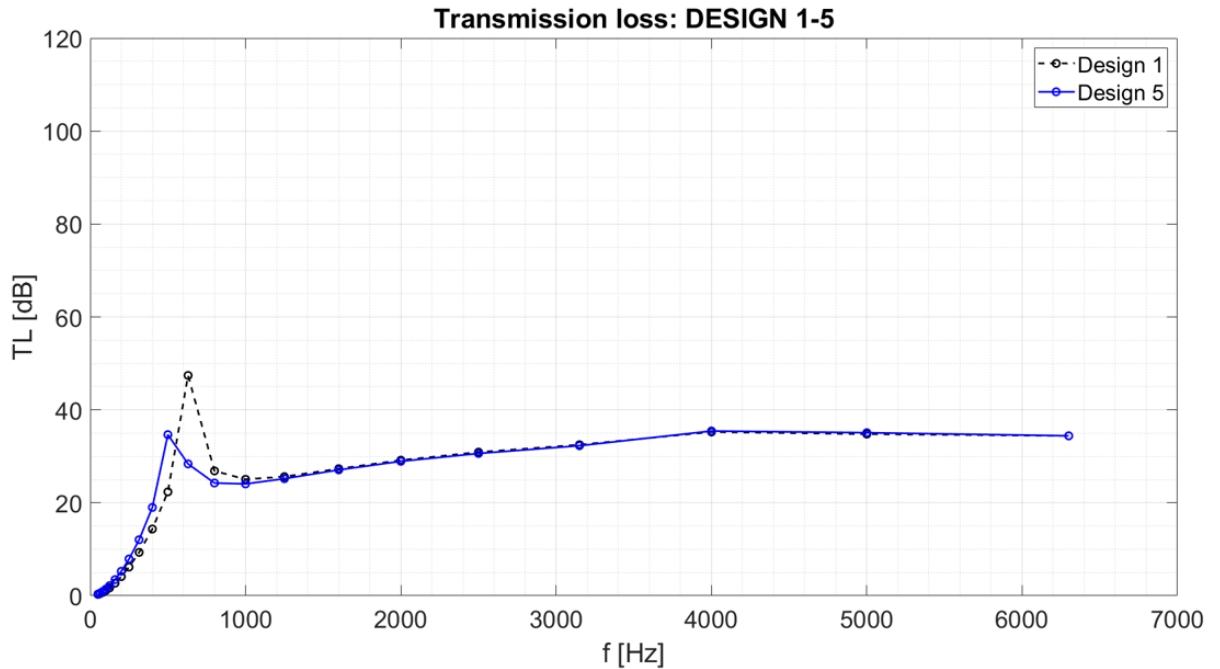


Figure 5.39: Transmission Loss 1,5

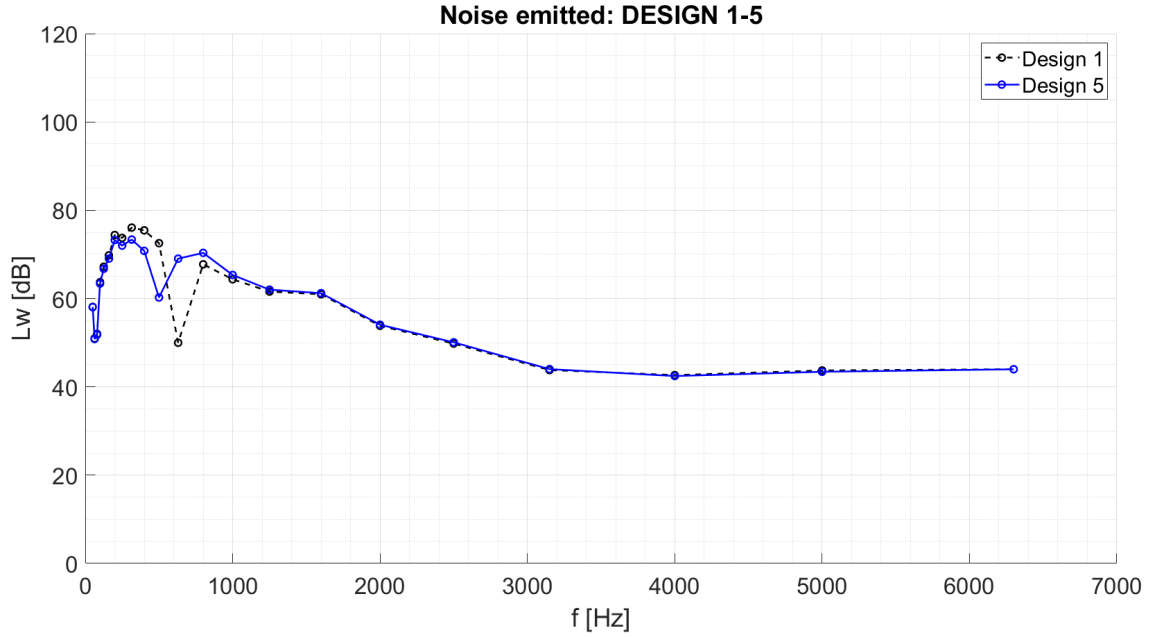


Figure 5.40: Sound power level 1,5

Table 5.24: Design 1,5

| DESIGN | $L_{w,Aeq}$ [dBA] |
|--------|-------------------|
| 1      | 82,42             |
| 5      | 80,5              |

Resonance frequency of Design 5 is  $f_r=530$  Hz. It is not too far to 630 Hz to guarantee an important attenuation even at this frequency, that presents the highest noise level without filter. Results correspond to expectative and the only important difference is at low frequencies. PART B of these two configurations is the same, so TL and  $L_w$  at high frequencies don't change.

At the end a final comparison is shown in Table 5.25, where each design is associated to another one. The instructions to read this table is reported in the following list:

- Consider a design in the first grey column (e.g. Design 1);
- Compare all characteristics of this Design, described in this dissertation (noise, pressure drop and size), to other designs in next columns. Obviously, red cells of the table is used to delete the comparison of same configurations.
- Make the same analysis to other designs in next rows.

Table 5.25: Final comparison

| DESIGN | 1     |   | 2     |   | 3     |   | 4     |   | 5     |   |
|--------|-------|---|-------|---|-------|---|-------|---|-------|---|
| 1      |       |   | Pdrop | ✗ | Pdrop | = | Pdrop | = | Pdrop | = |
|        |       |   | TL    | ✓ | TL    | ✓ | TL    | ✗ | TL    | ✗ |
|        |       |   | Size  | = | Size  | ✗ | Size  | ✓ | Size  | ✓ |
| 2      | Pdrop | ✓ |       |   | Pdrop | ✓ | Pdrop | ✓ | Pdrop | ✓ |
|        | TL    | ✗ |       |   | TL    | = | TL    | ✗ | TL    | ✗ |
|        | Size  | = |       |   | Size  | ✗ | Size  | ✓ | Size  | ✓ |
| 3      | Pdrop | = | Pdrop | ✗ |       |   | Pdrop | = | Pdrop | = |
|        | TL    | ✗ | TL    | = |       |   | TL    | ✗ | TL    | ✗ |
|        | Size  | ✓ | Size  | ✓ |       |   | Size  | ✓ | Size  | ✓ |
| 4      | Pdrop | = | Pdrop | ✗ | Pdrop | = |       |   | Pdrop | = |
|        | TL    | ✓ | TL    | ✓ | TL    | ✓ |       |   | TL    | ✓ |
|        | Size  | ✗ | Size  | ✗ | Size  | ✗ |       |   | Size  | ✗ |
| 5      | Pdrop | = | Pdrop | ✗ | Pdrop | = | Pdrop | = |       |   |
|        | TL    | ✓ | TL    | ✓ | TL    | ✓ | TL    | ✗ |       |   |
|        | Size  | ✗ | Size  | ✗ | Size  | ✓ | Size  | ✓ |       |   |

Table 5.26: Explication of the symbols

| RESULTS               | Symbols |
|-----------------------|---------|
| BETTER CONFIGURATION  | ✓       |
| WORSE CONFIGURATION   | ✗       |
| SIMILAR CONFIGURATION | =       |

Particularly, in the comparison between all designs, one of these is considered **better** than an other if:

- **Noise:**  $L_{w,A}$  is lower;
- **Pressure drop:** Pressure losses are lower;
- **Size:** filter is smaller.

If these conditions are not respected a design is **worse** than another one or, if the differences between them are really small, they are considered **similars**.

## 5.8 Next steps and further analysis

In the last paragraph of this dissertation some possible ideas to continue and improve this Thesis project will be presented.

The logical conclusion is about noise testing of all new filter configurations. It is fundamental to validate the methods that have been developed in this project.

In fact, in this way all final analytical results could be compared to experimental results in order to:

- Evaluate the **error rate** (percentual) between the results and make some consideration about its acceptability.
- Evaluate if new configurations represent an improvements respect to previous filters analyzed and if they are able to respect the initial objects of this project.
- Evaluate the acceptability of some hypotheses. For example if pressure drop is really dependent almost exclusively by concentrated losses or if noise level is more attenuated for a longer geometry. These results are independent from the first point of this list because they could represent a good starting point to start a new analysis trying to understand and correct the errors made.

Obviously, if the results will be considered acceptable, the validation of total model will be complete. Then, it will be possible to improve the model and to look for the best configuration.

As it has already mentioned the most important objects of this dissertation is the research of a correct compromise between noise performances, pressure losses and geometries of filters. Starting from the considerations of previous chapters, in next lines the expectative results are commented.

Firstly, the experimental results about pressure drop should be really near to analytical because of the validation of the model in Chapter 3.

Instead, the error rate in noise model should be higher because this method doesn't include some parameters that could influence final performances. For example, one of the problems of previous Thesis about noise was the inability of the inlet filter to attenuate noise level at high frequencies. In this case, even if the different structure of expansion chamber with extended pipes in inlet and outlet should improve noise performances, the results could be very far to reality. This because this analysis is made only considering fluidodynamic problems of acoustics and not mechanical aspects. Hence, probably only merging a **vibration test** to noise testing will be possible to investigate completely the problem.

Others possible solutions may be developed if experimental results won't guarantee the validation of the model proposed. For example an aspect to investigate could be evaluate what is the effect of a silencer in discharge part and not in intake. It is interesting to understand if changing the position of the filter the range of frequencies where there is an important noise attenuation is similar or different respect to the case of this Thesis. This solution could associate noise reduction of this particular case, a piston compressor, to others systems used to attenuate noise level in

others application. The most important is the muffler of the automotive applications.

Still considering this analogy, an hybrid solution typical of automotive applications could represent a possible idea, as shown in Fig. 5.41[12]. An hybrid silencer is an assembly of a reactive and a dissipative silencer. In fact, as it has already presented in Chapter 4, these two types of silencers have different way to attenuate noise level, one reflecting acoustic waves by abrupt area expansions or changes of impedance (reactive) and the other by dissipation of acoustic energy into heat (dissipative). The effects and the scopes of them are also very different. Reactive silencers have an important effect at low frequencies, ensuring an high noise reduction and low backpressure. Dissipative silencers have instead good effects at mid-high frequencies, so they have not the same noise reduction but an higher backpressure. Hence an hybrid solution may represent an optimal alternative to the configurations presented in this project.

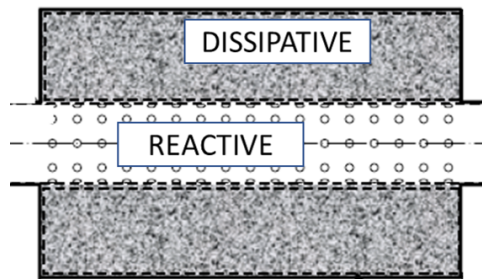


Figure 5.41: Hybrid solution

# Bibliography

- [1] *Basic knowledge of piston compressor*, Atlas Copco Group.
- [2] Professor Colin H Hansen, *FUNDAMENTALS OF ACOUSTICS*, Department of Mechanical Engineering, University of Adelaide.
- [3] Finn Jacobsen, Torben Poulsen, Jens Holger Rindel, Anders Christian Gade and Mogens Ohlrich (2011), *Fundamental of acoustics and noise control*, Department of Electrical Engineering, Technical University of Denmark.
- [4] ISO 9614-2:1996, *Determination of sound power levels of noise sources using sound intensity, PART 2-Measuring by scanning*.
- [5] ISO 3744:1995, *Determination of sound power levels of noise sources using sound pressure-Engineering method in an essentially free field over a reflecting plane*
- [6] M. Carello, A. Ivanov, L. Mazza *Pressure drop in pipe lines for compressed air: comparison between experimental and theoretical analysis*, Department of Mechanics, Politecnico di Torino.
- [7] Marco e Mario Doninelli *Tabelle e diagrammi Perdite di carico aria* , Caleffi.
- [8] R. Singh, W. Soedel *A Review of Compressor Lines Pulsation Analysis and Muffler Design Research -Part I: Pulsation Effects and Muffler Criteria*, International Compressor Engineering Conference, Purdue University.
- [9] Randall F. Barron (2001) *Industrial Noise Control and Acoustics* , Louisiana Tech University Ruston, Louisiana, U.S.A..
- [10] MIHAI BUGARU, OVIDIU VASILE, NICOLAE ENESCU(2006) *The Mufflers Modeling by Transfer Matrix Method*, University POLITEHNICA of Bucharest
- [11] Munjal, M.L., 1987, *Acoustics of Ducts and Mufflers*, 1st Ed., John Wiley and Sons, New York, 328 p.
- [12] Iljae Lee, M.S. (2005), *ACOUSTIC CHARACTERISTICS OF PERFORATED DISSIPATIVE AND HYBRID SILENCERS*, The Ohio State University
- [13] Md. Shahidullah Al Faruq, *An Experimental Investigation on Noise Reduction by Using Modified Helmholtz Resonator*, Bangladesh University of Engineering and Technology.



## Appendix A

# Filter design: 2D representations

In this appendix, all technical drawings are reported.

Firstly each filter assembly is presented. In these representations are shown all the useful 2D-views to describe better all total lengths of each design. In fact only the most important geometrical dimensions are marked, to evaluate the size of the filter (L and H of Fig. 5.30) and its possible obstruction in the structure.

Then, all filter parts and all their dimensions are reported. Total number of components used to create final 5 designs are 14, as shown in Table 5.29. The designation of each drawing regards the initial letter of each part (A=part A, B=part B, CP=connection part, F=foam material) and the number of model considered.

In the following table the decomposition of each filter is reported (see Table 5.20- Chapter V).

| <b><i>FILTER PARTS</i></b> |                 |                 |                  |                 |
|----------------------------|-----------------|-----------------|------------------|-----------------|
| <b><i>DESIGN</i></b>       | <b><i>A</i></b> | <b><i>B</i></b> | <b><i>CP</i></b> | <b><i>F</i></b> |
| 1                          | A1              | B1              | CP1              | F1              |
| 2                          | A2              | B2              | CP2              | F2              |
| 3                          | A1              | B3              | CP1              | F3              |
| 4                          | A1              | B4              | CP3              | F4              |
| 5                          | A3              | B1              | CP1              | F1              |

CONFIDENTIAL

1

2

3

4

5

6

7

8

9

10

A

B

C

D

E

F

G

SECTION A-A

SECTION A-A

SECTION B-B

SECTION B-B

Pos

Qty

Name

R/S

Comments

1

1

Part A

2

1

Part B

3

1

Connection part

4

4

Screw

M6- filter assembly

5

2

Screw

M6- head connection

6

1

Foam material

Tolerances, if not indicated in accordance to:

General tolerances

ATLAS COPCO STANDARD CLASS

130h - m

Name

DESIGN 2

Material

ABS

Treatment

Scale

1:2

Drawn by

Atlas Copco

Blank wt

Blank nr

Family

Blank nr

Blank wt

Blank nr

Family

Blank nr

Blank wt

Blank nr

Family

Blank nr

STATUS

PRELIMINARY

Ed

00

Posi- tion

Date

20.01.2020

Intr/ Appd

Parent 3D Model

Ed. Version 3D

Designation

DESIGN 2

Sheet

1 / 1

CONFIDENTIAL

This document is our property and that not without our permission be altered, copied, used for manufacturing or communicated to any other person or company.

SOLIDWORKS Educational Product. Solo per uso didattico.

93

CONFIDENTIAL

10 9 8 7 6 5 4 3 2 1

A B C D E F G

SECTION B-B

SECTION A-A

103 93 104 120

1 2 3 4 5 6

Parts list

| Pos | Qty | Name            | R/S | Comments            |
|-----|-----|-----------------|-----|---------------------|
| 1   | 1   | Part A          |     |                     |
| 2   | 1   | Part B          |     |                     |
| 3   | 1   | Connection part |     |                     |
| 4   | 4   | Screw           |     | M6- filter assembly |
| 5   | 2   | Screw           |     | M6- head connection |
| 6   | 1   | Foam material   |     |                     |

General tolerances  
130K - m

Design 4

ABS

Scale 1:2

Drawn by

Blank nr

Family

Compare

Replaces

Blank wt

Inv

Blank wt

Prod checked

Approved

Date 20.01.2020

Designation

DESIGN 4

Sheet 1 / 1

Ed. Version 3D

Parent 3D Model

Date 20.01.2020

Intr./Appd

Modified from

Post-  
tion

Ed

00

CONFIDENTIAL

This document is our property and that not without our permission be altered, copied, used for manufacturing or communicated to any other person or company.

SOLIDWORKS Educational Product. Solo per uso didattico.

00 Ed Post- tion

20.01.2020 Date

Intr./Appo

Parent 3D Model

Ed. Version 3D

PRELIMINARY

STATUS

ATLAS Copco

Scale 1:2

Drawn by

Blank wt

Blank nr

Family

Compare

Replaces

Drawing owner

Designation

Sheet 1 / 1

DESIGN 5

General tolerances

General tolerances

1300K - m

DESIGN 5

ABS

Material

Treatment

INVT

| Pos | Qty | Name            | R/S | Comments            |
|-----|-----|-----------------|-----|---------------------|
| 1   | 1   | Part A          |     |                     |
| 2   | 1   | Part B          |     |                     |
| 3   | 1   | Connection part |     |                     |
| 4   | 4   | Screw           |     | M6- filter assembly |
| 5   | 2   | Screw           |     | M6- head connection |
| 6   | 1   | Foam material   |     |                     |

Section A-A

Section B-B

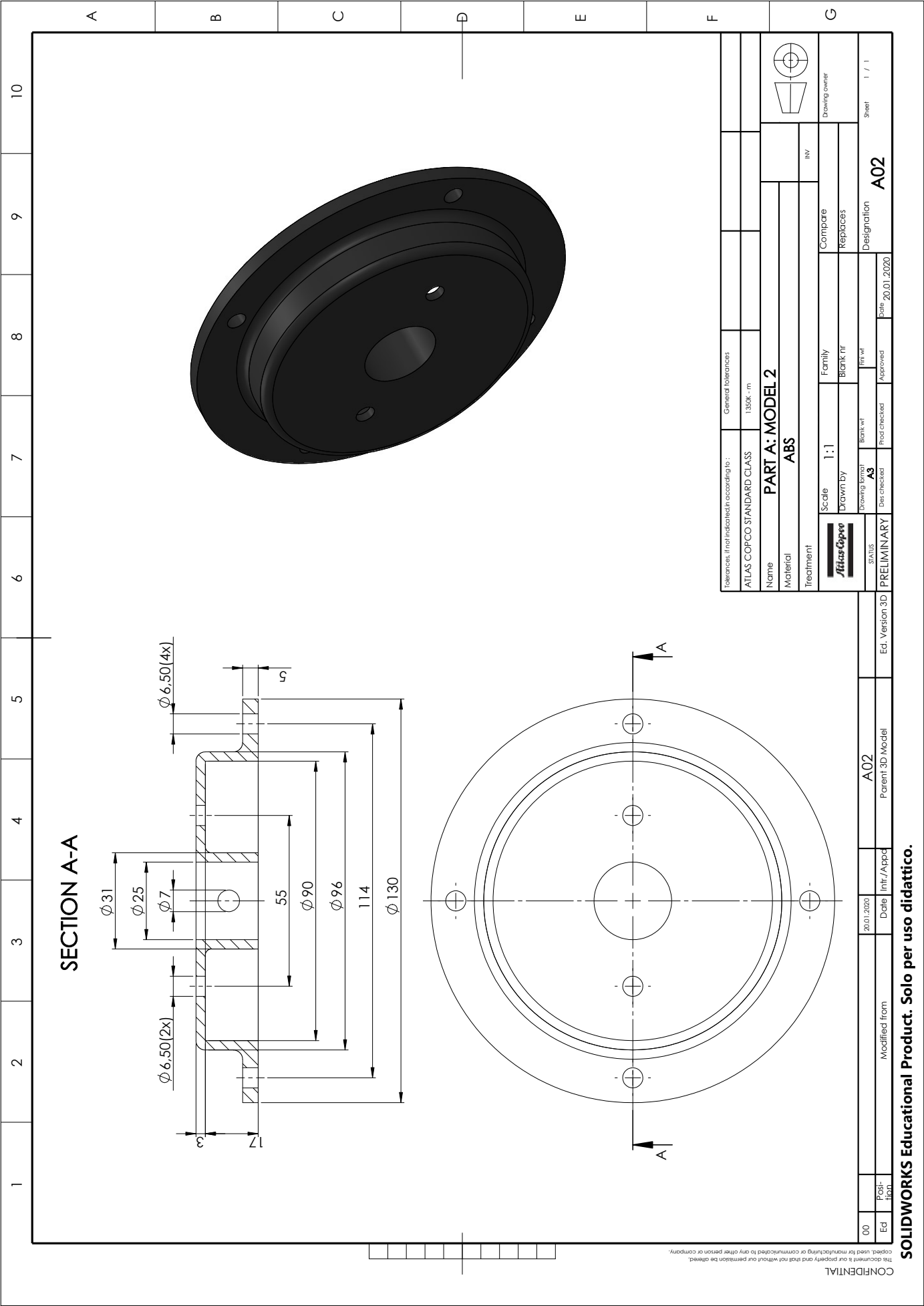
The drawing includes a 3D model of a mechanical part, a top view with dimensions 104 and 120, and two cross-sections. Section A-A shows internal features with dimensions 18 and 91. Section B-B shows a different cross-section with dimensions 104 and 120. A parts list table is provided, detailing the components and their quantities.

CONFIDENTIAL

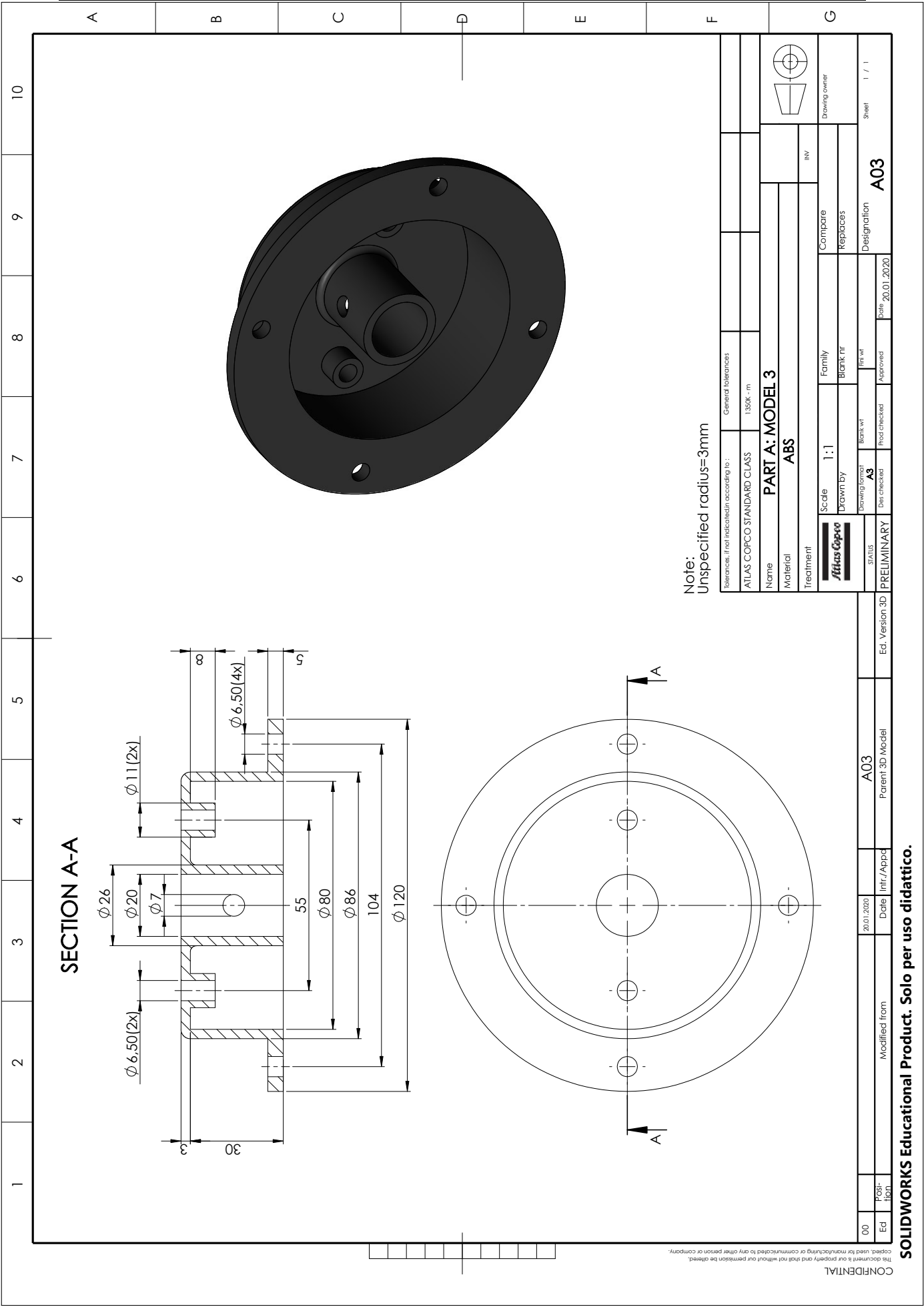
This document is not property and not without our permission be altered, copied, used for manufacturing or communicated to any other person or company.

SOLIDWORKS Educational Product. Solo per uso didattico.







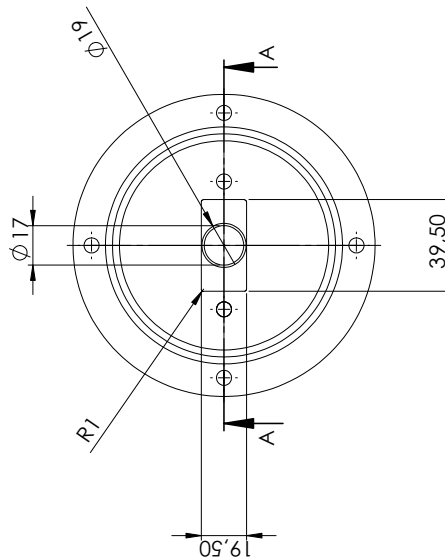
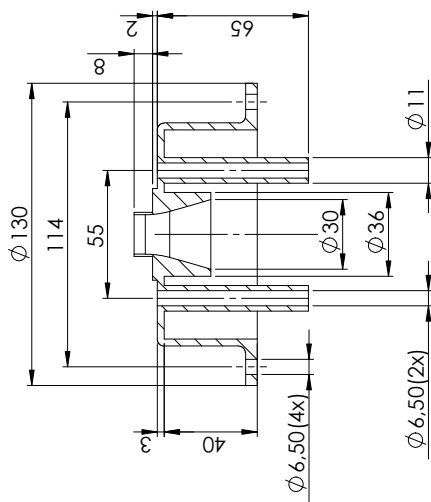


[illegible]

Note:  
Unspecified radius=3mm

[illegible]

**SOLIDWORKS Educational Product. Solo per uso didattico.**

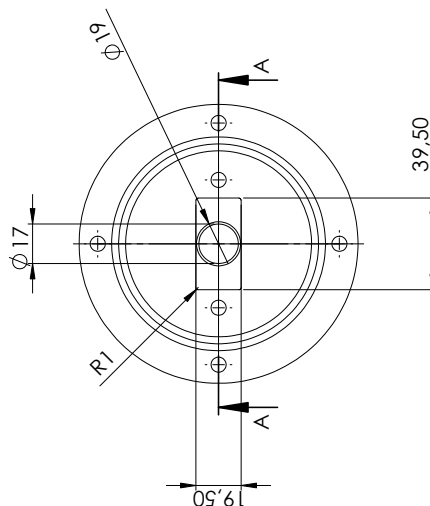


Note:  
Unspecified radius=3mm


[illegible]

Technical drawing of a 120mm diameter pipe with a 25mm diameter hole. The drawing shows the pipe with a 25mm diameter hole. The dimensions are as follows:

- Overall diameter:  $\varnothing 120$
- Hole diameter:  $\varnothing 25$
- Distance from hole center to pipe end: 104
- Distance from hole center to hole edge: 55
- Distance from hole edge to pipe end: 50
- Distance from hole center to hole edge (inner): 8
- Distance from hole center to hole edge (outer): 2
- Distance from hole center to hole edge (inner): 3
- Distance from hole center to hole edge (outer): 20
- Distance from hole center to hole edge (inner): 6.50 [4x]
- Distance from hole center to hole edge (outer): 6.50 (2x)
- Distance from hole center to hole edge (inner): 11 (2x)

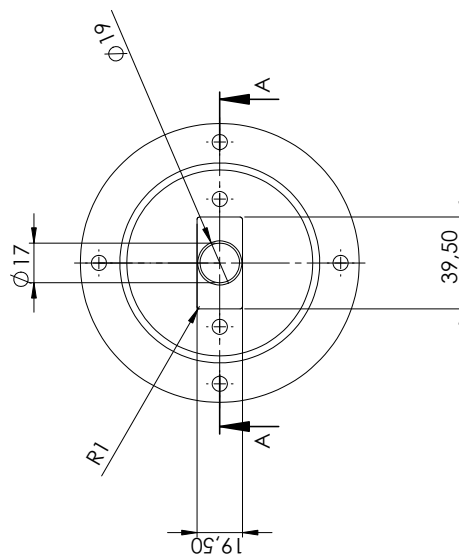


Note:  
Unspecified radius=3mm

|   |                |                    |              |          |               |
|---|----------------|--------------------|--------------|----------|---------------|
| Tolerances, if not indicated in accordance to :                                     |                | General tolerances |              |          |               |
| ATLAS COPCO STANDARD CLASS  |                | 130K - m           |              |          |               |
| <b>PART B: MODEL 3</b>  |                |                    |              |          |               |
| Name  |                |                    |              |          |               |
| Material  | ABS            |                    |              |          |               |
| Treatment   | INV            |                    |              |          |               |
|  | Scale          | 1 : 2              | Family       | Compare  | Drawing owner |
|   | Drawn by       |                    | Blank nr     | Replaces |               |
|   | Drawing format |                    | 1st ed       |          |               |
| STATUS  | Des checked    | A3                 | Prof checked | Approved | Designation   |
| BPEL / MINIBARY   |                |                    |              |          | B03           |
|   |                |                    |              |          | Sheet 1 / 1   |

|    |       |               |      |            |                 |
|----|-------|---------------|------|------------|-----------------|
| 00 |       | 20.01.2020    |      | B03        |                 |
| Ed | Posi- | Modified from | Date | Intr./Apod | Parent 3D Model |
|    |       |               |      |            | Ed. Version 3D  |

**SOLIDWORKS Educational Product. Solo per uso didattico.**



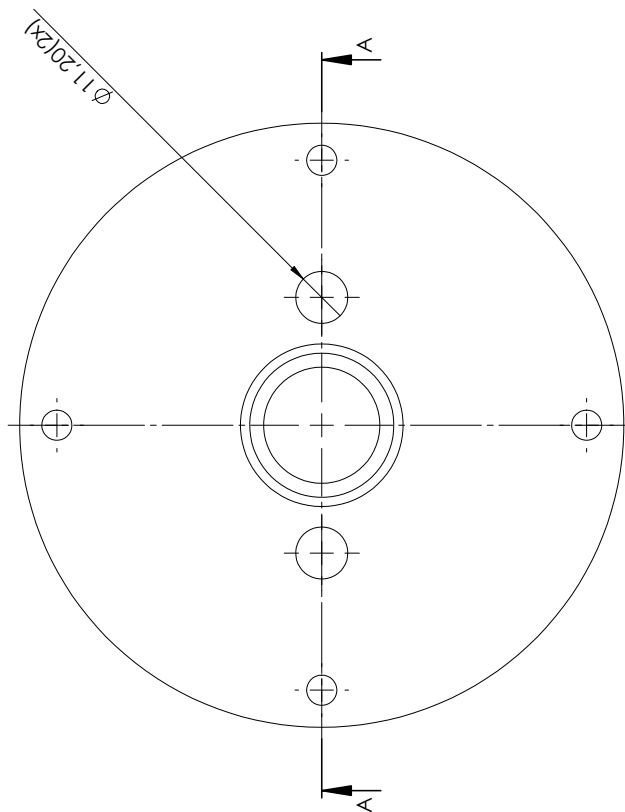
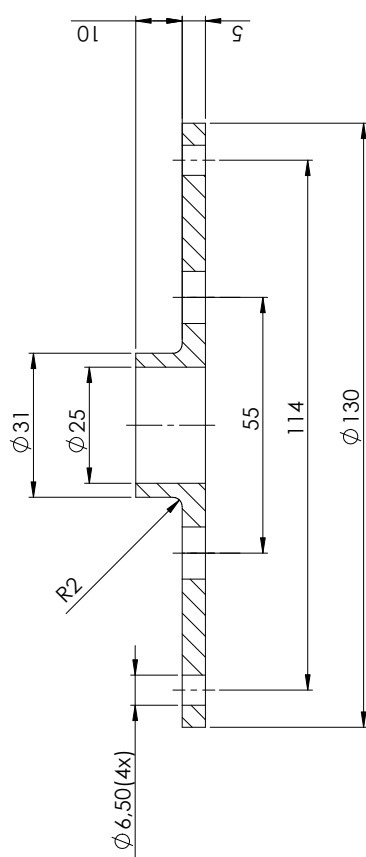
Note:  
Unspecified radius=3mm

|                        |  |  |       |                    |              |          |             |
|------------------------|--|--|-------|--------------------|--------------|----------|-------------|
|                        |  | Tolerance, if not indicated in accordance to : |       | General tolerances |              |          |             |
|                        |  | ATLAS COPCO STANDARD CLASS                     |       | 1350K - m          |              |          |             |
| <b>PART B: MODEL 4</b> |  |  |       |                    |              |          |             |
| Name                   |  |  |       |                    |              |          |             |
| Material               |  | ABS  |       |                    |              |          |             |
| Treatment              |  | INV  |       |                    |              |          |             |
|                        |  |  |       |                    |              |          |             |
|                        |  | Scale  | 1 : 2 |                    | Family       | Compare  |             |
|                        |  | Drawn by                                       |       |                    | Blank nr     | Replaces |             |
| Drawing format         |  | A3   |       | Blank wt           | Desigination |          |             |
| DESIGNED BY            |  | STATUS   |       | Des checked        | Approved     |          | Sheet 1 / 1 |
| PREPARED BY            |  |  |       | Part no. 01.0000   | <b>B04</b>   |          |             |

|    |       |               |            |            |                 |                |
|----|-------|---------------|------------|------------|-----------------|----------------|
| 00 |       |               | 20.01.2020 |            | B04             |                |
| Ed | Posi- | Modified from | Date       | Intr./Apod | Parent 3D Model | Ed. Version 3D |

**SOLIDWORKS Educational Product. Solo per uso didattico.**

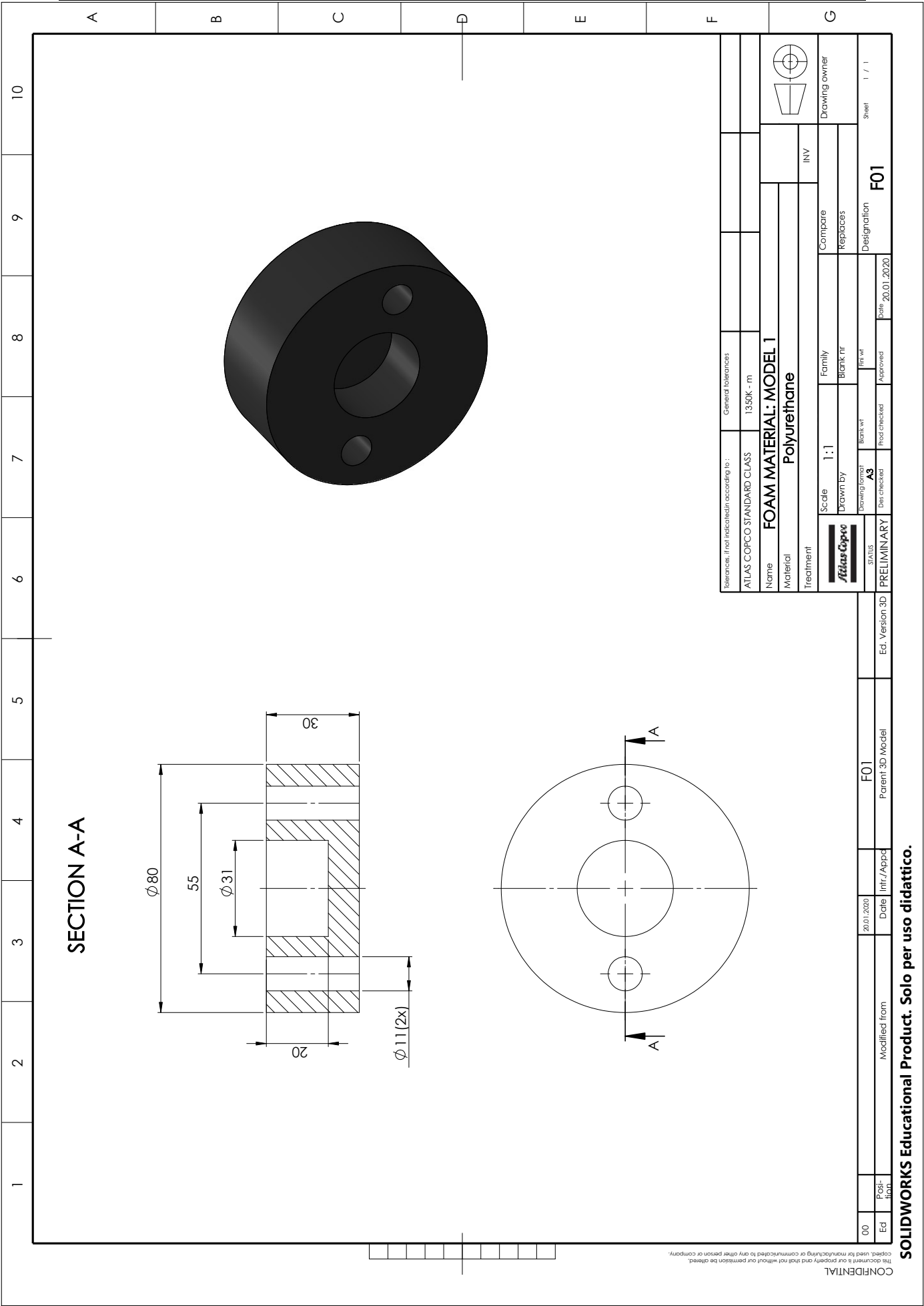


[illegible]

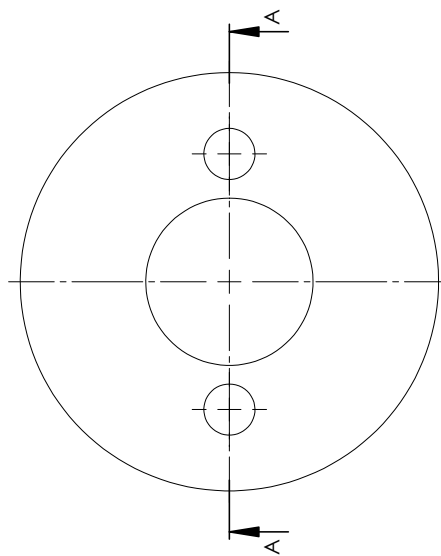
**SOLIDWORKS Educational Product. Solo per uso didattico.**



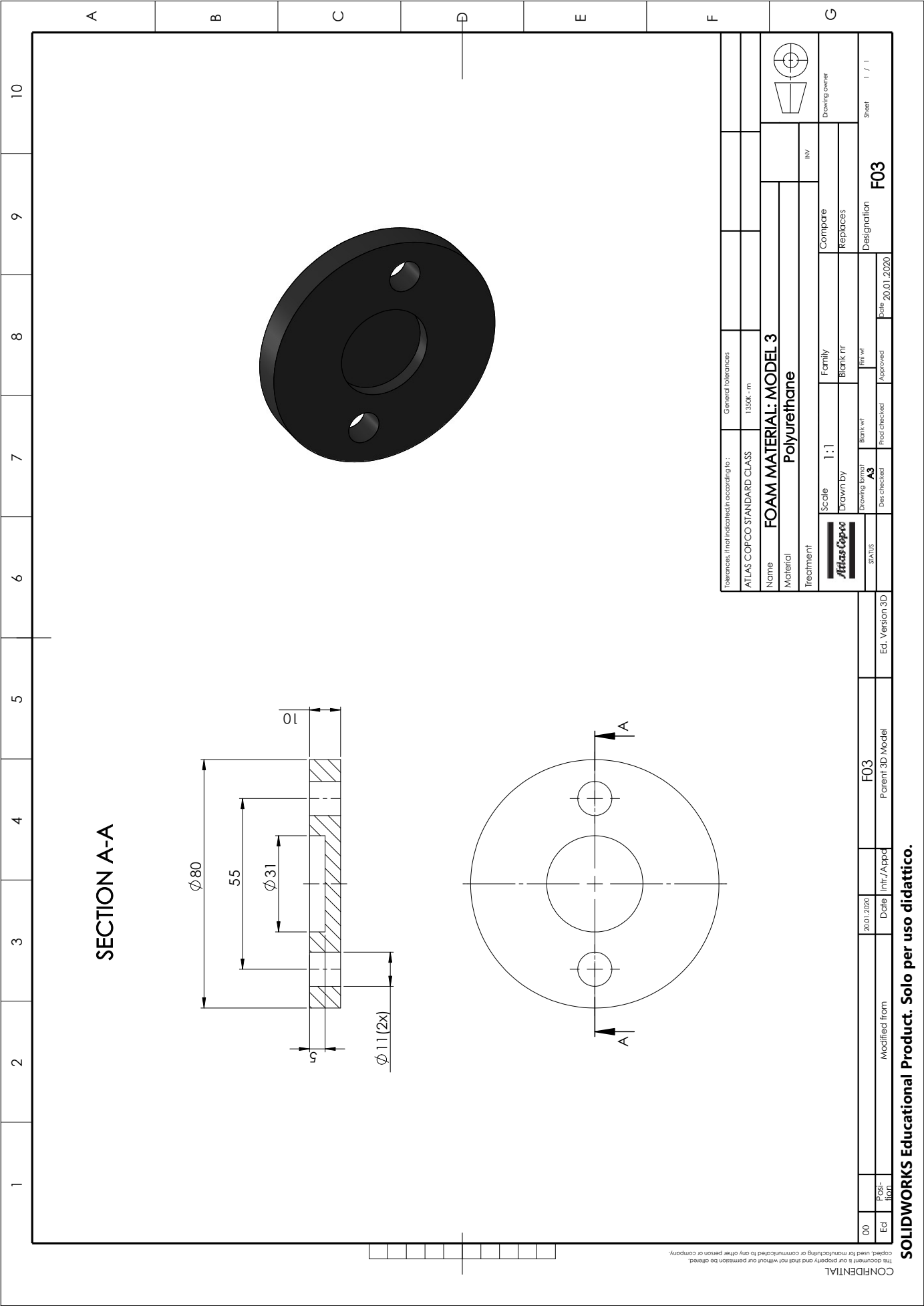




Technical drawing of a stepped shaft. The shaft has a total length of 90 and a total outer diameter of  $\phi 90$ . It consists of three main sections: a left section with a diameter of  $\phi 36$  and a length of 20, a middle section with a diameter of  $\phi 55$  and a length of 30, and a right section with a diameter of  $\phi 11$  and a length of 55. The shaft is shown with a cross-section view indicating the internal structure and the steps between the sections.

[illegible]

**SOLIDWORKS Educational Product. Solo per uso didattico.**



**SOLIDWORKS Educational Product. Solo per uso didattico.**